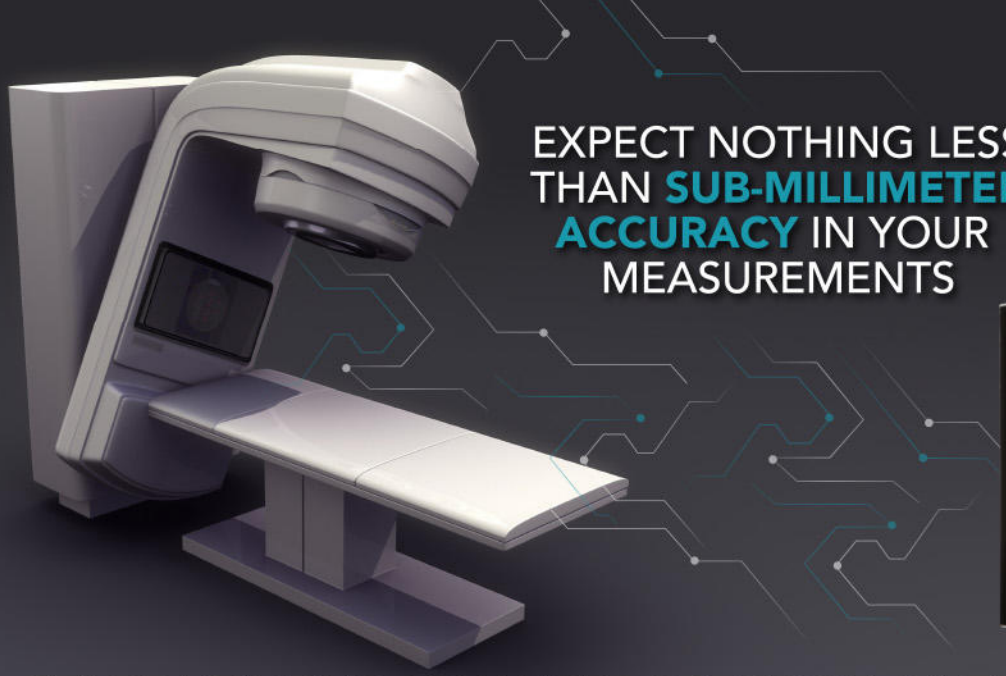

EXPECT NOTHING LESS THAN SUB-MILLIMETER ACCURACY IN YOUR MEASUREMENTS

RIT®

START UTILIZING ADVANCED PRECISION QA TODAY

THE RIT FAMILY OF PRODUCTS **VERSION 6.7.X**

3D Winston-Lutz Isocenter Optimization
The enhanced isocenter optimization routine allows for optimal cone detection, resulting in the utmost precision. The accuracy of this routine now surpasses sub-millimeter resolution. *(Pictured above)*

Cerberus 2.0: The Future of Complete Automation
Completely streamline your automated phantom analysis workflow with the new Cerberus. Cerberus operates in the background of your workstation, allowing for hands-free Imaging QA.

One-Click, Instant Automated Phantom Analyses

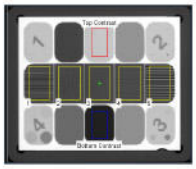

RIT's full suite of phantom analyses provides fast, robust, and accurate analysis of all imaging tests recommended in TG-142. The software now offers added support for the QCkV-1 phantom. *(Pictured right)*

Tolerance Customization and Management
RIT's new Tolerance Manager offers comprehensive customization of tolerance values for every measurement used in all automated phantom analyses. Tolerance profiles can be precisely-tailored to each individual machine in use.

CLICK HERE TO DOWNLOAD TODAY

Elekta Leaf Speed Analysis
RIT now offers fast and accurate automated analysis for Elekta MLC QA. The new Leaf Speed Analysis routine measures the consistency and accuracy of the MLC leaf speeds as they traverse the imager.

TomoTherapy® Registration for Patient QA
Easily perform exact dose comparisons with RIT's new TomoTherapy Registration routine. This new, innovative wizard uses a TomoTherapy® plan, dose map, and a film to determine position an dose accuracy using the red lasers. *(Pictured below)*

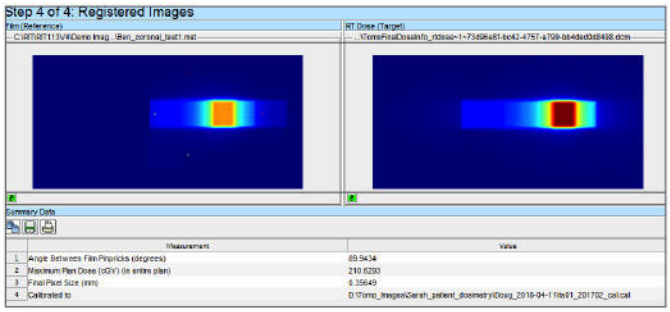

Streamline Your QA Workflow
Fully-customize your software experience with RIT's updated and dynamic interface. With the new ability to hide/display any features or sections, you can instantly access you most frequently-performed analysis routines.

Convenient, Cloud-Based Software Licensing
Easily manage your software licenses with RIT's new, flexible system at your convenience, 24/7/365 without the help of RIT Technical Support. Upgrading is now easier than ever.

RADIOLOGICAL IMAGING TECHNOLOGY, INC.
RADIMAGE.COM
(+1) 719.590.1077 x211 // sales@radimage.com

Connect with RIT
@RIT4QA

Supplement 2 for the 2004 update of the AAPM Task Group No. 43 Report: Joint recommendations by the AAPM and GEC-ESTRO

Mark J. Rivard[a)]
Department of Radiation Oncology, Tufts University School of Medicine, Boston, MA 02111, USA

Facundo Ballester
Unidad Mixta de Investigación en Radiofísica e Instrumentación Nuclear en Medicina (IRIMED), Instituto de Investigación Sanitaria La Fe (IIS-La Fe)-Universitat de Valéncia, Bujassot 46100, Spain

Wayne M. Butler
Schiffler Cancer Center, Wheeling Hospital, Wheeling, WV 26003, USA

Larry A. DeWerd
Accredited Dosimetry and Calibration Laboratory, University of Wisconsin, Madison, WI 53706, USA

Geoffrey S. Ibbott
Department of Radiation Physics, M.D. Anderson Cancer Center, Houston, TX 77030, USA

Ali S. Meigooni
Comprehensive Cancer Centers of Nevada, Las Vegas, NV 89169, USA

Christopher S. Melhus
Department of Radiation Oncology, Tufts University School of Medicine, Boston, MA 02111, USA

Michael G. Mitch
Radiation Physics Division, National Institute of Standards and Technology, Gaithersburg, MD 20899, USA

Ravinder Nath
Department of Therapeutic Radiology, Yale University School of Medicine, New Haven, CT 06510, USA

Panagiotis Papagiannis
Medical Physics Laboratory, Medical School, University of Athens, Athens, Greece

(Received 15 November 2016; revised 11 May 2017; accepted for publication 9 June 2017; published 8 August 2017)

Since the publication of the 2004 update to the American Association of Physicists in Medicine (AAPM) Task Group No. 43 Report (TG-43U1) and its 2007 supplement (TG-43U1S1), several new low-energy photon-emitting brachytherapy sources have become available. Many of these sources have satisfied the AAPM prerequisites for routine clinical purposes and are posted on the Brachytherapy Source Registry managed jointly by the AAPM and the Imaging and Radiation Oncology Core Houston Quality Assurance Center (IROC Houston). Given increasingly closer interactions among physicists in North America and Europe, the AAPM and the Groupe Européen de Curiethérapie-European Society for Radiotherapy & Oncology (GEC-ESTRO) have prepared another supplement containing recommended brachytherapy dosimetry parameters for eleven low-energy photon-emitting brachytherapy sources. The current report presents consensus datasets approved by the AAPM and GEC-ESTRO. The following sources are included: ^{125}I sources (BEBIG model I25.S17, BEBIG model I25.S17plus, BEBIG model I25.S18, Elekta model 130.002, Oncura model 9011, and Theragenics model AgX100); ^{103}Pd sources (CivaTech Oncology model CS10, IBt model 1031L, IBt model 1032P, and IsoAid model IAPd-103A); and ^{131}Cs (IsoRay Medical model CS-1 Rev2). Observations are included on the behavior of these dosimetry parameters as a function of radionuclide. Recommendations are presented on the selection of dosimetry parameters, such as from societal reports issuing consensus datasets (e.g., TG-43U1, AAPM Report #229), the joint AAPM/IROC Houston Registry, the GEC-ESTRO website, the Carleton University website, and those included in software releases from vendors of treatment planning systems. Aspects such as timeliness, maintenance, and rigor of these resources are discussed.

Links to reference data are provided for radionuclides (radiation spectra and half-lives) and dose scoring materials (compositions and mass densities). The recent literature is examined on photon energy response corrections for thermoluminescent dosimetry of low-energy photon-emitting brachytherapy sources. Depending upon the dosimetry parameters currently used by individual physicists, use of these recommended consensus datasets may result in changes to patient dose calculations. These changes must be carefully evaluated and reviewed with the radiation oncologist prior to their implementation.
 [https://doi.org/10.1002/mp.12430]

Key words: brachytherapy, dosimetry parameters, dosimetry protocol, TG-43

TABLE OF CONTENTS

1. INTRODUCTION

The American Association of Physicists in Medicine (AAPM) and the Groupe Européen de Curiethérapie-European Society for Radiotherapy & Oncology (GEC-ESTRO) endeavor to promote quality and standardization of clinical procedures such as brachytherapy. Since publication of the 1995 AAPM report by Task Group No. 43 (TG-43)[1] on interstitial brachytherapy source dosimetry, a 2004 update (TG-43U1)[2,3] and a 2007 supplement (TG-43U1S1)[4,5] have been published containing recommended standards and societal consensus datasets for brachytherapy dosimetry parameters of low-energy photon-emitting brachytherapy sources (†). The current report presents joint AAPM+GEC-ESTRO consensus datasets for 11 low-energy photon-emitting brachytherapy sources (‡) that have become available since the prior reports and have met the AAPM brachytherapy dosimetric prerequisites and the AAPM Calibration Laboratory Accreditation (CLA) subcommittee requirements.[2,6,7]

These sources are listed in Table IA with their schematic diagrams shown in Fig. 1. Production of five of these sources (models I25.S17, I25.S18, 9011, 1031L, and 1032P) has been discontinued. However, they are included to provide consensus data as a means of standardizing their dosimetry parameters for retrospective investigation of dose distribution comparisons among users, and also for retrospective analyses of patients previously treated with these sources. The current report has been reviewed and approved by the AAPM Brachytherapy Subcommittee and Therapy Physics Committee, the GEC-ESTRO Brachytherapy Physics Quality Assurance System working group, and the ESTRO Advisory Committee on Radiation Oncology Practice.

Since publication of the TG-43U1S1 report, a multisocietal report (TG-186) has become available to provide recommendations on the clinical use of model-based dose calculation algorithms (MBDCAs) in brachytherapy beyond the TG-43 formalism.[8] While this approach can address limitations of the TG-43 formalism (including the approximation of human tissue as water and the simplification of radiation scatter conditions), treatment planning systems (TPSs) using MBDCA are currently available only for high dose-rate ^{192}Ir brachytherapy sources. At ^{192}Ir photon energies, radiological differences between tissue and water are less important than for low-energy photon-emitting sources such as that included in the TG-43 report series. Given that most clinics worldwide still use TPSs based on the TG-43 dose calculation formalism, it is important to continue the presentation of recommended dosimetry parameters for consistent clinical use of low-energy brachytherapy sources.

2. DOSIMETRY DATASET REVIEW

Since publication of the 2004 and 2007 reports, manufacturers have increasingly adhered to AAPM recommendations for brachytherapy source characterization preceding clinical rollout, due in part to demand by medical physicists for manufacturer compliance with AAPM recommendations. Manufacturers and brachytherapy clinicians across the world have recognized the Brachytherapy Source Registry.[9] This Registry is managed jointly by the AAPM and the Imaging and Radiation Oncology Core Houston Quality Assurance Center (IROC Houston, formerly the Radiological Physics Center), and sets a rigorous paradigm for infrastructure of multicooperative group clinical trials. Standardization and

†Several sources included in the 2004 AAPM TG-43U1 report and the 2007 AAPM TG-43U1S1 report are no longer in production, but their data remain available on the online Joint AAPM/IROC Houston Brachytherapy Source Registry

‡Certain commercial equipment, instruments, and materials are identified in this work in order to specify adequately the experimental procedure. Such identification does not imply recommendation nor endorsement by the AAPM, the GEC-ESTRO, or the National Institute of Standards and Technology, nor does it imply that the material or equipment identified is necessarily the best available for these purposes.

dissemination of brachytherapy source datasets ensures clinical consistency across a wide variety of clinical settings. To provide guidance on the selection of dosimetry data, the following paragraph is presented (with permission) from the 2009 AAPM Summer School.[10]

> "Often, multiple dosimetry publications are available for a given brachytherapy source model, as well as different possible interpretations on how to select TG-43 protocol parameters and implement dose calculations for clinical treatment planning. This potential for confusion could cause variability in clinical practice and unnecessary variations in administered dose or even serious dose-calculation errors. A brief description is provided of the main publicly-accessible archives or databases of dosimetry datasets to provide guidance on choice of dosimetry parameters."

2.A. AAPM TG-43U1 and TG-43U1S1 reports

The AAPM 2004 and 2007 reports presented consensus datasets of TG-43 brachytherapy dosimetry parameters for 16 low dose-rate (LDR) ^{125}I and ^{103}Pd sources.[2–4] These critically evaluated consensus datasets used an established methodology and drew upon the strengths of the best papers available at the time. They constituted the AAPM recommendations for clinical dosimetry of these source models. The original data were interpolated or extrapolated into a uniform data format, for example, $g(r)$ data tabulated from 0.1 cm to 10 cm, with $F(r, \theta)$ and $\phi_{an}(r)$ data typically tabulated from 0.5 cm to 7 cm. Furthermore, background on the source design and rationale for consensus formulation were provided.

2.B. Brachytherapy source registry

The online Registry includes brachytherapy sources that may be used in clinical trials sponsored by the U.S. National Cancer Institute and conducted through the National Clinical Trials Network. Sources listed on the Registry must comply with the dosimetry prerequisites for low-energy sources as established by Williamson et al.,[6] and expanded upon by Rivard et al.,[2] and for high-energy sources as established by Li et al.[11] and expanded upon by Pérez-Calatayud et al.[12] These prerequisites call for published reference-quality measurements and Monte Carlo (MC) calculation of 2D single-source dose-rate distributions. Furthermore, they require the source manufacturer to have in place a robust calibration program with intercomparisons to the U.S. National Institute of Standards and Technology (NIST). The Registry is open to all types of brachytherapy sources, including high-energy photon-emitting brachytherapy sources.[12] For each source posted on the Registry, a brief description is included as well as links to the manufacturer, distributor(s), and dosimetry data publications used to qualify the source for Registry posting. The posting of a specific source model on the Registry does not imply existence of a societal consensus dataset. Clinical use of data from peer-reviewed scientific publications as posted on the Registry represents a reasonable choice for medical physicists, the source vendor, and clinical trial investigators for implementing newly marketed brachytherapy sources. When societal consensus datasets become available for specific source models, they also are posted on the Registry. Caution should be taken for the general clinical use (e.g., outside of a clinical protocol) of brachytherapy sources not posted on the Registry. Source manufacturers are encouraged to follow the procedures outlined on the Registry.

2.C. GEC-ESTRO datasets

The BRAchytherapyPHYsics Quality Assurance System (BRAPHYQS) working group of GEC-ESTRO manages an online database for brachytherapy dosimetry parameters and other related brachytherapy data.[13] To promote uniformity of clinical practice, GEC-ESTRO recommends TG-43 datasets for brachytherapy sources as follows:

> Category 1: Sources included in the Registry with AAPM or AAPM + GEC-ESTRO consensus datasets.[2–5,12]
>
> While the GEC-ESTRO methods used to recommend datasets are not yet formalized, datasets for these sources have historically been those recommended by the AAPM or jointly with the AAPM and GEC-ESTRO.
>
> Category 2: Sources not included in the Registry, but commercially available or commercially unavailable but still in clinical use.
>
> Datasets from any published papers in peer-review journals are examined, and a single dataset from one of the papers is selected without any data manipulation. Commercially unavailable sources are considered orphaned sources, which include certain models of ^{137}Cs and ^{60}Co sources.[12]

In addition, a table in Cartesian coordinates has been added to each source dataset for demonstrating consistency with its TG-43 data for quality assurance (QA) purposes. The GEC-ESTRO website posts available datasets in spreadsheet format for convenience of use. Currently, the GEC-ESTRO BRAPHYQS website is updated more frequently than the Registry and TPS vendor software releases. In the absence of AAPM-issued consensus datasets for any brachytherapy source, clinical users should verify the provenance of datasets posted on the ESTRO website, and ensure that the AAPM brachytherapy dosimetry prerequisites are satisfied.[2,6,7]

2.D. Carleton laboratory for radiotherapy physics

Another online venue for brachytherapy dosimetry parameter data is the Carleton University website.[14] Data for this evolving website was prepared in part by Taylor and Rogers,[15,16] and includes results of MC studies for ^{125}I, ^{103}Pd, ^{192}Ir, and ^{169}Yb sources. Key differences between this website and the other two venues are that the data were produced by a single research team and were derived with a single MC

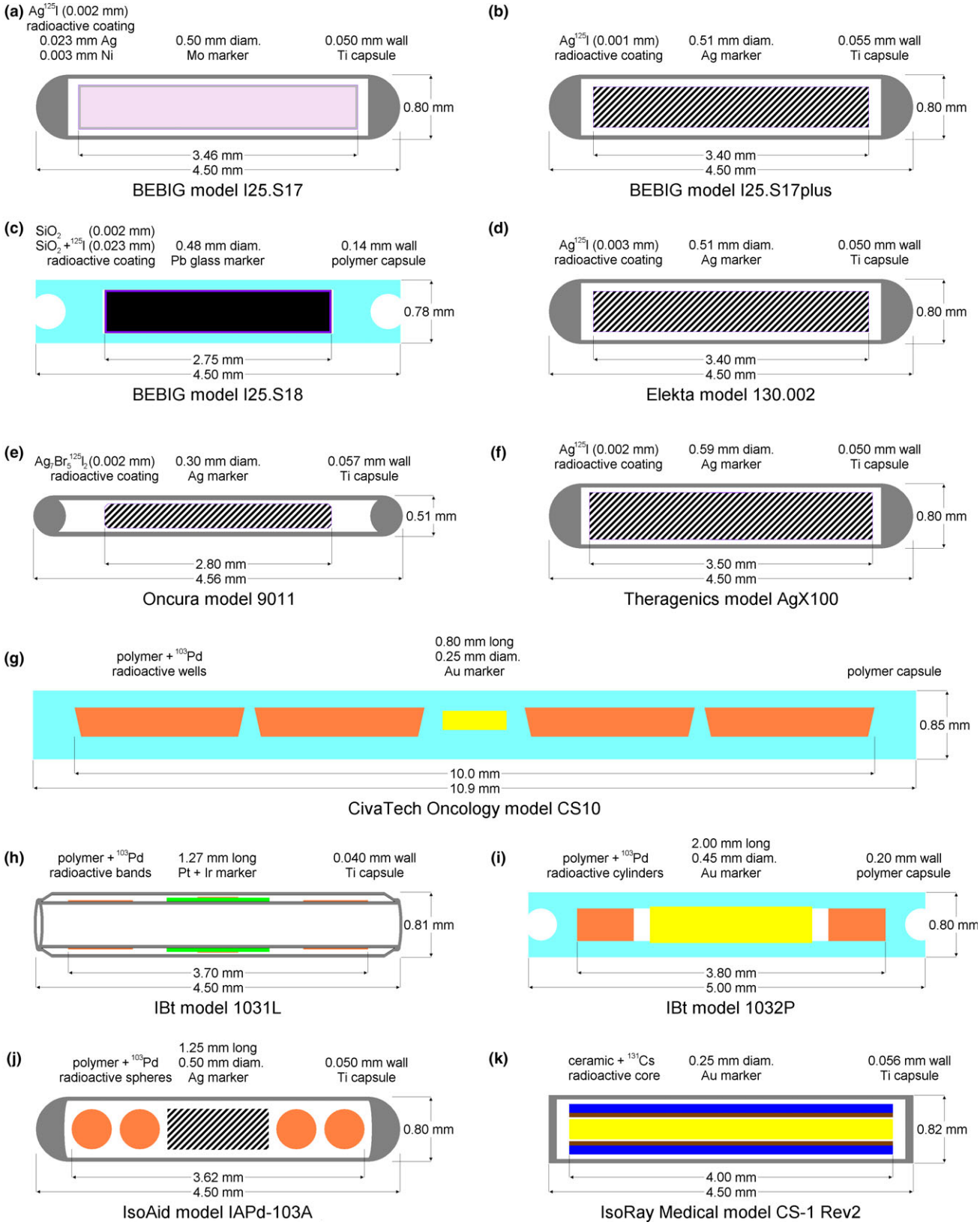

FIG. 1. Low-energy photon-emitting brachytherapy sources examined in the current report include: (a) BEBIG model I25.S17, (b) BEBIG model I25.S17plus, (c) BEBIG model I25.S18, (d) Elekta model 130.002, (e) Oncura model 9011, (f) Theragenics model AgX100, (g) CivaTech Oncology model CS10, (h) IBt model 1031L, (i) IBt model 1032P, (j) IsoAid model IAPd-103A, and (k) IsoRay Medical model CS-1 Rev2. A description of the design for each source model is included within the respective subsection of the Appendix. There is common color coding among the sources where gray is used for Ti, diagonal line pattern for Ag, black for Pb, pink for Mo, light blue for polymer, green for Pt(90% mass) + Ir(10% mass), yellow for Au, brown for quartz (SiO_2), purple for an ^{125}I compound, orange for a ^{103}Pd compound, and dark blue for a ^{131}Cs compound.

TABLE I. Transverse plane dose rates (cGy h^{-1} U^{-1}) as a function of distance for the 11 brachytherapy sources included in the current report. The 1D formalism of Eq. (10) from the 2004 AAPM TG-43U1 was used for all sources except the CivaTech model CS10 ^{103}Pd source, which used the 2D dose calculation formalism.

r (cm)	BEBIG S17	BEBIG S17plus	BEBIG S18	Elekta 130.002	Oncura 9011	Theragenics AgX100	CivaTech CS10	IBt 1031L	IBt 1032P	IsoAid IAPd-103A	IsoRay CS-1 Rev2
0.10	68.8	71.1	71.2	76.8	100.3	72.4	19.184	42.9	31.0	45.9	70.6
0.15	43.6	39.6	36.8	41.5	48.5	46.4	13.73	42.0	36.5	39.4	46.0
0.25	16.52	16.96	14.57	16.46	15.52	16.96	7.74	16.61	18.00	15.05	17.47
0.50	3.84	3.90	3.71	3.86	3.71	3.91	2.68	3.35	3.55	3.09	4.13
0.75	1.648	1.671	1.614	1.657	1.599	1.679	1.218	1.302	1.372	1.204	1.830
1.00	0.891	0.904	0.882	0.896	0.867	0.908	0.641	0.643	0.675	0.595	1.020
1.50	0.362	0.366	0.366	0.363	0.351	0.367	0.228	0.219	0.229	0.201	0.437
2.00	0.1820	0.1846	0.1885	0.1828	0.1772	0.1856	0.0982	0.0917	0.0955	0.0848	0.233
3.00	0.0631	0.0640	0.0678	0.0634	0.0614	0.0644	0.0244	0.0225	0.0232	0.0207	0.0887
4.00	0.0271	0.0274	0.0298	0.0272	0.0263	0.0276	0.00742	0.00686	0.00701	0.00633	0.0413
5.00	0.01299	0.01319	0.01489	0.01308	0.01261	0.01324	0.00255	0.00238	0.00239	0.00218	0.0214
6.00	0.00669	0.00682	0.00777	0.00675	0.00651	0.00686	0.000950	0.000872	0.000891	0.000816	0.01178
7.00	0.00364	0.00371	0.00424	0.00368	0.00354	0.00373	0.000378	0.000353	0.000355	0.000329	0.00679
8.00	0.00206	0.00210	0.00238	0.00207	0.00199	0.00211	0.0001588	0.0001523	0.0001472	0.0001410	0.00404
9.00	0.001190	0.001217	0.001367	0.001202	0.001163	0.001228	0.0000696	0.0000715	0.0000647	0.0000641	0.00246
10.00	0.000709	0.000722	0.000878	0.000713	0.000693	0.000727	0.0000327	0.0000354	0.0000305	0.0000314	0.001529

radiation transport code (BrachyDose™) developed by Taylor et al.[17] Compared to results from most other dosimetry investigators, these online datasets generally have higher spatial resolution and include tabulated dose rates very close to the source capsule. The majority of consensus datasets included in this report (see the Appendix) have as their origin the Carleton University website with results based on the methods of Taylor and Rogers.[15,16]

In addition to the TG-43 dosimetry parameters, dose-rate contributions are presented separately for primary, single-scattered, and multiple-scattered photons for high-energy sources. This method follows the formalism by Russell et al.[18] that could be used in convolution/superposition methods[19] to calculate dose distributions around brachytherapy sources in heterogeneous media and under bounded conditions.

3. AGREEMENT ON CONSENSUS DATASETS FOR CLINICAL IMPLEMENTATION

The methodology described in Section IV of the 2004 AAPM TG-43U1 report[2] was used to prepare the consensus datasets in the current report (i.e., TG-43U1S2). The AAPM+GEC-ESTRO consensus datasets for the sources included in the current report are provided in Tables AI–AXIV of the Appendix. For QA purposes, dose-rate distributions per unit source strength (i.e., U) are presented in Table I, calculated using the 1D dose calculation formalism as similar to the 2004 and 2007 AAPM reports.[2,4] Additional data for QA purposes are included in Tables II–XII in the polar coordinate system and in Tables XIII–XXIII in an along-away format having a consistent grid, where "along" is the distance along the source long axis and "away" is the distance away from the source axis of symmetry. The Appendix also contains descriptions of each source and provides details regarding how consensus datasets were obtained. Dosimetry investigators for a given source model were contacted directly if details required for the appraisal of their data were omitted from the salient publications. Consensus data in boldface indicate that values are interpolated[4] so that datasets for all sources share a common mesh; data are *italicized* if they were acquired from a candidate dataset differing from the principal dataset; and extrapolated data are underlined. In some instances, datasets are thinned to minimize high-resolution values at large distances while maintaining interpolation errors $\leq 2\%$ for the purposes of calculating dose-rate distributions. For brevity, the values of unity for $F(r, \theta = 90°)$ are not shown. To keep bilinear interpolation errors $\leq 2\%$, the radial and angular resolution of $F(r, \theta)$ data may vary across source models. Consensus dosimetry parameters are defined as having subscript '$_{CON}$' preceding the variable.

Since publication of the TG-43U1S1 report, a multisocietal report (TG-138)[20] has become available to provide recommendations on the evaluation of uncertainties associated with calculating single-source dose distributions. It was reported that source calibrations for individual, low-energy photon-emitting brachytherapy sources have a standard uncertainty of 1.3% when measured in a clinic with NIST-traceable calibrations. The standard uncertainties for measured (EXP) and MC-estimated values of the dose-rate constant Λ were reported in TG-138 as 2.9% and 2.1%, respectively. In the current report, consensus values for measured and MC-estimated values of Λ are given, along with evaluation of their uncertainties. The TG-138 report also includes evaluation of uncertainties for other brachytherapy dosimetry parameters and for the dose determination in a TPS using the TG-43 dose calculation formalism. At the reference position of 1 cm on the source transverse plane, the TG-138 reports an uncertainty of 4.4% for calculating dose from low-energy brachytherapy sources. Medical physicists are encouraged to consider the magnitude of

TABLE II. Dose rates (cGy h^{-1} U^{-1}) per unit source strength for the BEBIG model S17 ^{125}I source using the 2D formalism of Eq. (1) from the 2004 AAPM TG-43U1 report.

	r (cm)									
Polar angle θ (°)	0.10	0.25	0.50	0.75	1	2	3	5	7.5	10
0		6.26	0.977	0.471	0.286	0.0772	0.0310	0.00737	0.001744	0.000476
2		6.30	0.981	0.491	0.321	0.0930	0.0373	0.00858	0.001909	0.000513
5		6.77	1.543	0.731	0.418	0.1004	0.0378	0.00857	0.001923	0.000518
7		8.40	1.691	0.760	0.438	0.1046	0.0394	0.00887	0.001960	0.000525
10		12.85	1.945	0.868	0.494	0.1144	0.0424	0.00936	0.00206	0.000551
15		17.41	2.51	1.074	0.594	0.1305	0.0472	0.01017	0.00221	0.000581
20		20.5	2.99	1.244	0.676	0.1438	0.0511	0.01089	0.00233	0.000618
25		21.7	3.34	1.376	0.741	0.1541	0.0544	0.01144	0.00243	0.000632
30	157.2	21.7	3.60	1.478	0.792	0.1629	0.0571	0.01185	0.00251	0.000657
40	108.0	19.63	3.93	1.621	0.868	0.1756	0.0609	0.01258	0.00264	0.000693
50	85.3	16.59	4.11	1.713	0.917	0.1845	0.0638	0.01310	0.00274	0.000710
60	72.9	15.66	4.15	1.773	0.951	0.1909	0.0656	0.01339	0.00281	0.000731
70	65.9	15.01	3.94	1.785	0.967	0.1954	0.0672	0.01370	0.00286	0.000736
80	62.2	14.63	3.91	1.712	0.935	0.1964	0.0677	0.01388	0.00291	0.000751
90	61.1	14.51	3.91	1.716	0.933	0.1905	0.0664	0.01362	0.00284	0.000737

TABLE III. Dose rates (cGy h^{-1} U^{-1}) per unit source strength for the BEBIG model S17plus ^{125}I source using the 2D formalism of Eq. (1) from the 2004 AAPM TG-43U1 report.

	r (cm)									
Polar angle θ (°)	0.25	0.50	0.75	1	1.5	2	3	5	7	10
0	6.72	0.964	0.473	0.281	0.1351	0.0779	0.0315	0.00769	0.00234	0.000522
2	6.75	0.981	0.509	0.337	0.1747	0.0990	0.0385	0.00892	0.00260	0.000535
5	7.51	1.699	0.790	0.445	0.1944	0.1039	0.0389	0.00879	0.00261	0.000530
7	14.98	2.04	0.896	0.504	0.219	0.1157	0.0428	0.00943	0.00277	0.000557
10	19.43	2.60	1.097	0.604	0.253	0.1314	0.0476	0.01029	0.00296	0.000591
15	22.4	3.08	1.269	0.686	0.283	0.1450	0.0516	0.01100	0.00314	0.000620
20	23.2	3.45	1.404	0.754	0.306	0.1559	0.0549	0.01156	0.00328	0.000646
25	22.7	3.71	1.508	0.806	0.326	0.1649	0.0576	0.01196	0.00340	0.000666
30	20.1	4.04	1.655	0.882	0.354	0.1781	0.0617	0.01273	0.00359	0.000700
40	16.91	4.20	1.746	0.933	0.373	0.1874	0.0647	0.01328	0.00373	0.000725
50	15.89	4.20	1.798	0.966	0.387	0.1941	0.0668	0.01366	0.00383	0.000744
60	15.16	3.97	1.802	0.977	0.394	0.1983	0.0683	0.01394	0.00391	0.000754
70	14.71	3.94	1.728	0.947	0.394	0.1986	0.0686	0.01403	0.00393	0.000762
80	14.51	3.93	1.726	0.940	0.382	0.1927	0.0669	0.01380	0.00387	0.000752
90	6.72	0.964	0.473	0.281	0.1351	0.0779	0.0315	0.00769	0.00234	0.000522

uncertainties throughout the process of entering dosimetry parameters into a TPS (or checking their accuracy for the case where data are preloaded into the TPS). Methods and examples of how these have been evaluated for the sources included in the current report are given in the Appendix.

4. CONSENSUS DATASET RECOMMENDATIONS FOR CLINICAL USE

Based on the aforementioned online resources (i.e., Registry, ESTRO website, and Carleton University website) for brachytherapy TG-43 dosimetry parameters, the AAPM and GEC-ESTRO recommend that medical physicists use data from the following sources for clinical purposes, in decreasing order of preference:

(a) Societal consensus data such as from the 2004 AAPM TG-43U1 report,[2] the 2007 AAPM TG-43U1S1 report,[4] the 2012 AAPM+GEC-ESTRO report,[12] or the current report (TG-43U1S2).
(b) Data posted on the Registry, where the medical physicist checks for agreement with data in the original publication(s).
(c) If a given source model is not posted on the Registry, this suggests that the AAPM dosimetric practice standards may not have been met. The burden then falls upon the

TABLE IV. Dose rates (cGy h^{-1} U^{-1}) per unit source strength for the BEBIG model S18 ^{125}I source using the 2D formalism of Eq. (1) from the 2004 AAPM TG-43U1 report.

	r (cm)								
Polar angle θ (°)	0.5	1	2	3	4	5	6	7	10
0	1.899	0.586	0.1483	0.0559	0.0256	0.01286	0.00674	0.00378	0.000772
10	3.24	0.774	0.1721	0.0625	0.0277	0.01389	0.00725	0.00398	0.000822
20	3.59	0.844	0.1810	0.0650	0.0288	0.01431	0.00751	0.00409	0.000850
30	3.72	0.868	0.1845	0.0665	0.0293	0.01460	0.00761	0.00416	0.000859
40	3.76	0.876	0.1870	0.0673	0.0296	0.01476	0.00770	0.00418	0.000870
50	3.77	0.890	0.1891	0.0679	0.0299	0.01494	0.00777	0.00426	0.000879
60	3.71	0.891	0.1896	0.0684	0.0301	0.01497	0.00783	0.00427	0.000884
70	3.74	0.895	0.1912	0.0685	0.0302	0.01510	0.00788	0.00429	0.000886
80	3.71	0.894	0.1911	0.0687	0.0302	0.01506	0.00787	0.00430	0.000891
90	3.75	0.893	0.1917	0.0687	0.0302	0.01508	0.00786	0.00431	0.000889

TABLE V. Dose rates (cGy h^{-1} U^{-1}) per unit source strength for the Elekta model 130.002 ^{125}I source using the 2D formalism of Eq. (1) from the 2004 AAPM TG-43U1 report.

	r (cm)									
Polar angle θ (°)	0.1	0.2	0.5	0.7	1	2	3	5	7	10
0			0.954	0.543	0.288	0.0758	0.0312	0.00758	0.00231	0.000479
2			1.006	0.571	0.323	0.0904	0.0360	0.00827	0.00246	0.000498
5			1.547	0.831	0.419	0.0997	0.0377	0.00858	0.00254	0.000510
7			1.717	0.868	0.432	0.1033	0.0387	0.00879	0.00262	0.000516
10			1.931	0.982	0.485	0.1120	0.0418	0.00929	0.00270	0.000540
15			2.46	1.213	0.582	0.1276	0.0463	0.00997	0.00290	0.000576
20		51.9	2.93	1.411	0.663	0.1410	0.0504	0.01071	0.00305	0.000603
25	225	43.9	3.27	1.563	0.729	0.1522	0.0536	0.01130	0.00320	0.000635
30	160.3	37.0	3.54	1.686	0.780	0.1611	0.0564	0.01180	0.00333	0.000654
40	108.9	29.8	3.92	1.871	0.861	0.1746	0.0608	0.01254	0.00355	0.000690
50	85.6	26.3	4.12	1.993	0.919	0.1854	0.0640	0.01314	0.00371	0.000716
60	73.1	24.1	4.15	2.07	0.960	0.1925	0.0664	0.01359	0.00382	0.000737
70	66.2	22.6	4.00	2.07	0.974	0.1976	0.0680	0.01392	0.00388	0.000751
80	62.5	21.8	4.00	2.02	0.954	0.1981	0.0683	0.01396	0.00392	0.000753
90	61.4	21.6	4.00	2.03	0.954	0.1940	0.0670	0.01374	0.00386	0.000747

user to perform an analysis, similar to the procedure described herein, to ensure that source calibrations are NIST-traceable within an acceptable level of accuracy[20] and that available published and unpublished dosimetry data exhibit an acceptable level of rigor and redundancy to safely treat patients. Early adopters of a new source should work closely with the vendor, the vendor's dosimetry consultant, and the TPS vendor to ensure that the conditions outlined in the relevant AAPM recommendations are met.[2,7,11,12] Coordinated action by the medical community using a particular source model, rather than isolated and possibly inconsistent analyses by individuals, is preferred to maximize uniformity of dosimetric practice. For a product with a track record of use for which the vendor Registry application (e.g., a source approved in Europe, but new to North America) has not yet been accepted, users should consider following GEC-ESTRO recommendations and cooperate with the vendor to assure calibration traceability to a primary standard.[21] If available, datasets on the ESTRO or Carleton University websites may also be useful.

4.A. Treatment planning system and source vendor dosimetry recommendations

The AAPM and GEC-ESTRO recommend that values for the brachytherapy dosimetry parameters specific to each source model be uniformly adopted by all medical physicists for clinical treatment planning. This approach supports consistency of the worldwide practice of brachytherapy. Depending upon the dose calculation protocol and the values currently used by individual physicists, adoption of these data may result in changes to patient dose calculations. These changes must be carefully evaluated and reviewed with the radiation oncologist preceding implementation of the current protocol. In all instances the medical

TABLE VI. Dose rates (cGy h^{-1} U^{-1}) per unit source strength for the Oncura model 9011 ^{125}I source using the 2D formalism of Eq. (1) from the 2004 AAPM TG-43U1 report.

	r (cm)									
Polar angle θ (°)	0.1	0.25	0.5	0.7	1	2	3	5	7	10
0		3.72	0.871	0.490	0.269	0.0738	0.0296	0.00739	0.00218	0.000432
2		4.02	0.988	0.625	0.348	0.0875	0.0336	0.00768	0.00228	0.000461
5		5.81	1.211	0.649	0.339	0.0857	0.0332	0.00763	0.00229	0.000474
7		6.76	1.324	0.715	0.371	0.0921	0.0351	0.00800	0.00238	0.000487
10		9.98	1.732	0.894	0.445	0.1041	0.0387	0.00864	0.00253	0.000520
15	370	13.84	2.38	1.169	0.559	0.1227	0.0444	0.00961	0.00277	0.000554
20	261	15.81	2.87	1.388	0.652	0.1379	0.0489	0.01035	0.00296	0.000589
25	191.3	16.72	3.20	1.548	0.721	0.1494	0.0525	0.01098	0.00312	0.000617
30	151.9	17.08	3.43	1.663	0.772	0.1585	0.0554	0.01149	0.00325	0.000640
40	110.2	16.93	3.71	1.812	0.842	0.1714	0.0594	0.01221	0.00344	0.000674
50	89.3	16.34	3.85	1.901	0.886	0.1799	0.0621	0.01273	0.00357	0.000699
60	77.5	15.52	3.93	1.956	0.915	0.1856	0.0640	0.01309	0.00367	0.000716
70	70.7	15.13	3.95	1.984	0.931	0.1893	0.0652	0.01331	0.00372	0.000724
80	67.2	14.89	3.92	1.979	0.937	0.1910	0.0658	0.01344	0.00375	0.000731
90	66.1	14.82	3.93	1.981	0.933	0.1901	0.0656	0.01341	0.00376	0.000733

TABLE VII. Dose rates (cGy h^{-1} U^{-1}) per unit source strength for the Theragenics model AgX100 ^{125}I source using the 2D formalism of Eq. (1) from the 2004 AAPM TG-43U1 report.

	r (cm)									
Polar angle θ (°)	0.1	0.25	0.5	0.7	1	2	3	5	7	10
0	15.34	2.28	1.228	0.642	0.312	0.1762	0.0707	0.01671	0.00512	0.001086
2	15.69	2.27	1.230	0.696	0.362	0.2071	0.0807	0.01852	0.00557	0.001120
5	16.09	3.31	1.754	0.888	0.400	0.2174	0.0833	0.01896	0.00565	0.001159
7	17.96	3.60	1.865	0.951	0.426	0.2299	0.0869	0.01973	0.00583	0.001195
10	28.8	4.25	2.184	1.086	0.478	0.2546	0.0947	0.02094	0.00614	0.001234
15	40.4	5.61	2.76	1.327	0.561	0.2926	0.1060	0.02285	0.00661	0.001318
20	47.8	6.73	3.24	1.521	0.629	0.3240	0.1152	0.02445	0.00703	0.001393
25	50.3	7.58	3.61	1.676	0.683	0.3490	0.1231	0.02579	0.00737	0.001447
30	50.2	8.18	3.89	1.796	0.727	0.3690	0.1292	0.02690	0.00763	0.001496
40	45.5	8.95	4.29	1.973	0.792	0.3995	0.1386	0.02861	0.00807	0.001574
50	38.1	9.35	4.53	2.088	0.837	0.4209	0.1454	0.02982	0.00840	0.001629
60	35.9	9.51	4.69	2.168	0.869	0.4362	0.1503	0.03068	0.00863	0.001676
70	34.3	8.95	4.71	2.218	0.891	0.4472	0.1538	0.03135	0.00881	0.001699
80	33.3	8.91	4.51	2.136	0.891	0.4496	0.1553	0.03172	0.00888	0.001723
90	33.0	8.91	4.51	2.130	0.864	0.4362	0.1512	0.03106	0.00874	0.001700

physicist should carefully document the origin of the brachytherapy dosimetry parameter data and provide a rationale for why a given dataset and/or website tabulation was chosen. Toward commissioning a new brachytherapy source or an existing source with new data, the physicist should perform TPS phantom tests to evaluate the data and calculated results preceding clinical use.

The TPS vendors for low-energy LDR brachytherapy sources generally include dosimetry parameters in their software for a variety of source models. These data are often the most readily available to medical physicists. TPS vendors may use datasets that consist of unpublished data from dosimetry investigations they have commissioned or sponsored, with these data not having undergone critical review by a sanctioned committee within a professional society. Due to the dynamic market for low-energy LDR sources, TPS vendors may update their software as new publications containing TG-43 dosimetry parameters become available. However, the medical physicist should exercise caution if electing to adopt vendor-supplied dosimetry data since recommendations and selection criteria by the TPS vendor or source model vendor may be unknown or atypical. Furthermore, the interpolation and extrapolation methods used in the TPS should be validated.[4,5] The TPS vendor and source vendor should state whether or not a given source model is on the Registry to facilitate the medical physicist task. In the

TABLE VIII. Dose rates (cGy h^{-1} U^{-1}) per unit source strength for the CivaTech model CS10 ^{103}Pd source using the 2D formalism of Eq. (1) from the 2004 AAPM TG-43U1 report.

	r (cm)									
Polar angle θ (°)	0.1	0.25	0.5	0.75	1	2	3	5	7	10
0				2.63	0.900	0.0923	0.0214	0.00219	0.000341	0.0000243
2				2.69	0.933	0.1000	0.0234	0.00238	0.000356	0.0000309
5				2.84	1.003	0.1081	0.0250	0.00253	0.000372	0.0000334
7			28.1	2.84	1.020	0.1104	0.0256	0.00256	0.000375	0.0000328
10			19.92	2.79	1.023	0.1121	0.0260	0.00261	0.000381	0.0000327
15		48.2	13.18	2.63	1.008	0.1131	0.0263	0.00264	0.000385	0.0000331
20		34.7	9.74	2.44	0.979	0.1129	0.0264	0.00265	0.000386	0.0000332
25		26.7	7.68	2.25	0.944	0.1121	0.0263	0.00265	0.000387	0.0000330
30	53.1	21.5	6.33	2.07	0.905	0.1111	0.0262	0.00265	0.000388	0.0000331
40	37.1	15.20	4.70	1.772	0.827	0.1081	0.0258	0.00263	0.000386	0.0000330
50	28.7	11.76	3.78	1.551	0.760	0.1051	0.0254	0.00261	0.000383	0.0000329
60	23.9	9.74	3.24	1.396	0.708	0.1023	0.0250	0.00258	0.000381	0.0000329
70	21.1	8.55	2.91	1.294	0.670	0.1001	0.0246	0.00256	0.000379	0.0000328
80	19.62	7.94	2.73	1.236	0.648	0.0986	0.0244	0.00255	0.000377	0.0000327
90	19.18	7.74	2.68	1.218	0.641	0.0982	0.0244	0.00255	0.000378	0.0000327

TABLE IX. Dose rates (cGy h^{-1} U^{-1}) per unit source strength for the IBt model 1031L ^{103}Pd source using the 2D formalism of Eq. (1) from the 2004 AAPM TG-43U1 report.

	r (cm)									
Polar angle θ (°)	0.1	0.25	0.5	0.75	1	2	3	5	7.5	10
0		38.0	0.860	0.352	0.206	0.0421	0.01156	0.001382	0.0001454	0.0000255
2		36.5	1.034	0.445	0.257	0.0429	0.01107	0.001256	0.0001345	0.0000235
5		30.4	1.765	0.615	0.306	0.0460	0.01180	0.001331	0.0001383	0.0000246
7		27.8	2.22	0.740	0.348	0.0497	0.01256	0.001399	0.0001448	0.0000247
10		29.8	2.54	0.815	0.381	0.0535	0.01338	0.001473	0.0001511	0.0000263
15		26.5	2.83	0.949	0.443	0.0616	0.01517	0.001648	0.0001650	0.0000276
20		27.0	2.96	1.041	0.496	0.0685	0.01680	0.001792	0.0001793	0.0000284
25	94.6	25.9	3.08	1.097	0.526	0.0736	0.01805	0.001931	0.0001893	0.0000307
30	82.7	23.9	3.19	1.150	0.555	0.0777	0.01897	0.00203	0.0001968	0.0000316
40	58.0	19.77	3.38	1.244	0.604	0.0853	0.0208	0.00222	0.000215	0.0000338
50	47.3	16.59	3.47	1.322	0.648	0.0917	0.0225	0.00237	0.000229	0.0000351
60	41.8	14.46	3.48	1.373	0.680	0.0968	0.0237	0.00249	0.000239	0.0000367
70	39.4	13.17	3.44	1.391	0.695	0.0997	0.0244	0.00258	0.000248	0.0000372
80	38.3	12.45	3.41	1.395	0.701	0.1015	0.0248	0.00262	0.000250	0.0000382
90	37.9	12.19	3.40	1.398	0.701	0.1020	0.0249	0.00265	0.000253	0.0000386

absence of societal consensus datasets, the medical physicist should determine the origin of the vendor-supplied data (by contacting the vendor), evaluate its quality (see Section IV of the 2004 TG-43U1 report) and document its appropriateness for clinical purposes in the physicist's commissioning report.

5. REFERENCE DATA FOR BRACHYTHERAPY DOSIMETRY INVESTIGATIONS

5.A. Radionuclide source spectra

The TG-43U1 report (2004) included source photon spectra for ^{125}I and ^{103}Pd.[2] These were based on spectra recommended on August 12, 2000 by the National Nuclear Data Center (NNDC)[22] of Brookhaven National Laboratory. The spectra recommended by the NNDC are based on scientific publications prepared on a regular basis to formally evaluate the radiation emissions and nuclear energy levels for nuclides having a given atomic mass. These publications are generally in the journal Nuclear Data Sheets, and focus on nuclear energy levels and related gamma rays. However, the NNDC also includes values for radionuclide half-lives and associated x rays (i.e., energies and intensities). Since issuing the TG-43U1 report, new experimental and theoretical spectral evaluations have become available for both ^{125}I and ^{103}Pd, and there is a need to provide data for ^{131}Cs.

TABLE X. Dose rates (cGy h^{-1} U^{-1}) per unit source strength for the IBt model 1032P ^{103}Pd source using the 2D formalism of Eq. (1) from the 2004 AAPM TG-43U1 report.

	r (cm)									
Polar angle θ (°)	0.1	0.25	0.5	0.75	1	2	3	5	7.5	10
0		4.37	4.19	1.292	0.580	0.0743	0.01764	0.001823	0.0001735	0.0000248
2		38.1	4.19	1.294	0.580	0.0743	0.01772	0.001827	0.0001747	0.0000241
5		52.8	4.19	1.294	0.583	0.0751	0.01797	0.001844	0.0001761	0.0000243
7		50.8	4.18	1.303	0.588	0.0762	0.01822	0.001876	0.0001784	0.0000248
10		60.6	4.19	1.321	0.600	0.0782	0.01871	0.001927	0.0001834	0.0000250
15		47.4	4.18	1.348	0.618	0.0816	0.01954	0.00201	0.0001913	0.0000265
20		39.6	4.13	1.372	0.635	0.0849	0.0204	0.00209	0.0001985	0.0000273
25		33.0	4.06	1.389	0.652	0.0881	0.0213	0.00219	0.000207	0.0000281
30	79.0	27.8	3.99	1.406	0.668	0.0912	0.0220	0.00226	0.000214	0.0000289
40	54.3	20.6	3.82	1.417	0.686	0.0951	0.0230	0.00236	0.000224	0.0000301
50	40.3	16.25	3.63	1.405	0.689	0.0972	0.0236	0.00243	0.000228	0.0000306
60	32.1	13.64	3.46	1.382	0.686	0.0981	0.0239	0.00247	0.000232	0.0000313
70	27.5	12.11	3.32	1.358	0.680	0.0981	0.0239	0.00248	0.000235	0.0000313
80	25.2	11.36	3.22	1.339	0.675	0.0977	0.0238	0.00248	0.000233	0.0000318
90	24.4	11.14	3.19	1.329	0.671	0.0975	0.0238	0.00245	0.000231	0.0000315

TABLE XI. Dose rates (cGy h^{-1} U^{-1}) per unit source strength for the IsoAid model IAPd-103A ^{103}Pd source using the 2D formalism of Eq. (1) from the 2004 AAPM TG-43U1 report.

	r (cm)									
Polar angle θ (°)	0.1	0.25	0.5	0.75	1	2	3	5	7.5	10
0		6.85	0.890	0.346	0.1767	0.0285	0.00745	0.000870	0.0000974	0.00001737
2		6.97	0.898	0.349	0.1785	0.0287	0.00755	0.000865	0.0000972	0.00001745
5		7.65	0.936	0.360	0.1834	0.0293	0.00769	0.000884	0.0000979	0.00001750
7		8.47	0.976	0.373	0.1886	0.0300	0.00788	0.000907	0.0000998	0.00001792
10		10.74	1.088	0.405	0.203	0.0320	0.00838	0.000948	0.0001042	0.00001877
15		16.25	1.382	0.498	0.246	0.0377	0.00968	0.001090	0.0001179	0.0000200
20		20.5	1.818	0.636	0.309	0.0456	0.01156	0.001273	0.0001331	0.0000220
25		22.0	2.24	0.786	0.379	0.0544	0.01352	0.001465	0.0001505	0.0000243
30	151.2	21.4	2.59	0.918	0.442	0.0624	0.01537	0.001648	0.0001656	0.0000259
40	85.9	18.44	3.07	1.115	0.538	0.0753	0.01842	0.001947	0.0001924	0.0000289
50	58.4	15.81	3.32	1.257	0.611	0.0856	0.0208	0.00219	0.000214	0.0000317
60	44.6	14.05	3.39	1.333	0.660	0.0933	0.0227	0.00237	0.000231	0.0000334
70	37.4	12.97	3.38	1.366	0.682	0.0974	0.0237	0.00249	0.000240	0.0000338
80	33.7	12.37	3.35	1.369	0.686	0.0990	0.0242	0.00250	0.000245	0.0000350
90	32.5	12.17	3.33	1.372	0.693	0.0994	0.0243	0.00255	0.000245	0.0000353

Rivard et al. examined the sensitivity of such brachytherapy dosimetry parameters as the Λ to the choice of brachytherapy source photon spectrum for ^{125}I, ^{103}Pd, and ^{192}Ir point sources.[23] They observed that the differences in the selected photon spectra did not substantially (< 0.2%) alter kerma or dose deposition as a function of depth, or dosimetry parameters such as Λ. However, differences of about 2% were observed when tracking dose delivery per disintegration, but not in Λ, $g(r)$, or $F(r, \theta)$.

For several ^{125}I and ^{103}Pd brachytherapy seeds, Rodriguez and Rogers[24] similarly examined the influence of selected photon source spectra on Λ and the transmitted spectrum on the seed transverse plane after propagating through the seed capsule, and found that reasonable choices of the photon source spectrum did not substantially alter Λ. Comparisons between their MC calculations and measurements by others of transmitted ^{125}I photon spectrum at 31 keV indicated better agreement when using the spectrum in the National Council on Radiation Protection and Measurements (NCRP) Report No. 58 (NCRP 58)[25] in comparison to the ^{125}I spectrum recommended in the TG-43U1 report. Additionally, the transmitted ^{103}Pd photon intensity at 23 keV indicated better agreement when using the NNDC spectrum recommended in 2000 in comparison to the ^{103}Pd spectrum recommended in the 2004 TG-43U1 report. These findings prompted a deeper examination of the utilized spectra. The source photon

TABLE XII. Dose rates (cGy h^{-1} U^{-1}) per unit source strength for the IsoRay model CS-1 Rev2 ^{131}Cs source using the 2D formalism of Eq. (1) from the 2004 AAPM TG-43U1 report.

	r (cm)								
Polar angle θ (°)	0.1	0.25	0.5	1	2	3	5	7	10
0		29.3	4.25	2.04	0.942	0.205	0.0778	0.01874	0.00602
5		31.3	4.08	1.935	0.911	0.206	0.0782	0.01881	0.00596
10		32.8	4.00	1.826	0.836	0.1876	0.0724	0.01777	0.00572
15		31.5	3.67	1.692	0.794	0.1831	0.0714	0.01765	0.00570
20		28.3	3.45	1.650	0.789	0.1846	0.0720	0.01781	0.00575
25		26.6	3.62	1.747	0.836	0.1940	0.0752	0.01848	0.00593
30		25.8	3.86	1.864	0.889	0.204	0.0786	0.01915	0.00613
40	185.4	24.0	4.04	1.957	0.932	0.212	0.0813	0.01969	0.00629
50	145.9	22.2	4.15	2.02	0.965	0.219	0.0836	0.0202	0.00643
60	100.2	19.29	4.25	2.11	1.009	0.228	0.0870	0.0209	0.00666
70	79.3	17.24	4.25	2.14	1.034	0.234	0.0892	0.0214	0.00682
80	67.9	15.85	4.20	2.15	1.048	0.238	0.0907	0.0218	0.00692
90	61.3	14.95	4.14	2.15	1.054	0.241	0.0917	0.0220	0.00700

TABLE XIII. Dose rates (cGy h^{-1} U^{-1}) per unit source strength for the BEBIG model S17 ^{125}I source in along-away format.

	Away (cm)									
Along (cm)	0	0.5	1	1.5	2	3	4	5	6	7
0.0		3.906	0.933	0.379	0.1905	0.0664	0.0285	0.01362	0.00700	0.00380
0.5	0.977	1.896	0.747	0.344	0.1816	0.0651	0.0282	0.01353	0.00698	0.00380
1.0	0.286	0.592	0.410	0.243	0.1449	0.0579	0.0263	0.01294	0.00677	0.00371
1.5	0.1340	0.239	0.215	0.1553	0.1052	0.0480	0.0232	0.01181	0.00632	0.00353
2.0	0.0772	0.1184	0.1187	0.0971	0.0732	0.0381	0.01971	0.01047	0.00575	0.00326
2.5	0.0470	0.0658	0.0696	0.0621	0.0502	0.0295	0.01628	0.00904	0.00513	0.00297
3.0	0.0310	0.0403	0.0431	0.0403	0.0345	0.0222	0.01319	0.00766	0.00449	0.00265
3.5	0.0207	0.0258	0.0278	0.0269	0.0240	0.01660	0.01050	0.00638	0.00387	0.00234
4.0	0.01434	0.01736	0.01858	0.01831	0.01678	0.01235	0.00824	0.00526	0.00328	0.00204
4.5	0.01016	0.01201	0.01273	0.01271	0.01193	0.00918	0.00643	0.00427	0.00276	0.001757
5.0	0.00737	0.00853	0.00895	0.00897	0.00854	0.00686	0.00500	0.00345	0.00230	0.001496
5.5	0.00538	0.00611	0.00638	0.00643	0.00621	0.00515	0.00388	0.00276	0.001892	0.001264
6.0	0.00399	0.00448	0.00463	0.00468	0.00455	0.00388	0.00302	0.00221	0.001551	0.001061
6.5	0.00300	0.00333	0.00340	0.00345	0.00337	0.00294	0.00235	0.001761	0.001268	0.000886
7.0	0.00228	0.00251	0.00254	0.00257	0.00253	0.00224	0.001828	0.001400	0.001035	0.000738

spectra in NCRP 58 were prepared in 1984. All K_β transition x rays were grouped into a single value in NCRP 58, while the source spectra in the TG-43U1 report did not include $K_{\beta4}$ and $K_{\beta5}$ transition x rays. Adding the $K_{\beta4}$ and $K_{\beta5}$ transition x rays to the ^{125}I and ^{103}Pd spectra in the TG-43U1 report, the relative intensities of the 31 keV and 23 keV x rays both increased by 3%.

So what should be the reference disintegration spectra data for radionuclides used in low-energy photon-emitting sources? The NNDC website comprehensively presents gamma-ray energies and intensities for numerous radionuclides, but it is currently missing some of the lower intensity x rays. The NIST website[26] on x-ray transitions includes most possible transitions for all elements and has high accuracy for the reported energies, but does not include the x-ray intensities. Other websites such as that developed by the Department of Physics, Lund University, Sweden and the Lawrence Berkeley National Laboratory (Berkeley, CA, USA) appear to comprehensively include gamma rays and x rays (and half-lives) associated with a given radionuclide.[27] However, the Lund reference data were last updated on February 28, 1999. Yet another website recommending reference data is from the Laboratoire National Henri Becquerel (LNHB)[28] in Saclay, France, which provides an assortment of pertinent data such as radionuclide half-lives, nuclear disintegration processes, and gamma- and x-ray energies and their intensities. While the LNHB website is updated every few years (most

TABLE XIV. Dose rates (cGy h^{-1} U^{-1}) per unit source strength for the BEBIG model S17plus ^{125}I source in along-away format.

	Away (cm)									
Along (cm)	0	0.5	1	1.5	2	3	4	5	6	7
0.0		3.925	0.940	0.382	0.1927	0.0669	0.0286	0.01380	0.00711	0.00387
0.5	0.964	1.935	0.758	0.349	0.1839	0.0659	0.0283	0.01369	0.00707	0.00385
1.0	0.281	0.602	0.416	0.247	0.1473	0.0588	0.0265	0.01309	0.00685	0.00376
1.5	0.1351	0.243	0.218	0.1576	0.1068	0.0488	0.0235	0.01200	0.00642	0.00357
2.0	0.0779	0.1194	0.1200	0.0984	0.0742	0.0386	0.0200	0.01067	0.00587	0.00332
2.5	0.0477	0.0664	0.0702	0.0627	0.0508	0.0297	0.01655	0.00923	0.00524	0.00303
3.0	0.0315	0.0408	0.0435	0.0406	0.0347	0.0224	0.01339	0.00782	0.00459	0.00271
3.5	0.0211	0.0261	0.0280	0.0270	0.0241	0.01676	0.01065	0.00651	0.00395	0.00239
4.0	0.01469	0.01746	0.01866	0.01840	0.01688	0.01249	0.00836	0.00535	0.00335	0.00208
4.5	0.01050	0.01216	0.01282	0.01282	0.01204	0.00928	0.00654	0.00435	0.00281	0.001796
5.0	0.00769	0.00870	0.00903	0.00907	0.00864	0.00694	0.00509	0.00351	0.00233	0.001533
5.5	0.00559	0.00627	0.00645	0.00651	0.00628	0.00522	0.00395	0.00281	0.001926	0.001299
6.0	0.00414	0.00461	0.00469	0.00473	0.00460	0.00394	0.00307	0.00225	0.001584	0.001089
6.5	0.00310	0.00343	0.00347	0.00349	0.00341	0.00299	0.00238	0.001791	0.001298	0.000906
7.0	0.00234	0.00258	0.00259	0.00260	0.00255	0.00227	0.001851	0.001429	0.001056	0.000750

TABLE XV. Dose rates (cGy h^{-1} U^{-1}) per unit source strength for the BEBIG model S18 ^{125}I source in along-away format.

	Away (cm)									
Along (cm)	0	0.5	1	1.5	2	3	4	5	6	7
0.0		3.75	0.893	0.371	0.1917	0.0687	0.0302	0.01508	0.00786	0.00431
0.5	1.899	1.824	0.702	0.329	0.1775	0.0662	0.0295	0.01481	0.00776	0.00426
1.0	0.586	0.675	0.415	0.241	0.1448	0.0593	0.0276	0.01408	0.00748	0.00412
1.5	0.264	0.307	0.236	0.1629	0.1090	0.0502	0.0248	0.01300	0.00702	0.00391
2.0	0.1483	0.1633	0.1395	0.1073	0.0789	0.0407	0.0214	0.01164	0.00643	0.00364
2.5	0.0874	0.0953	0.0865	0.0718	0.0561	0.0321	0.01806	0.01016	0.00577	0.00332
3.0	0.0559	0.0598	0.0559	0.0484	0.0399	0.0249	0.01495	0.00869	0.00508	0.00299
3.5	0.0370	0.0389	0.0373	0.0335	0.0286	0.01915	0.01205	0.00731	0.00441	0.00265
4.0	0.0256	0.0265	0.0257	0.0236	0.0207	0.01471	0.00960	0.00607	0.00377	0.00231
4.5	0.01791	0.01848	0.01813	0.01689	0.01516	0.01115	0.00761	0.00498	0.00318	0.00200
5.0	0.01286	0.01322	0.01304	0.01222	0.01111	0.00847	0.00598	0.00405	0.00266	0.001707
5.5	0.00923	0.00947	0.00940	0.00891	0.00823	0.00644	0.00469	0.00326	0.00220	0.001447
6.0	0.00674	0.00689	0.00686	0.00656	0.00610	0.00491	0.00368	0.00261	0.001805	0.001240
6.5	0.00502	0.00510	0.00506	0.00487	0.00456	0.00375	0.00288	0.00209	0.001476	0.001066
7.0	0.00378	0.00382	0.00378	0.00364	0.00343	0.00287	0.00225	0.001672	0.001226	0.000914

recently March 24, 2014) and includes photons from ^{125}I, it does not include ^{103}Pd or ^{131}Cs. Based on review of the available references, at this time there is no single, ideal reference for brachytherapy photon spectra. Therefore, it is recommended that source photon spectrum be selected to achieve a combination of accuracy and thoroughness appropriate to the task at hand and the radionuclide being simulated. While not substantial for the accuracy of low-energy brachytherapy source dosimetry, choice of the photon spectrum could improve the accuracy for other investigations such as comparisons of MC results to spectroscopic measurements[29] for the validation of the MC source model.[24] As an example, Table XXIV has been prepared for ^{131}Cs as this has not been included in prior reports containing consensus brachytherapy dosimetry parameters. The x-ray photon energies were taken from the NIST website and the x-ray intensities were taken from the Lund website. In this example, the approach for low-energy photon-emitting sources differs from that recommended for high-energy photon-emitting brachytherapy dosimetry in the AAPM Report #229 (Section 5.B.1)[12] due to typically the greater importance of x rays for low-energy sources and the greater importance of gamma rays for high-energy sources.

5.B. Radionuclide half-lives

In addition to source spectra emitted by radionuclides used in brachytherapy, the TG-43U1 report also included

TABLE XVI. Dose rates (cGy h^{-1} U^{-1}) per unit source strength for the Elekta model 130.002 ^{125}I source in along-away format.

	Away (cm)									
Along (cm)	0	0.5	1	1.5	2	3	4	5	6	7
0.0		4.004	0.954	0.387	0.1940	0.0670	0.0287	0.01374	0.00709	0.00386
0.5	0.954	1.889	0.754	0.348	0.1834	0.0656	0.0283	0.01363	0.00705	0.00384
1.0	0.288	0.583	0.410	0.245	0.1464	0.0586	0.0265	0.01303	0.00684	0.00375
1.5	0.1332	0.234	0.213	0.1552	0.1058	0.0486	0.0235	0.01197	0.00640	0.00356
2.0	0.0758	0.1159	0.1173	0.0965	0.0732	0.0384	0.0200	0.01065	0.00584	0.00330
2.5	0.0468	0.0646	0.0685	0.0614	0.0500	0.0296	0.01647	0.00919	0.00521	0.00301
3.0	0.0312	0.0398	0.0424	0.0397	0.0342	0.0222	0.01328	0.00778	0.00456	0.00269
3.5	0.0209	0.0255	0.0273	0.0264	0.0238	0.01655	0.01054	0.00647	0.00394	0.00238
4.0	0.01459	0.01711	0.01822	0.01800	0.01658	0.01231	0.00827	0.00531	0.00333	0.00207
4.5	0.01040	0.01191	0.01254	0.01248	0.01177	0.00915	0.00647	0.00432	0.00279	0.001779
5.0	0.00758	0.00851	0.00886	0.00881	0.00842	0.00683	0.00503	0.00348	0.00232	0.001514
5.5	0.00552	0.00613	0.00633	0.00633	0.00610	0.00512	0.00389	0.00279	0.001908	0.001278
6.0	0.00408	0.00448	0.00461	0.00462	0.00447	0.00385	0.00301	0.00222	0.001562	0.001072
6.5	0.00305	0.00332	0.00340	0.00341	0.00332	0.00291	0.00233	0.001764	0.001274	0.000892
7.0	0.00231	0.00249	0.00255	0.00254	0.00249	0.00221	0.001814	0.001400	0.001036	0.000740

TABLE XVII. Dose rates (cGy h^{-1} U^{-1}) per unit source strength for the Oncura model 9011 ^{125}I source in along-away format.

	Away (cm)									
Along (cm)	0	0.5	1	1.5	2	3	4	5	6	7
0.0		3.927	0.933	0.378	0.1901	0.0656	0.0280	0.01341	0.00691	0.00376
0.5	0.878	1.815	0.720	0.333	0.1763	0.0633	0.0274	0.01319	0.00682	0.00372
1.0	0.271	0.577	0.399	0.236	0.1408	0.0562	0.0254	0.01252	0.00656	0.00360
1.5	0.1275	0.228	0.210	0.1514	0.1024	0.0467	0.0225	0.01147	0.00614	0.00341
2.0	0.0736	0.1108	0.1152	0.0947	0.0713	0.0371	0.01917	0.01020	0.00561	0.00317
2.5	0.0450	0.0606	0.0668	0.0602	0.0489	0.0286	0.01586	0.00883	0.00500	0.00289
3.0	0.0297	0.0367	0.0410	0.0389	0.0334	0.0215	0.01284	0.00749	0.00438	0.00259
3.5	0.01992	0.0233	0.0262	0.0257	0.0232	0.01612	0.01021	0.00624	0.00378	0.00229
4.0	0.01389	0.01553	0.01738	0.01741	0.01613	0.01200	0.00802	0.00513	0.00321	0.001994
4.5	0.00991	0.01074	0.01186	0.01205	0.01142	0.00891	0.00627	0.00417	0.00269	0.001717
5.0	0.00723	0.00765	0.00831	0.00849	0.00816	0.00666	0.00488	0.00336	0.00224	0.001464
5.5	0.00526	0.00548	0.00591	0.00608	0.00592	0.00499	0.00378	0.00269	0.001845	0.001239
6.0	0.00389	0.00403	0.00428	0.00440	0.00432	0.00375	0.00293	0.00215	0.001512	0.001041
6.5	0.00291	0.00300	0.00314	0.00323	0.00320	0.00283	0.00227	0.001710	0.001236	0.000868
7.0	0.00220	0.00226	0.00234	0.00240	0.00238	0.00215	0.001768	0.001361	0.001006	0.000721

recommendations for half-life values. Examining the aforementioned references, there typically was good agreement in the reported values for radionuclide half-life. For ^{125}I, ^{103}Pd, and ^{131}Cs, these were 59.407(10) days, 16.991(34) days, and 9.689(1) days, respectively, with variations between evaluations of less than 0.4%, 0.2%, and 0.01%, respectively. For the reasons outlined above for reference photon spectra, the AAPM and GEC-ESTRO recommend the NNDC website[22] as the reference for brachytherapy radionuclide half-life values. This recommendation for low-energy photon-emitting sources is consistent with the corresponding recommendation made in the AAPM Report #229 (Section 5.B.1) on high-energy photon-emitting brachytherapy dosimetry.[12]

5.C. Reference dose scoring media

The TG-43U1 report made recommendations for the composition and mass density of air and water. While the composition of air at various levels of humidity was included, only dry air (0% humidity) should be used for determinations of air-kerma strength. The composition (by percentage mass) of dry air is 75.527% N, 23.178% O, 1.283% Ar, and 0.012% C. The mass density of dry air is a function of temperature and pressure. At 22 °C and 101.325 kPa as used in North America, the mass density for dry air is 1.197 mg/cm^3.[30] Correcting for a standard temperature of 20 °C as used in Europe, the mass density of dry air at 101.325 kPa is 1.205 mg/cm^3.

TABLE XVIII. Dose rates (cGy h^{-1} U^{-1}) per unit source strength for the Theragenics model AgX100 ^{125}I source in along-away format.

	Away (cm)									
Along (cm)	0	0.5	1	1.5	2	3	4	5	6	7
0.0		3.981	0.952	0.386	0.1950	0.0676	0.0290	0.01388	0.00718	0.00390
0.5	1.018	1.928	0.763	0.352	0.1858	0.0667	0.0287	0.01381	0.00715	0.00389
1.0	0.287	0.599	0.417	0.248	0.1481	0.0593	0.0268	0.01322	0.00694	0.00380
1.5	0.1393	0.241	0.218	0.1581	0.1073	0.0491	0.0237	0.01209	0.00649	0.00361
2.0	0.0788	0.1185	0.1202	0.0986	0.0745	0.0389	0.0201	0.01074	0.00592	0.00335
2.5	0.0480	0.0657	0.0702	0.0628	0.0510	0.0300	0.01664	0.00929	0.00528	0.00306
3.0	0.0316	0.0402	0.0434	0.0407	0.0349	0.0225	0.01345	0.00788	0.00462	0.00274
3.5	0.0210	0.0256	0.0279	0.0270	0.0242	0.01686	0.01070	0.00656	0.00398	0.00242
4.0	0.01455	0.01717	0.01860	0.01837	0.01693	0.01255	0.00841	0.00539	0.00338	0.00211
4.5	0.01030	0.01189	0.01274	0.01275	0.01200	0.00934	0.00658	0.00438	0.00283	0.001811
5.0	0.00747	0.00845	0.00897	0.00902	0.00861	0.00699	0.00512	0.00353	0.00236	0.001542
5.5	0.00545	0.00607	0.00640	0.00648	0.00627	0.00524	0.00397	0.00283	0.001945	0.001303
6.0	0.00404	0.00445	0.00465	0.00471	0.00459	0.00395	0.00308	0.00227	0.001593	0.001092
6.5	0.00302	0.00331	0.00343	0.00347	0.00340	0.00300	0.00239	0.001803	0.001300	0.000909
7.0	0.00229	0.00249	0.00255	0.00258	0.00255	0.00228	0.001865	0.001433	0.001058	0.000754

TABLE XIX. Dose rates (cGy h^{-1} U^{-1}) per unit source strength for the CivaTech model CS10 ^{103}Pd source in along-away format.

	Away (cm)									
Along (cm)	0	0.5	1	1.5	2	3	4	5	6	7
0.0		2.678	0.641	0.228	0.0982	0.0244	0.00742	0.00255	0.000950	0.000378
0.5		1.906	0.524	0.201	0.0901	0.0232	0.00717	0.00248	0.000932	0.000372
1.0	0.900	0.672	0.306	0.1426	0.0705	0.0200	0.00650	0.00231	0.000879	0.000355
1.5	0.245	0.243	0.1539	0.0879	0.0492	0.01598	0.00554	0.00205	0.000800	0.000329
2.0	0.0923	0.1020	0.0767	0.0509	0.0320	0.01193	0.00448	0.001740	0.000703	0.000296
2.5	0.0425	0.0482	0.0397	0.0292	0.0200	0.00851	0.00347	0.001425	0.000598	0.000259
3.0	0.0214	0.0246	0.0214	0.01676	0.01230	0.00587	0.00260	0.001130	0.000495	0.000221
3.5	0.01147	0.01315	0.01186	0.00977	0.00755	0.00396	0.001895	0.000874	0.000399	0.0001850
4.0	0.00642	0.00734	0.00678	0.00578	0.00464	0.00264	0.001355	0.000662	0.000317	0.0001515
4.5	0.00370	0.00421	0.00395	0.00346	0.00287	0.001747	0.000955	0.000492	0.000247	0.0001222
5.0	0.00219	0.00248	0.00236	0.00211	0.001794	0.001154	0.000668	0.000361	0.0001889	0.0000970
5.5	0.001340	0.001495	0.001434	0.001306	0.001133	0.000763	0.000463	0.000263	0.0001429	0.0000759
6.0	0.000836	0.000916	0.000886	0.000817	0.000722	0.000505	0.000321	0.0001899	0.0001073	0.0000592
6.5	0.000531	0.000572	0.000557	0.000518	0.000464	0.000336	0.000222	0.0001365	0.0000798	0.0000460
7.0	0.000341	0.000362	0.000354	0.000332	0.000302	0.000225	0.0001538	0.0000978	0.0000595	0.0000354

The response of a reentrant open to air well-type or thimble ionization chamber to changes in atmospheric pressure does not behave exactly as would be expected for an ideal gas, and the differences can be significant for large changes in pressure. Several papers have examined this issue for both low-energy photon-emitting brachytherapy sources and for kilovoltage x rays.[31,32,33,34,35]

For water, the recommended composition of H_2O and mass density of 0.998 g/cm^3 are unchanged from the TG-43U1 report. The values of brachytherapy dosimetry parameters are generally provided in terms of dose to water in water – the reference medium for brachytherapy dose calculations. The TG-186 report and other authors have discussed the complex issues related to reporting dose to other media, which can be significantly different in low-energy brachytherapy.[8]

5.D. TLD dosimetry corrections

While no single method can be considered ideal for experimental dosimetry of low-energy brachytherapy sources, thermoluminescent dosimeters (TLDs) are the most commonly employed and have been utilized for all sources considered in this report. The energy dependence

TABLE XX. Dose rates (cGy h^{-1} U^{-1}) per unit source strength for the IBt model 1031L ^{103}Pd source in along-away format.

	Away (cm)									
Along (cm)	0	0.5	1	1.5	2	3	4	5	6	7
0.0		3.395	0.701	0.241	0.1020	0.0249	0.00763	0.00265	0.000967	0.000390
0.5	0.860	1.484	0.514	0.204	0.0914	0.0235	0.00733	0.00257	0.000944	0.000382
1.0	0.206	0.399	0.248	0.1310	0.0680	0.01995	0.00657	0.00236	0.000887	0.000364
1.5	0.0844	0.1362	0.1112	0.0732	0.0443	0.01541	0.00551	0.00206	0.000802	0.000336
2.0	0.0421	0.0545	0.0520	0.0393	0.0270	0.01110	0.00436	0.001725	0.000701	0.000301
2.5	0.0212	0.0249	0.0257	0.0213	0.01600	0.00763	0.00330	0.001381	0.000591	0.000264
3.0	0.01156	0.01256	0.01329	0.01184	0.00943	0.00507	0.00241	0.001071	0.000483	0.000223
3.5	0.00646	0.00676	0.00716	0.00669	0.00561	0.00333	0.001705	0.000809	0.000386	0.0001852
4.0	0.00376	0.00381	0.00401	0.00386	0.00338	0.00216	0.001181	0.000605	0.000302	0.0001512
4.5	0.00225	0.00221	0.00232	0.00227	0.00205	0.001384	0.000809	0.000444	0.000234	0.0001224
5.0	0.001382	0.001322	0.001374	0.001357	0.001247	0.000887	0.000557	0.000322	0.0001780	0.0000977
5.5	0.000845	0.000798	0.000826	0.000822	0.000768	0.000577	0.000381	0.000233	0.0001346	0.0000771
6.0	0.000525	0.000492	0.000510	0.000509	0.000484	0.000380	0.000261	0.0001673	0.0001020	0.0000606
6.5	0.000338	0.000315	0.000325	0.000324	0.000311	0.000253	0.0001803	0.0001207	0.0000770	0.0000474
7.0	0.000220	0.000205	0.000211	0.000209	0.000202	0.0001698	0.0001254	0.0000879	0.0000582	0.0000369

TABLE XXI. Dose rates (cGy h^{-1} U^{-1}) per unit source strength for the IBt model 1032P ^{103}Pd source in along-away format.

	Away (cm)									
Along (cm)	0	0.5	1	1.5	2	3	4	5	6	7
0.0		3.19	0.671	0.230	0.0975	0.0238	0.00725	0.00245	0.000911	0.000362
0.5	4.19	1.634	0.514	0.200	0.0888	0.0226	0.00699	0.00241	0.000901	0.000359
1.0	0.580	0.489	0.273	0.1351	0.0682	0.01946	0.00630	0.00224	0.000852	0.000343
1.5	0.1855	0.1755	0.1290	0.0796	0.0462	0.01535	0.00535	0.001981	0.000772	0.000316
2.0	0.0743	0.0733	0.0618	0.0445	0.0291	0.01131	0.00430	0.001683	0.000681	0.000284
2.5	0.0348	0.0347	0.0311	0.0247	0.01774	0.00794	0.00330	0.001371	0.000579	0.000249
3.0	0.01764	0.01766	0.01639	0.01381	0.01064	0.00537	0.00244	0.001079	0.000477	0.000211
3.5	0.00950	0.00949	0.00899	0.00787	0.00639	0.00356	0.001765	0.000827	0.000383	0.0001758
4.0	0.00532	0.00531	0.00509	0.00458	0.00386	0.00233	0.001249	0.000622	0.000300	0.0001435
4.5	0.00308	0.00307	0.00297	0.00270	0.00235	0.001531	0.000867	0.000459	0.000230	0.0001147
5.0	0.001823	0.001809	0.001768	0.001631	0.001447	0.000995	0.000602	0.000333	0.0001749	0.0000904
5.5	0.001109	0.001099	0.001075	0.001004	0.000899	0.000651	0.000413	0.000239	0.0001315	0.0000707
6.0	0.000680	0.000675	0.000662	0.000626	0.000570	0.000428	0.000282	0.0001711	0.0000979	0.0000554
6.5	0.000429	0.000426	0.000418	0.000397	0.000364	0.000281	0.0001921	0.0001217	0.0000728	0.0000432
7.0	0.000272	0.000270	0.000265	0.000252	0.000234	0.0001847	0.0001318	0.0000867	0.0000544	0.0000330

of TLDs has been identified as a significant source of uncertainty in experimental dosimetry of low-energy sources.[2,36,37] In brachytherapy dosimetry, this dependence was traditionally accounted for by the "relative energy response correction" $E(r)$, defined to account also for all phenomena associated with experimental and calibration irradiations in a protocol, such as detector volume averaging and self-attenuation, and the nonliquid water equivalence of employed phantoms.[38]

Since the publication of the 2004 TG-43U1 report[2] and its 2007 supplement,[4] a terminology has been introduced to rigorously describe dosimeter characteristics,[39,40] and important work has been reported on the complexity of using TLD dosimetry for low-energy sources.[41–45] In this terminology,[39,44] $D_{med}(Q)$ is the absorbed dose to the medium $_{med}$ at the point of measurement (normally the detector midpoint) in the absence of the detector for a given radiation quality Q. This is related to the detector measurement for the same radiation quality $M(Q)$ and the absorbed dose calibration coefficient for the detector $N_{D,med}(Q)$ according to:

$$D_{med}(Q) = M(Q)\, N_{D,med}(Q). \tag{1}$$

The inverse of $N_{D,med}(Q)$ is the absorbed dose sensitivity $S_{AD,med}$. Thus, Eq. (1) can be rearranged as:

$$S_{AD,med}(Q) = \frac{M(Q)}{D_{med}(Q)}. \tag{2}$$

TABLE XXII. Dose rates (cGy h^{-1} U^{-1}) per unit source strength for the IsoAid model IAPd-103A ^{103}Pd source in along-away format.

	Away (cm)									
Along (cm)	0	0.5	1	1.5	2	3	4	5	6	7
0.0		3.33	0.693	0.235	0.0994	0.0243	0.00738	0.00255	0.000947	0.000379
0.5	0.890	1.375	0.500	0.1984	0.0892	0.0229	0.00706	0.00246	0.000923	0.000372
1.0	0.1767	0.298	0.226	0.1249	0.0657	0.01939	0.00632	0.00226	0.000866	0.000355
1.5	0.0632	0.0857	0.0926	0.0665	0.0417	0.01481	0.00533	0.00200	0.000784	0.000327
2.0	0.0285	0.0333	0.0397	0.0339	0.0245	0.01047	0.00417	0.001674	0.000685	0.000293
2.5	0.01400	0.01537	0.01813	0.01744	0.01397	0.00704	0.00312	0.001335	0.000575	0.000255
3.0	0.00745	0.00788	0.00897	0.00911	0.00789	0.00457	0.00224	0.001032	0.000469	0.000215
3.5	0.00413	0.00427	0.00469	0.00490	0.00453	0.00293	0.001571	0.000773	0.000373	0.0001779
4.0	0.00239	0.00243	0.00260	0.00273	0.00261	0.001854	0.001076	0.000569	0.000289	0.0001447
4.5	0.001423	0.001436	0.001504	0.001571	0.001538	0.001171	0.000730	0.000412	0.000220	0.0001153
5.0	0.000870	0.000871	0.000895	0.000930	0.000920	0.000743	0.000494	0.000294	0.0001658	0.0000906
5.5	0.000543	0.000540	0.000546	0.000564	0.000561	0.000475	0.000333	0.000209	0.0001235	0.0000704
6.0	0.000344	0.000341	0.000343	0.000352	0.000351	0.000306	0.000225	0.0001487	0.0000917	0.0000548
6.5	0.000223	0.000221	0.000221	0.000224	0.000223	0.0001996	0.0001529	0.0001054	0.0000678	0.0000423
7.0	0.0001462	0.0001446	0.0001441	0.0001455	0.0001450	0.0001319	0.0001050	0.0000752	0.0000504	0.0000325

TABLE XXIII. Dose rates (cGy h^{-1} U^{-1}) per unit source strength for the IsoRay model CS-1 Rev2 ^{131}Cs source in along-away format.

	Away (cm)									
Along (cm)	0	0.5	1	1.5	2	3	4	5	6	7
0.0		4.10	1.056	0.455	0.242	0.0923	0.0429	0.0222	0.01223	0.00705
0.5	4.25	2.08	0.833	0.404	0.225	0.0890	0.0419	0.0218	0.01207	0.00698
1.0	0.942	0.745	0.493	0.298	0.1845	0.0801	0.0392	0.0208	0.01164	0.00677
1.5	0.392	0.334	0.279	0.202	0.1396	0.0681	0.0352	0.01924	0.01096	0.00645
2.0	0.205	0.1794	0.1653	0.1335	0.1017	0.0556	0.0306	0.01734	0.01011	0.00604
2.5	0.1212	0.1070	0.1032	0.0900	0.0731	0.0443	0.0259	0.01527	0.00914	0.00556
3.0	0.0778	0.0694	0.0677	0.0614	0.0524	0.0346	0.0215	0.01320	0.00812	0.00504
3.5	0.0519	0.0469	0.0459	0.0429	0.0380	0.0268	0.01759	0.01123	0.00712	0.00451
4.0	0.0362	0.0329	0.0322	0.0306	0.0277	0.0207	0.01422	0.00943	0.00615	0.00399
4.5	0.0257	0.0237	0.0231	0.0222	0.0205	0.01593	0.01145	0.00785	0.00526	0.00348
5.0	0.01874	0.01745	0.01691	0.01632	0.01527	0.01231	0.00915	0.00649	0.00446	0.00302
5.5	0.01383	0.01294	0.01252	0.01215	0.01151	0.00953	0.00730	0.00532	0.00375	0.00259
6.0	0.01038	0.00978	0.00943	0.00916	0.00873	0.00740	0.00582	0.00436	0.00314	0.00221
6.5	0.00786	0.00745	0.00717	0.00697	0.00668	0.00577	0.00464	0.00355	0.00261	0.00188
7.0	0.00602	0.00574	0.00551	0.00535	0.00514	0.00451	0.00371	0.00288	0.00217	0.00159

Further, $S_{AD,med}(Q)$ can be partitioned into two components as:

$$S_{AD,med}(Q) = \frac{M(Q)}{D_{med}(Q)} = \frac{M(Q)}{\overline{D_{TLD}}(Q)} \frac{\overline{D_{TLD}}(Q)}{D_{med}(Q)} = \frac{1}{k_{bq}(Q)} \frac{1}{f(Q)}, \quad (3)$$

where $\overline{D_{TLD}}(Q)$ is the average absorbed dose in TLD for a given radiation quality Q, $k_{bq}(Q)$ is the intrinsic energy dependence, which is associated with the signal formation process of the dosimeter and its dependence on the linear energy transfer of the radiation,[36,41,46–49] and it can only be determined experimentally if one uses MC or other techniques to calculate $f(Q)$ and thereby extract $k_{bq}(Q)$ from the measured value of $S_{AD,med}(Q)$, and $f(Q)$ is the absorbed dose energy dependence, which depends on medium and TLD cross-sections, TLD self-attenuation and volume averaging, and can be estimated using MC simulation techniques.

In view of the different experimental (Q) and calibration (Q_0) radiation qualities employed in the dosimetry of brachytherapy sources using TLDs, the measured signal is corrected using the relative absorbed dose sensitivity[44] as

$$S^{rel}_{AD,med} = \frac{S_{AD,med}(Q)}{S_{AD,med}(Q_0)} = \frac{1}{k^{rel}_{bq}} \frac{1}{f^{rel}}, \quad (4)$$

TABLE XXIV. Half-life and photon spectrum for ^{131}Cs dosimetry. X-ray transitions are listed after the elemental symbol for the daughter nuclide (i.e., Xe). Subgroups are enumerated for the K_α and K_β transitions, while the mean energies and total intensities are given for the other transitions, e.g., $L_\gamma = L_{\gamma 1} + L_{\gamma 2} + L_{\gamma 3}$.

^{131}Cs (half-life = 9.689 ± 0.016 days)	
Photon energy (keV)	Photons per disintegration
3.760 Xe $L_{\eta+\iota}$	0.0037
4.109 Xe L_α	0.0702
4.479 Xe L_β	0.06302
5.138 Xe L_γ	0.00844
29.112 Xe $K_{\alpha 3}$	0.000022
29.461 Xe $K_{\alpha 2}$	0.211
29.782 Xe $K_{\alpha 1}$	0.389
33.562 Xe $K_{\beta 3}$	0.0364
33.624 Xe $K_{\beta 1}$	0.0702
33.881 Xe $K_{\beta 5}$	0.00071
34.419 Xe $K_{\beta 2}$	0.0213
34.496 Xe $K_{\beta 4}$	0.00412
	0.8781 total photons per disintegration
30.411 mean (> 10 keV photons)	0.7328 total (≥ 10 keV photons)

resulting in the application of two distinct correction factors to account for the energy dependence of TLD readings; the relative absorbed dose sensitivity f^{rel} and the relative intrinsic energy dependence k_{bq}^{rel} defined in the above equation. When the measurement is performed in a phantom medium different than the calibration medium, there also needs to be a detector response correction for the phantom material. The relationship of $E(r)$ with quantities defined in this terminology is straightforward as

$$E(r) = \frac{S_{AD,med}^{rel}(Q)}{P_{phant}} = \frac{1}{k_{bq}^{rel}} \frac{1}{f^{rel}} \frac{1}{P_{phant}}, \quad (5)$$

where P_{phant} is a correction for the nonliquid water equivalence of the utilized plastic phantoms, given by the ratio of dose to water at a given point in water medium to dose to water at the same point in the phantom medium for the experimental radiation quality.[44] The P_{phant} correction is very sensitive to the details of phantom composition, and an independent check is advisable since small changes in the fraction by weight of higher Z elements can cause up to 10% changes in P_{phant} at these low photon energies.[44]

Given that varying terminologies have been employed in the literature, and $E(r)$ has often been quoted to describe corrections not fully compliant with its formal definition (for examples and a relevant discussion, please refer to the TG-43U1 report[2] and Rodriquez and Rogers[44]), wider adoption of the new terminology will promote clarity and uniformity in reporting experimental results. Moreover, reporting the value of the above three correction factors explicitly, along with the corresponding calculation methods or provenance, facilitates review of experimental results and their swift update as progress is made in the field and new knowledge becomes available. In a recent, comprehensive study on the effect of improved TLD dosimetry for derivation of Λ values for low-energy brachytherapy sources, Rodriquez and Rogers[44] have provided a wealth of information including a review of the terminology in the context of using TLDs for dosimetry for low-energy brachytherapy sources; key methodological information regarding the calculation of the f^{rel} and P_{phant} correction factors using MC simulation; a review of corresponding values in the literature, as well as simulation results of these factors; the dependence of f^{rel} on radiation quality and TLD shape and size; and the dependence of P_{phant} on phantom material, composition, and density.

With the appropriate experimental methodology[2] and under the best possible circumstances, the uncertainty of dose per unit S_K at r_0 = (1 cm, 90°) measured using TLDs could be better than 3% if the uncertainty in the relative intrinsic energy dependence correction were to be reduced to 2%.[37] The hypothesis of k_{bq}^{rel} equal to unity prevailed in TLD dosimetry studies of low-energy sources until the work of Davis et al. and subsequent high-quality determinations of k_{bq} reported in the literature.[42–45] See reference[37] for a review. Davis et al.[41] reported a TLD over-response under 200 keV relative to ^{60}Co (k_{bq} decrease) up to 10% (0.6% Type A uncertainty, k = 1) for LiF:Mg,Ti TLD chips using low-energy x-ray beams. Corresponding results of Nunn et al.[42] and Carlsson Tedgren et al.[43] were 13% (3.5% combined standard uncertainty, k = 1) and 7% (1.9% combined standard uncertaintiy, k = 1), respectively. Carlsson Tedgren et al.[43] discussed differences between their results and those of previous studies in view of TLD handling (annealing and read out parameters) and formulation, and expressed concern regarding the applicability of determinations obtained using x-ray beams to other photon fields. They concluded that if universally valid corrections for the energy dependence of TLD readings were to be achieved, this would require the combination of accurate dosimetry and standardized handling protocols. On the other hand, Massillon-JL et al.[50] concluded that differences observed between k_{bq}^{rel} results in the literature are most likely due to nonlinearity effects, and details of the irradiation for its experimental determination (including energy-spectra and phantom geometry/composition conditions) rather than TLD protocol details.

More recently, Reed et al.[45] measured the k_{bq}^{rel} of LiF:Mg, Ti TLD chips for the radiation quality of one ^{125}I seed without silver components, one ^{125}I seed with silver components, and a ^{103}Pd seed model, all relative to ^{60}Co. They obtained k_{bq}^{rel} results of 0.883 ± 0.011, 0.870 ± 0.012, and 0.871 ± 0.013, respectively, with combined standard uncertainties (k = 1). These results were found to be lower than corresponding results of previous studies for comparable qualities, with differences from the former being greater than their expanded uncertainties (k = 2). As also discussed by the authors, this was attributed to the same factors reported by Carlsson Tedgren et al.[43]

Rodriquez and Rogers[44] used a different approach. They performed a rigorous literature review of 23 TLD

experimental determinations of Λ values for low-energy brachytherapy seeds. After replacing the original f^{rel} and P_{phant} corrections by their own results calculated using MC methods, they arrived at a global k_{bq}^{rel} value through minimizing the difference between modified-measured and their MC-calculated Λ values, but without considering differences in TLD handling protocols in the original experimental studies. The k_{bq}^{rel} results and standard uncertainties were 0.931 ± 0.013 and 0.922 ± 0.022 for ^{125}I and ^{103}Pd seeds, respectively.

While these results are well within the range of corresponding findings of studies[41–43] employing x-ray beams, they are significantly higher than corresponding findings of Reed et al.[45] On average, the measured Λ values (as revised by Rodriquez and Rogers[44] to include their f^{rel}, P_{phant}, and k_{bq}^{rel} corrections) were 4.3% and 5.9% lower than the original values for ^{103}Pd and ^{125}I seeds, respectively. As expected, a closer agreement was observed between these revised Λ values and their corresponding MC calculations. This agreement led Rodriquez and Rogers[44] to propose adopting the MC-calculated values for clinical purposes rather than the averaged consensus values.

There is reluctance to eliminate the independent check of MC dosimetry through experimental dosimetry. The latter is a means to assure that a component of Type B uncertainty (i.e., uncertainty evaluated by means other than statistical analysis) does not go unnoticed in MC calculations for low-energy brachytherapy source dosimetry. A review of recommendations for the computational and experimental dosimetric characterization of low-energy sources is necessary to evaluate alternative means of corroborating results from MC studies. It is prudent to continue with the past methodology for consensus derivation until this topic is resolved. In the interim, the methodological recommendations in the TG-43U1 report for experimental dosimetry apply, especially the recommendation that in utilizing measured or MC-based TLD corrections, experimental dosimetry investigators should confirm that the associated measurement methodology matches their reference dosimetry technique with regard to TLD type and size, annealing and readout technique, and megavoltage beam calibration technique. Specifically, one should no longer use a value of 1.4 as the value of $S_{AD,med}^{rel}$ since the literature values were based on outdated primary standards and protocols that no longer apply and/or simple theoretical models that are no longer thought valid. For the purposes of measurement reporting, the AAPM and GEC-ESTRO recommend that dosimetry investigators utilize the TLD correction terminology summarized above. Additional research is needed with regard to the effect of TLD handling on k_{bq}^{rel} and the potential for universally valid corrections for the energy dependence of TLD readings based on modern primary standards and dosimetry protocols.

6. SUMMARY

Consensus datasets from the AAPM and GEC-ESTRO are presented for 11 low-energy photon-emitting brachytherapy sources. Based on radionuclide, there are general trends evident for the examined sources. For the ^{125}I sources, all values for ${}_{\mathrm{CON}}\Lambda$ are within 1.2% of an average value of 0.942 cGy h^{-1} U^{-1}, except for the model S18 source, which has plastic encapsulation instead of titanium. Similarly, all values of ${}_{\mathrm{CON}}\Lambda$ for the ^{103}Pd sources are within 0.6% of an average value of 0.697 cGy h^{-1} U^{-1}, except for the model CS10 and model 1032P sources, which have plastic encapsulations instead of titanium. Consistency of these results is expected given the similarities of the source models and the magnitude of the uncertainties associated with deriving the ${}_{\mathrm{CON}}\Lambda$ values. When considering all sources including the single ^{131}Cs source, there is a general trend of increasing values of ${}_{\mathrm{CON}}\Lambda$ as the radionuclide photon energy increases. Except for the model S18 (unique in emitting Pb characteristic x rays), the ${}_{\mathrm{MC}}\Lambda/{}_{\mathrm{EXP}}\Lambda$ ratio for all sources is within 5% of the average value of 0.961. This ratio varies by less than 1% when examining only ^{125}I or ^{103}Pd sources.

Values for ${}_{\mathrm{CON}}g_{\mathrm{L}}(r)$ also exhibit energy-dependent behavior where the steeper gradients are more gradual in moving from ^{103}Pd to ^{125}I to ^{131}Cs. Behavior of the ${}_{\mathrm{CON}}g_{\mathrm{L}}(r)$ data for the model S18 source is notable in that the dose falloff is more gradual than that for other ^{125}I sources.

Values for ${}_{\mathrm{CON}}\phi_{\mathrm{an}}(r)$ are nearly constant within a few percent for all sources for $r \geq 1$ cm. As r decreases from 1 cm, ${}_{\mathrm{CON}}\phi_{\mathrm{an}}(r)$ values increase due to volume averaging of higher dose rates for small polar angles. This effect is more pronounced for the ^{131}Cs and ^{103}Pd sources than for the ^{125}I sources.

Depending upon the dosimetry parameters currently used by individual physicists, use of these recommended consensus datasets may result in changes to patient dose calculations. These changes could globally cause patient dose calculations to be higher or lower, the single-source dose distributions could have a different shape, and/or the range for which data are interpolated or extrapolated could be altered. The reason for any changes must be carefully evaluated and reviewed with the radiation oncologist prior to their implementation.

ACKNOWLEDGMENTS

Some authors (MJR; LAD; GSI; ASM; PP) have received research support (GE Healthcare, CivaTech Oncology, and IsoRay Medical; GE Healthcare, CivaTech Oncology, and IsoRay Medical; IsoRay Medical; International Brachytherapy and IsoAid; and Elekta AB and BEBIG GmbH), respectively, to perform dosimetry studies for the sources included herein. We thank Robert van der Laarse for his assistance in the preparation of the QA tables and David Rogers for fruitful discussion on preliminary versions of this report.

APPENDIX

DERIVATION OF MODEL-SPECIFIC BRACHYTHERAPY DOSIMETRY PARAMETERS

The methods for deriving consensus datasets of brachytherapy dosimetry parameters have been previously described in

detail in previous reports.[2,4] To match the NIST wide-angle free-air chamber (WAFAC) measurement geometry as used for source calibrations in the measurement of Λ, results of MC simulations of the NIST WAFAC measurement geometry were used in favor of the MC estimations of air-kerma strength at a point on the source transverse plane. For sources used outside the U.S. such as in Europe with different calibration approaches, small differences between delivered and expected dose may result when a different calibration standard is used for measurements performed to derive Λ versus measurements of sources assayed for clinical applications. The same issue holds true for MC simulations of the calibration standards. As in the TG-43U1 (2004) report,[2] the terms S_K and s_K are defined to indicate measured and MC-simulated values for air-kerma strength. Because values for the active length L or effective length L_{eff} are limited in TPS software to 0.001 cm resolution, derivations of L or L_{eff} are similarly constrained. The ${}_{CON}g_P(r)$ values were obtained from ${}_{CON}g_L(r)$ values using the ratio of the point- and line-source geometry functions with ${}_{CON}L$ (or ${}_{con}L_{eff}$). As recommended in the 2004 AAPM TG43-U1 report,[2] the ${}_{CON}\phi_{an}(r)$ values were derived from ${}_{CON}F(r, \theta)$ by numerical integration of the dose rate with respect to solid angle. Uncertainty assessments for individual results were quoted from the original studies, but developed further when published information was missing. While the majority of these were evaluated following the generic uncertainty assessment scheme in the 2004 AAPM TG-43U1 report,[2] the reader is referred to the corresponding studies for details. While less prevalent than in the TG-43U1 (2004)[2] and TG-43U1S1 (2007)[4] reports, some of the studies using MC methods had photoatomic cross-section libraries with suspect values. Results from these MC studies were excluded from derivation of ${}_{CON}g_L(r)$ values, but included for derivation of ${}_{CON}\Lambda$ and ${}_{CON}F(r, \theta)$ values.

All mention of water is to liquid water unless otherwise noted. During the time span subtended by the measurements in the cited publications, there were corporate changes to the LiF TLD manufacturer, known throughout the years as St. Gobain Bicron (Wermelskirchen, Germany), Harshaw/Bicron (Solon, OH, USA), Harshaw, Inc. (Oakwood Village, OH, USA), and currently Thermo Scientific, Inc. (Waltham, MA, USA). Listed alphabetically by manufacturer for ^{125}I, ^{103}Pd, and ^{131}Cs sources, each source model and specifics used to obtain the dosimetry parameters are provided in the following sections.

A1. BEBIG MODEL I25.S17 ^{125}I SOURCE

The IsoSeed™ model I25.S17 ^{125}I source was manufactured by Eckert & Ziegler BEBIG GmbH (Berlin, Germany). It is no longer in production, but previously met the AAPM brachytherapy dosimetric prerequisites and the AAPM CLA subcommittee requirements. This source, see Fig. 1(a), consisted of a cylindrical molybdenum marker with 3.40 mm outer length and a 0.50 mm diameter that was coated with a 3 μm thick layer of nickel, followed by a 23 μm thick layer of pure silver with a 2 μm thick layer of silver iodide containing ^{125}I. The ^{125}I-coated marker was encapsulated within a titanium tube having a 0.050 mm wall thickness and hemispherical endwelds 0.40 mm in radius. The outside dimensions of the cylindrical capsule are 4.50 mm in length and 0.80 mm in diameter.

In 2005, Lymperopoulou et al. published the results of both TLD measurements and MC estimations of the dosimetric characteristics of this source.[51] Measurements were performed with TLD-100 rods in two SolidWater™ phantoms (GfM Weiterstadt, Germany). Since relatively large TLD rods were used, Lymperopoulou et al. considered the effects of volume averaging and shift in the point of measurement. A total of 11 sources were used in the measurements, three of which were calibrated at NIST in terms of air-kerma strength. The statistical (Type A) component of uncertainty varied, with a value of 0.3% at r_0 on the transverse plane and maximum value of 9% obtained at r=5 cm and small polar angles. MC studies were performed using both a code written by the authors and the MCNPX (version 2.4.0) photon transport simulation code to calculate the dose-rate distribution in water. Photon cross-section libraries equivalent to DLC-146 were used. Air-kerma strength MC estimations s_K were performed in vacuum in two ways, namely using either a point detector scoring voxel or a scoring volume on the source transverse plane at 30 cm that subtended a cone of 7.6° half-angle to simulate the NIST WAFAC calibration geometry. The Ti characteristic x-ray production was either suppressed using MC software options or a 5 keV cutoff energy was used in the MCNPX simulation software.

In 2008, Taylor and Rogers published the results of MC calculations of TG-43 dosimetry parameters for 27 sources,[15] including the model I25.S17 source. MC studies were performed with an EGSnrc-based user-code called BrachyDose, which used a track-length estimator to score collision kerma per history in each voxel. XCOM photon cross-section data was employed, as well as photon spectra from the TG-43U1 report. By simulating up to 4×10^{10} histories, Type A uncertainties were less than 2% for dosimetry parameters calculated at 10 cm from the source. s_K was calculated in vacuum with a 5 keV photon cutoff to maintain consistency with the NIST WAFAC standard. Results were reported for both a point-like detector and for a voxel subtending a solid angle similar to that of the NIST WAFAC measurement geometry.

A1.1. Model I25.S17 dose-rate constant

Lymperopoulou et al. reported a TLD-measured value of Λ in water of (0.951 ± 0.044) cGy h^{-1} U^{-1}. For the NIST WAFAC geometry, their MC value was (0.914 ± 0.014) cGy h^{-1} U^{-1}. Their TLD results were selected as the ${}_{EXP}\Lambda$. Their TLD and MC results agreed within their respective uncertainties. Taylor and Rogers obtained a value Λ of (0.916 ± 0.002) cGy h^{-1} U^{-1} using voxel sizes that simulated the WAFAC measurement geometry. The MC results of Lymperopoulou et al. and from Taylor and Rogers agreed within 0.2% (within their respective uncertainties), giving an average ${}_{MC}\Lambda$ value of (0.915 ± 0.007) cGy h^{-1} U^{-1}. The

average of $_{EXP}\Lambda$ and $_{MC}\Lambda$ yielded $_{CON}\Lambda$ = (0.933 ± 0.025) cGy h^{-1} U^{-1}. The $_{MC}\Lambda$ value was 3.8% lower than the $_{EXP}\Lambda$ value and within the standard uncertainty of the measurements.

A1.2. Model I25.S17 radial dose function

For calculating the geometry function, $G(r, \theta)$, Lymperopoulou et al. used the line-source approximation with L = 0.34 cm. To measure $g_L(r)$, TLDs were placed in a SolidWater™ phantom at radial distances ranging from 1 cm to 7 cm on the source transverse plane with results corrected for water. MC estimations covered a larger range from 0.10 cm to 10 cm. The differences between their measured and calculated values of $g_L(r)$ were within 2% for $r \leq 5$ cm with a maximum difference of 7% at r = 7 cm. Taylor and Rogers used L = 0.346 cm, differing from Lymperopoulou et al. by 60 μm to account for the thickness of the various coatings applied to the cylindrical molybdenum marker. For direct comparison, the $g_L(r)$ data of Lymperopoulou et al. were renormalized using $G_L(r, \theta)$ with a consensus value of $_{CON}L$ = 0.346 cm. This inclusion of the coating thickness in derivation of $_{CON}L$ affected results only by 1.0% at r = 0.1 cm, 0.4% at r = 0.25 cm, and 0.1% at r = 0.5 cm. The MC studies of Taylor and Rogers spanned a range of 0.05–10 cm with a finer resolution than MC results from Lymperopoulou et al.

Comparing the $g_L(r)$ data from the two MC studies, with both using L = 0.346 cm, agreement was within 1.5% over all distances. The $g_L(r)$ results obtained using MC methods from both research teams agreed with TLD-measured values of Lymperopoulou et al. to within 3% for 1–5 cm and within 7% for 5–7 cm. Because there was good agreement among the three datasets as described above, the candidate dataset (i.e., Taylor and Rogers) covering the largest range and having the highest resolution was chosen as the consensus dataset for $_{CON}g_L(r)$.

A1.3. Model I25.S17 anisotropy functions

Lymperopoulou et al. measured $F(r, \theta)$ using TLDs placed at radial distances of 1, 1.5, 2, 3, and 5 cm from the source, with angles ranging from 2° to 60°, depending on the distance. Their MC study of the 2D anisotropy function was performed at radial distances of 0.5, 1, 1.5, 2, 3, 5, and 7 cm from the source, with variable angular sampling. The measurement and simulation approaches used L = 0.340 cm and indicated agreement within the Type A measurement uncertainties. Taylor and Rogers calculated $F(r, \theta)$ at radial distances of 0.10, 0.15, 0.25, 0.5 0.75, 1, 2, 3, 4, 5, 7.5, and 10 cm from the source, also with variable angular sampling.

To perform a direct comparison as was previously done for the $g_L(r)$ values, the MC and TLD $F(r, \theta)$ data from Lymperopoulou et al. were renormalized using $G_L(r, \theta)$ calculated with $_{CON}L$ = 0.346 cm. Subsequently, the MC-based $F(r, \theta)$ data from both research teams agreed within 8% for $\theta > 5°$. The maximum discrepancy was 23% near the end of the source at $P(r$ = 0.5 cm, θ = 5°) with the Lymperopoulou et al. results consistently being lower than those from Taylor and Rogers. The MC and TLD $F(r, \theta)$ data from Lymperopoulou et al. agreed within 8% at all common positions. The Taylor and Rogers MC results agreed within 9% with the renormalized TLD results of Lymperopoulou et al., except at $P(r$ = 1 cm, θ = 10°) where the difference was 13%. Given the good agreement among the three datasets except in close proximity to the source ends, the candidate dataset (i.e., Taylor and Rogers) covering the largest radial and angular range and having the highest resolution was chosen as the consensus 2D anisotropy function dataset $_{CON}F(r, \theta)$.

A2. BEBIG MODEL I25.S17PLUS ^{125}I SOURCE

The model I25.S17plus ^{125}I source is also manufactured by Eckert & Ziegler BEBIG GmbH (Berlin, Germany). It is currently posted on the Registry and consists of a cylindrical silver marker with a 3.4 mm length and a 0.51 mm diameter that is coated with a 1 μm thick layer of silver iodide containing ^{125}I, see Fig. 1(b). The ^{125}I-coated Ag marker is encapsulated within a titanium tube having a 0.055 mm wall thickness and 0.41 mm thick hemispherical endwelds. The outside dimensions of the cylindrical capsule are 4.50 mm in length and 0.80 mm in diameter. A $_{CON}L$ = 0.34 cm value was used.

Moutsatsos et al. reported results of measurements in model 457 SolidWater™ (Gammex, Inc., Middleton, WI, USA) using a batch of 100 TLD-100 1 mm^3 cubes.[52] TLDs were calibrated using 6 MV photons from a linac with a k_{bq}^{rel} factor of 0.916 ± 0.023 based on the work of Kennedy et al.[53] TLD response in SolidWater™ was corrected to derive dose to water in water using MC methods with the MCNP6 v.6.1 radiation transport code using 5 × 10^{10} photon histories and similar methods to Pantelis et al.[54] To measure $g_L(r)$, TLDs were placed in the SolidWater™ phantom on the source transverse plane at 1–7 cm with 0.5 cm spacing with results corrected for water.

Pantelis et al. reported results of MC calculations on the dosimetric characteristics of this source.[54] The MCNP5 code (version 1.60)[55] was used for radiation transport simulations with the default photon cross-section libraries. The *FMESH4 tally was used in combination with mass-energy absorption coefficients from the NIST XCOM database to convert photon energy fluence to absorbed dose.[56] The source was positioned at the center of a 30 cm diameter spherical water phantom, and 3 × 10^9 histories were simulated, resulting in Type A uncertainties of < 0.2% for r < 5 cm. MC methods to derive s_K to air in vacuum with 10^9 histories were determined over a cylindrical voxel having a half-angle of 7.6° to simulate the NIST WAFAC measurement geometry. Compared to measurements by Moutsatsos et al., the MC simulations by Pantelis et al. covered a larger range from 0.10 cm to 10 cm with higher spatial resolution. Unique to the study by Pantelis et al. was inclusion of a 2D map of dosimetric uncertainties attributed to the variations in source design as observed through dimensional

measurements of ten seeds. This approach relaxes the need for dosimetric measurements of an increased number of sources and provides confidence intervals for associated dosimetry parameters at all points to facilitate comparisons to experimentally measured results as well as the preparation of consensus data.

A2.1. Model I25.S17plus dose-rate constant

Moutsatsos et al. reported a TLD-measured value of ${}_{EXP}\Lambda$ in water of (0.956 ± 0.043) cGy h^{-1} U^{-1}. For the NIST WAFAC geometry, Pantelis et al. reported the MC-calculated value of ${}_{MC}\Lambda$ as (0.925 ± 0.019) cGy h^{-1} U^{-1}. An equally weighted average of ${}_{EXP}\Lambda$ and ${}_{MC}\Lambda$ yielded ${}_{CON}\Lambda$ = (0.940 ± 0.025) cGy h^{-1} U^{-1}. The ${}_{MC}\Lambda$ value was 3.3% lower than the ${}_{EXP}\Lambda$ value and within the standard uncertainty of the measurements.

A2.2. Model I25.S17plus radial dose function

The differences between the measured and calculated values of $g_L(r)$ were within 3% for $r \leq 3.5$ cm with a maximum difference of 8.5% at $r = 7$ cm. This level of agreement between measured and simulated results is typical for an ^{125}I source at large distances. Due to the larger radial range and higher resolution, the MC results of Pantelis et al. were selected for ${}_{CON}g_L(r)$.

A2.3. Model I25.S17plus anisotropy functions

Moutsatsos et al. measured $F(r, \theta)$ at radii of 1, 1.5, 2, 3, 4, and 5 cm and polar angles of 0°, 30°, 60°, and 90° using four sources and four measurements per source. Pantelis et al. simulated the 2D anisotropy function over $0.25 \leq r \leq 10$ cm and for $0° \leq \theta \leq 90°$ with 1° increments. At positions common to both studies, the agreement between the measured and calculated values of $F(r, \theta)$ was within 4% for 30° and 60°. At 0° the TLD results were 12% larger than the MC results, except for at $r = 5$ cm where they were only 5% larger. Given the relatively good agreement between the candidate datasets and the higher spatial and angular resolution of the study by Pantelis et al., their MC results were selected and used for the ${}_{CON}F(r, \theta)$ dataset.

A3. BEBIG MODEL I25.S18 ^{125}I SOURCE

The SmartSeed™ model I25.S18 ^{125}I source was manufactured by Eckert & Ziegler BEBIG GmbH (Berlin, Germany), formerly of IBt-Bebig. It is no longer in production, but previously met the AAPM brachytherapy dosimetric prerequisites and the AAPM CLA subcommittee requirements. The source consisted of a cylindrical leaded-glass radiopaque marker 2.75 mm long and 0.48 mm in diameter with a 23 μm thick quartz layer containing ion-implanted ^{124}Xe which was transmuted to ^{125}I through neutron irradiation.[57] This core is subsequently coated with an additional 2 μm thick quartz layer for radioactive containment. The capsule is composed of a biocompatible polymer (i.e., polyacryletheretherketone) with a length of 4.50 mm, outer diameter of 0.78 mm, and wall thickness of 0.14 mm, see Fig. 1(c). The capsule ends have spherical cutouts to permit stranding of the sources.

Abboud et al.[57] reported dosimetry results of TLD measurements and MC estimations, and used ${}_{CON}L$ = 0.275 cm for the length of the ^{125}I-coated radiopaque marker. Measurements performed using TLD-100 1 mm^3 cubes calibrated with 6 MV photons from a linac. Five sources were sent to NIST for WAFAC calibration, and two of these sources were sent to Abboud et al. for cross-calibrating additional sources for TLD measurements. An energy response correction factor of 1.40 was used. TLD measurements were performed within a 20 × 20 × 10 cm^3 phantom of model WT1 SolidWater™ (model 457, Radiation Measurement, Inc., Middletown, WI, USA).

Abboud et al.[57] also reported on MC dosimetry results with the MCNP5 radiation transport code and the MCPLIB04 photoatomic cross-section library. Dose in medium was estimated using two separate scoring methods. The measurement environment and materials were simulated in the same manner as done for dose to water for correcting TLD response to dose to water results. The 2 m diameter water phantom was modeled in two ways: (a) with 1 mm^3 spherical scoring voxels, and (b) with scoring voxels determined by the intersection of spherical shells and cones in 2° increments. To reduce statistical uncertainties, 10^9 photon histories were simulated to provide standard uncertainties (statistical) of 0.2% and 1.3% in water at 1 cm and 5 cm, respectively. Air kerma was also modeled in two ways: (a) at 5 cm from the source in air (F6 tally) and (b) in a 2-cm-thick ring of air centered 2 m from the source in vacuum and restricted to within 2° of the source transverse plane (*F4 tally). A total of 10^9 photon histories were used for both MC estimations of s_K.

While the TG-43U1 dosimetry protocol specifies a photon energy cutoff of 5 keV, Abboud et al. also evaluated the influence of photon energy cutoffs of 1 keV and 14 keV on dose to water and Λ. These two additional energy cutoffs were used to investigate the contributions of characteristic x-rays from xenon (~5 keV) and lead (~12 keV) because this source model has a polymer-based encapsulation and would not filter these low-energy photon emissions. Abboud et al. determined that the xenon x rays had negligible dosimetric contributions even for close distances. However, the lead x rays contributed 8.7% and 2.7% to the total dose on the source transverse plane at $r = 0.1$ cm and $r = 0.5$ cm, respectively, being negligible at $r = 1.0$ cm.

New to the field of brachytherapy is a source having a value of Λ that is strongly dependent on choice of energy cutoff. Due to diverse disease sites having different pertinent radial distances, one energy cutoff value for Λ may appear not to be appropriate. However, the process of NIST-traceable source calibrations and clinical treatment planning favors consistent use of the 5 keV cutoff. A more realistic simulation of the NIST WAFAC measurement geometry, with inclusion of an

aluminum filter and spectroscopy-based corrections to air-kerma rate, would enhance the comparisons between simulated and measured results for Λ, thought to be especially important for sources having x-rays between 5 keV and 20 keV.

A3.1. Model I25.S18 dose-rate constant

Abboud et al. reported a TLD-measured value in water of (0.885 ± 0.060) cGy h^{-1} U^{-1}, which was selected for ${}_{EXP}\Lambda$. To strictly comply with the S_K definition, only results from the 5 keV cutoff were considered for the candidate data. The results from two separate scoring methods were (0.895 ± 0.024) cGy h^{-1} U^{-1} and (0.905 ± 0.024) cGy h^{-1} U^{-1}, where a 2.7% uncertainty was identified in the text. The average of these two methods yielded ${}_{MC}\Lambda$ = (0.900 ± 0.017) cGy h^{-1} U^{-1}. The average of TLD and MC results yielded ${}_{CON}\Lambda$ = (0.893 ± 0.032) cGy h^{-1} U^{-1}. The ${}_{MC}\Lambda$ value was 1.7% higher than the ${}_{EXP}\Lambda$ value and within the standard uncertainty of the measurements.

A3.2. Model I25.S18 radial dose function

Abboud et al. evaluated $g_L(r)$ with TLDs in the WT1 phantom at 1, 1.5, 2, 3, 4, 5, 6, and 7 cm and with MCNP5 in water from 0.1 cm to 10 cm. Comparisons of MC-derived dose rates in WT1 to TLD-measured dose rates at common positions agreed on average within 2% with a maximum difference of 5% at r = 7 cm. Given the MC results covered a larger radial range and had a higher resolution than the TLD results, the MC results of Abboud et al. were selected for ${}_{CON}g_L(r)$.

A3.3. Model I25.S18 anisotropy functions

Abboud et al. evaluated $F(r, \theta)$ in WT1 using TLD measurements and MC estimations at 2, 3, 5, and 7 cm and from 0° to 90° with 10° binning. Over the 36 common positions, these results were in 1.5% agreement on average with a maximum difference of 3.7%. The MC-derived $F(r, \theta)$ values in water had the same angular binning, but covered a radial range from 0.5 cm to 10 cm. Due to the higher resolution of MC results in water and no need to perform medium correction factors for the TLD results, the MC results of Abboud et al. were adopted for ${}_{CON}F(r, \theta)$. Abboud et al. did not report ${}_{EXP}\phi_{an}(r)$ values. Examining their ${}_{MC}\phi_{an}(r)$ values, a 2.3% discontinuity was observed between 5 cm and 6 cm. The 1D ${}_{MC}\phi_{an}(r)$ results published in Abboud et al. were not in agreement with values calculated using numerical integration of the dose rate with respect to solid angle. After correspondence with the authors, it was determined that the methods used in Abboud et al. to obtain ${}_{MC}\phi_{an}(r)$ did not follow the 2004 TG-43U1 report formalism.

A4. ELEKTA MODEL 130.002 ^{125}I SOURCE

The selectSeed™ model 130.002 ^{125}I source is manufactured by Eckert & Ziegler BEBIG, GmbH (Berlin, Germany) and distributed by Nucletron (Veenendaal, the Netherlands), a subsidiary of Elekta AB (Stockholm, Sweden). The source is currently posted on the Registry, and may be implanted interstitially either manually or using a commercially available robotic brachytherapy system.[58–60] It has ^{125}I adsorbed on a cylindrical silver rod contained within a tubular titanium capsule. The titanium capsule is 4.5 mm long with inner and outer diameters of 0.70 mm and 0.80 mm, respectively, see Fig. 1(d). Hemispherical endwelds (0.4 mm thick) are made using laser welding to encase a silver rod 3.4 mm long and 0.51 mm diameter coated with a 3 μm thick silver halide layer containing ^{125}I.

Anagnostopoulos et al. reported results of measurements in a $(30\ cm)^3$ SolidWater™ phantom (GfM Weiterstadt, Germany) using TLD-100 rods calibrated using 6 MV photons from a linac.[61] Source calibrations were initially performed for three model 130.002 ^{125}I sources calibrated at the PTB (Braunschweig, Germany) in a manner similar to the NIST WAFAC approach to remove contributions from Ti characteristic x rays. Six sources were later sent to NIST to establish a U.S. primary calibration standard and permit traceable calibrations for measurements of Λ.[62]

Karaiskos et al. reported results of MC estimations on the dosimetry parameters for the model 130.002 ^{125}I source using a generalized MC code that was developed in-house specifically for brachytherapy dosimetry investigations.[63] While no identifying name or version of this code was declared, the MC code used by the University of Athens group has been well-validated under a variety of circumstances appropriate for radiation transport calculations for brachytherapy sources. Photoatomic interaction cross-sections from Scofield,[64] Hubbell et al.,[65] and Hubbell and Øverbø[66] were used. The MC code uses NIST XCOM mass-energy absorption coefficients from Hubbell and Seltzer,[56] and atomic data from Plechaty et al.[67] were used for characteristic x-ray generation. Both Anagnostopoulos et al. and Karaiskos et al. used ${}_{CON}L$ = 0.34 cm for their derivations of brachytherapy dosimetry parameters. While ^{125}I coating thicknesses of 3 μm and 10 μm were examined, only the 3 μm results were pertinent to the model 130.002 source available to users. The 30 cm diameter water phantom was divided into 0.1 cm and 1° voxels for a total of 27,000 scoring cells. The dose-rate constant was simulated using 10^9 photon histories in air and in vacuum on the source transverse plane within a 5 m diameter sphere at distances ranging from 1 cm to 500 cm. Air-kerma strength and dose to water were calculated by multiplying photon energy fluences calculated on the surface of each voxel by the corresponding mass-energy absorption coefficients. There was no volume averaging on the source transverse plane of 90° ± 7.6° to simulate the NIST WAFAC measurement geometry. Consequently, additional MC studies by Lymperopoulou et al.[51] were used for estimation of ${}_{MC}\Lambda$, as suggested by Papagiannis et al.[62] MC estimations of dose to water by Karaiskos et al.[63] utilized 10^9 photon histories. MC simulations were also performed by Taylor and Rogers[15] with L = 0.34 cm and similar methods as described for the model I25.S17 ^{125}I source in Appendix Section A1.

A4.1. Model 130.002 dose-rate constant

Anagnostopoulos et al.[61] measured (0.902 ± 0.065) cGy h^{-1} U^{-1} in SolidWater™, which was corrected to (0.938 ± 0.065) cGy h^{-1} U^{-1} for water using distance-dependent phantom correction factors as calculated by Karaiskos et al.[63] To strictly comply with CLA source calibration recommendations, Papagiannis et al.[62] reported (0.987 ± 0.077) cGy h^{-1} U^{-1} for sources having NIST traceability. This latter value was selected as ${}_{EXP}\Lambda$.

Karaiskos et al.[63] estimated Λ without incorporating s_K volume averaging for the NIST WAFAC aperture and reported (0.954 ± 0.005) cGy h^{-1} U^{-1} where the uncertainty was attributed solely to statistics. Lymperopoulou et al.[51] reported (0.950 ± 0.014) cGy h^{-1} U^{-1} for the same geometry and a MC-estimated value of (0.925 ± 0.014) cGy h^{-1} U^{-1} approximating the WAFAC geometry. Also, from MC studies of the WAFAC, Taylor and Rogers calculated (0.917 ± 0.002) cGy h^{-1} U^{-1} where the uncertainty was attributed solely to statistics. Averaging the WAFAC simulation values from Lymperopoulou et al. and Taylor and Rogers,[15] a value of (0.921 ± 0.007) cGy h^{-1} U^{-1} was obtained for ${}_{MC}\Lambda$. An equally weighted average of ${}_{EXP}\Lambda$ and ${}_{MC}\Lambda$ yielded ${}_{CON}\Lambda$ = (0.954 ± 0.043) cGy h^{-1} U^{-1}. The ${}_{MC}\Lambda$ value was 6.7% lower than the ${}_{EXP}\Lambda$ value and within the standard uncertainty of the measurements.

A4.2. Model 130.002 radial dose function

Anagnostopoulos et al. evaluated $g_L(r)$ with TLDs in the SolidWater™ phantom from 1 cm to 7 cm with 0.5 cm increments. Results from Karaiskos et al. were used to correct TLD response to obtain $g_L(r)$ in water. Karaiskos et al. reported $g_L(r)$ in water from 0.1 cm to 10 cm. Comparisons of MC-derived dose rates in SolidWater™ from Karaiskos et al. to TLD-measured dose rates in SolidWater™ from Anagnostopoulos et al. at common positions exhibited agreement within 2% on average with a maximum difference of 6% at r = 7 cm. Comparisons of MC-based $g_L(r)$ results between Karaiskos et al. and Taylor and Rogers indicated agreement within 0.3% on average with maximum differences of 2.2% at r = 0.1 cm and 1.5% at r = 10 cm. Given the MC results from Karaiskos et al. covered a larger radial range and had a higher resolution than the TLD results from Anagnostopoulos et al., and that Karaiskos et al. had hands-on experience with the model 130.002 ^{125}I seed, the $g_L(r)$ results of Karaiskos et al. were selected for ${}_{CON}g_L(r)$.

A4.3. Model 130.002 anisotropy functions

Anagnostopoulos et al. measured $F(r, \theta)$ at radii of 1, 1.5, 2, 3, 4, 5, and 7 cm and polar angles of 0°, 30°, 60°, and 90°. Since relatively large TLD rods were used, Anagnostopoulos et al. considered the effects of volume averaging and shift in the point of measurement. For the nominal polar angles of 0°, 30°, 60°, and 90°, these effects amounted to a less than 1° angular shift at r = 7 cm. However, the measurements at r=1 cm corresponded to effective polar angles of 10°, 31°, 60°, and 90°, respectively. To perform a direct comparison with Karaiskos et al. MC results at the same positions, the authors were contacted[68] and a high-resolution dataset was obtained with sampling at the same radial resolution as their $g_L(r)$ results, but with 1° angular binning and centered on integer values of polar angles unlike in their Table III.[63] At r = 1 cm, the simulated results 4.6%, 4.5%, and 0.5% higher than the measured results at 10°, 31°, and 60°, respectively. At larger distances, agreement was within 5% and typically within 2%. Taylor and Rogers[15] also evaluated $F(r, \theta)$ for the model 130.002 ^{125}I source, covering the same radial and angular range as Karaiskos et al., but with less frequent binning. At positions common to both MC-based datasets, the results of Taylor and Rogers and Karaiskos et al. were in agreement within 0.6% on average with maximum differences of 5.1% at $F(r = 0.1$ cm, $\theta = 5°)$ and 4.4% at $F(r = 10$ cm, $\theta = 3°)$. Given the good agreement between the candidate datasets and the higher spatial and angular resolution of the study by Karaiskos et al., their MC results were selected as the ${}_{CON}F(r, \theta)$ dataset.

A5. ONCURA MODEL 9011 ^{125}I SOURCE

The THINSeed™ model 9011 ^{125}I source was introduced in 2010 by Oncura, Inc. (Princeton, NJ, USA) and distributed by GE Healthcare, Inc., (Arlington Heights, IL, USA). It is no longer in production, but previously met the AAPM brachytherapy dosimetric prerequisites and the AAPM CLA subcommittee requirements. The source was posted on the Registry and was similar to the also discontinued model 6711 source in that it had a 2 μm thick layer of ^{125}I adsorbed onto a cylindrical silver rod contained within a titanium capsule. However, the model 9011 source had a smaller outer diameter (0.51 mm) than the 6711 source with improved visualization with computed tomography (CT) imaging.[69,70] The capsule outer length was 4.56 mm, hemispherical capsule ends, and a 0.057 mm wall thickness of titanium tubing, see Fig. 1(e). There are three publications on dosimetry for this source, all using ${}_{CON}L$ = 0.28 cm.

Rivard[71] reported results of MC estimations on the dosimetry parameters for the model 9011 ^{125}I source using version 1.40 of the MCNP5 radiation transport code and the *F4 and F6 tally estimators for determinations of air kerma and absorbed dose to water, respectively. Comparisons were also made to the model 6711 ^{125}I source. The ^{125}I photon energy spectrum was taken from the NNDC website. The mass-energy absorption coefficients used to convert photon energy fluence in vacuum to air kerma were taken from NIST.[56] The photoatomic cross-section libraries were based on ENDF/B-VI.[72] Air kerma was scored using a 5 keV energy cutoff in vacuum 30 cm from the source in a voxel covering 90.0° ± 7.6° whose center was positioned on the source transverse plane to approximate the NIST WAFAC measurement geometry. Absorbed dose to water was scored

in a 40 cm diameter spherical water phantom at 0.05, 0.075, 0.1, 0.15, 0.2, 0.25 cm and from $0.3 \le r \le 15$ cm in 0.1 cm increments, and from $0° \le \theta \le 180°$ in 1° increments. MC calculations in vacuum and water both used 2×10^9 photon histories. The Ag marker was visually confirmed to have ends beveled 0.05 mm to 45° as reported for the model 6711 source by Dolan et al.[73] Rivard simulated the silver marker with a 2.00 μm thick layer of BrI and AgI in a 2.5:1 molecular ratio.[71]

Kennedy et al.[53] reported dosimetry results of TLD measurements and MC estimations of the model 9011 ^{125}I source, with comparisons also made to the model 6711 ^{125}I source. Measurements performed using TLD-100 1 mm^3 cubes calibrated with ^{60}Co photons based on the methods of Nunn et al.[42] Irradiations were performed in two high-purity $11 \times 30 \times 30$ cm^3 polymethyl methacrylate (PMMA) phantoms having independent composition analyses. This material was chosen over solid water mixtures due to the reduced uncertainties when correcting measured results to yield absorbed dose to water. One phantom was drilled to accommodate TLDs for measurements of $g_L(r)$ while the other phantom had holes drilled for $F(r, \theta)$ measurements. In all cases, at least 5 cm of backscattering material at each detector position was added so that measurements were performed under appropriately large scatter conditions. Following the CLA recommendations,[7] two model 9011 ^{125}I sources were calibrated at NIST. These same two sources were used for measurements of Λ. To yield dose to water, Kennedy et al. corrected measurements in phantom through simulating the experimental conditions using MCNP5 version 1.50 with the same cross-section libraries and similar methods as Rivard.[71] MC studies in water ranged from 0.05 cm to 15 cm for $g_L(r)$ and $F(r, \theta)$ with the latter parameter having polar angle coverage of $0° \le \theta \le 180°$ with 1° increments. MC estimations of air kerma using a 5 keV energy cutoff were scored in vacuum 30 cm from the source in a voxel covering $90.0° \pm 7.6°$ whose center was positioned on the source transverse plane to approximate the NIST WAFAC measurement geometry. All MC calculations by Kennedy et al. utilized 10^{10} photon histories, the ^{125}I photon spectrum recommended in the 2004 AAPM TG-43U1 report,[2] and the Ag marker coated with a 1.75 μm thick layer of AgBr and AgI in a 2.5:1 molecular ratio.

Mason et al.[74] reported dosimetry results of MC calculations for the model 9011 ^{125}I source, mainly for evaluating measurements of a MOSFET detector. The MCNPX (version 2.5.0)[75] photon transport simulation code was used to calculate air kerma and absorbed dose in water using the F6 tally. MC estimation of air kerma in a voxel approximating the NIST WAFAC measurement geometry used a 5 keV energy cutoff. The ^{125}I photon spectrum recommended in the 2004 AAPM TG-43U1 report was used. The radioactive layer coating the Ag marker was 1.75 μm thick and composed of AgBr and AgI in a 2.5:1 molecular ratio as specified by Kennedy et al. Mason et al. did not specify the number of photon histories, but the statistical uncertainties for all cells were reported to be below 1%.

A5.1. Model 9011 dose-rate constant

Rivard reported MC results of $\Lambda = (0.914 \pm 0.021)$ cGy h^{-1} U^{-1}.[71] Kennedy et al.[53] reported MC results of $\Lambda = (0.923 \pm 0.004)$ cGy h^{-1} U^{-1} and a TLD-measured value in PMMA for Λ in water of (0.940 ± 0.055) cGy h^{-1} U^{-1}. Mason et al.[74] reported MC results of $\Lambda = 0.926$ cGy h^{-1} U^{-1}; no uncertainty was provided, but was assumed to be on the order of 1%. Rodriguez and Rogers reported MC results of $\Lambda = (0.930 \pm 0.002)$ cGy h^{-1} U^{-1}.[44] The TLD value from Kennedy et al.[53] was selected as $_{EXP}\Lambda$. The Λ MC results from Kennedy et al., Mason et al., and Rodriguez and Rogers all agreed within a range of 0.4% about the average. The Λ MC results from Rivard were 1.0% lower than those from Kennedy et al., with the difference attributed to the coating layer having a different composition.[53] Consequently, the results from Kennedy et al., Mason et al., and Rodriguez and Rogers were used for selecting $_{MC}\Lambda = (0.926 \pm 0.003)$ cGy h^{-1} U^{-1}. An equally weighted average of $_{EXP}\Lambda$ and $_{MC}\Lambda$ yielded $_{CON}\Lambda = (0.933 \pm 0.028)$ cGy h^{-1} U^{-1}. The $_{MC}\Lambda$ value was 1.5% lower than the $_{EXP}\Lambda$ value and within the standard uncertainty of the measurements.

A5.2. Model 9011 radial dose function

Mason et al. calculated $g_L(r)$ at seven distances. These results were on average within 0.01% of the results at positions in common with Kennedy et al. and differed by no more than 0.5% from 0.2 cm to 5 cm. Differences in calculated $g_L(r)$ results between Rivard and Kennedy et al. were 0.8%, 2.5%, and 3.2% at 2, 5, and 10 cm, respectively, and were attributed to the silver rod coating used by Rivard. Furthermore, Rivard initially transposed $g_L(r)$ results for the model 6711 and model 9011 sources,[71] which were later corrected.[76] The simulated results of Kennedy et al. were lower by 2.1%, 5.3%, 6.6%, 9.4%, and 19.2% than their measured results at 2, 5, 7, 9, and 10 cm, respectively, which was considered good agreement given the experimental uncertainties. Because of the good agreement with other $g_L(r)$ datasets, the large radial range of 0.2 cm to 12 cm, and the high resolution, the MC-based $g_L(r)$ results of Kennedy et al. were selected for $_{CON}g_L(r)$, with the values at 0.10 cm and 0.15 cm selected from Rivard.

A5.3. Model 9011 anisotropy functions

Mason et al.[74] calculated $F(r, \theta)$ at 0.5, 1, 2, and 5 cm and polar angles of 0°, 30°, and 60°. Their results were within 2% of those from Rivard at common positions, except for at $\theta = 0°$ where their results differed by 1.9%, 11%, 9%, and 5% at 0.5, 1, 2, and 5 cm, respectively. For the TLD results of Kennedy et al.,[53] comparison of $F(r, \theta)$ at 42 common positions with the MC results of Rivard were in agreement within 4.8% on average, with the largest differences similarly occurring along the source long axis with discrepancies of 15.5% at $F(r = 1$ cm, $\theta = 0°)$ and 12.7% at $F(r = 2$ cm, $\theta = 0°)$. Kennedy et al. reported $F(r, \theta)$ MC results from 0° to

90° for 0.5, 1, 2, 3, 4, and 5 cm. At 42 common positions, the MC results of Kennedy et al. and Rivard were in agreement within 1.0% on average with maximum differences of 5.7% at $F(r = 0.5\ \text{cm}, \theta = 0°)$ and 8.2% at $F(r = 3\ \text{cm}, \theta = 0°)$. The relatively higher $F(r, \theta = 0°)$ values of Kennedy et al. were attributed to their thinner endwelds in comparison to Rivard. At $\theta \geq 10°$, agreement for all distances was always within 0.5%. Given the good agreement with the other datasets and the larger range of radii and polar angles covered by the MC-based $F(r, \theta)$ dataset from Rivard,[71] it was selected for ${}_{\text{CON}}F(r, \theta)$.

A6. THERAGENICS MODEL AGX100 ^{125}I SOURCE

The I-Seed™ model AgX100 ^{125}I source was introduced in 2010 by Theragenics, Corp. (Buford, GA, USA), and is currently posted on the Registry. It has a 2 μm thick coating of $Ag^{125}I$ adsorbed onto a cylindrical silver rod (3.50 mm length and 0.59 mm diameter) without beveled ends. This is contained within a titanium capsule having a 4.50 mm outer length and a 0.80 mm outer diameter, see Fig. 1(f). The titanium tubing wall thickness is 0.05 mm. Both publications on dosimetry for this source used ${}_{\text{CON}}L = 0.35$ cm. The source has hemispherical endwelds that can range from 0.4 to 0.6 mm in thickness across different sources.

Mourtada et al.[77] reported results of MC calculations on the dosimetry parameters using the MCNPX (version 2.5.0)[75] photon transport simulation code and the MCPLIB04 photoatomic cross-section library. MC estimation of air kerma with 10^8 photon histories using a 5 keV energy cutoff were obtained in vacuum within a voxel covering 90.0° ± 7.5° whose center was positioned on the source transverse plane to approximate the NIST WAFAC measurement geometry. The MCNPX pedep tally estimator was used for calculating air kerma in vacuum and absorbed dose to water. MC estimations of dose to water with 3.15×10^9 photon histories covered a radial range of 0.01 to 10 cm with radial binning no greater than 0.05 cm, with 1° binning for $0° \leq \theta \leq 90°$. The ^{125}I photon spectrum recommended in the 2004 AAPM TG-43U1 report was used.

Chen et al.[79] reported results of measurements in a model 457 SolidWater™ phantom (Radiation Measurements, Inc., Middleton, WI, USA) using TLD-100 1 mm^3 cubes calibrated with 6 MV photons from a linac. TLD response in the phantom was corrected to derive dose to water in water using a MC-derived correction based on the MC study by Mourtada et al.[77] Measurements of Λ were linked to source strength calibrations reported by the manufacturer using equipment calibrated with sources calibrated with the NIST WAFAC. Measurements in SolidWater™ ranged from 0.5 cm to 7 cm in 0.5 cm increments for evaluation of $g_L(r)$, and from 1 cm to 6 cm in 1 cm increments and $0° \leq \theta \leq 90°$ with 10° increments for evaluation of $F(r, \theta)$.

A6.1. Model AgX100 dose-rate constant

Mourtada et al.[77] calculated $\Lambda = (0.918 \pm 0.024)$ cGy h^{-1} U^{-1} using the NIST WAFAC geometry for estimation of s_K. Rodriguez and Rogers reported MC results of $\Lambda = (0.900 \pm 0.002)$ cGy h^{-1} U^{-1} also using the NIST WAFAC geometry.[44] The average of these values was chosen for ${}_{\text{MC}}\Lambda = (0.909 \pm 0.024)$ cGy h^{-1} U^{-1}, instead of the (0.943 ± 0.024) cGy h^{-1} U^{-1} value suggested by Mourtada et al. and also by Chen et al., based on pointwise determination of s_K not accounting for volume averaging of the NIST WAFAC. Chen et al.[78] measured $\Lambda = (0.995 \pm 0.066)$ cGy h^{-1} U^{-1} using nine separate TLD experiments that were performed with three different AgX100 sources. Chen et al.[78] also measured Λ using a high-purity germanium detector. This photon spectrometry technique is a combination of measurements and MC methods, and produced a value of (0.957 ± 0.042) cGy h^{-1} U^{-1}.[29] However, the spectrometry technique is not traceable to a primary standard dosimetry laboratory, has been shown to be systematically incorrect,[24] and therefore was not used for derivation of ${}_{\text{EXP}}\Lambda$. Consequently, the TLD result of Chen et al.[78] was selected for ${}_{\text{EXP}}\Lambda$. In combination with the ${}_{\text{MC}}\Lambda$ result, a value of ${}_{\text{CON}}\Lambda = (0.952 \pm 0.043)$ cGy h^{-1} U^{-1} was determined. The ${}_{\text{MC}}\Lambda$ value was 8.6% lower than the ${}_{\text{EXP}}\Lambda$ value and within the combined standard uncertainty of the measurements and MC estimations.

A6.2. Model AgX100 radial dose function

Chen et al. measured $g_L(r)$ from 0.5 cm to 7.0 cm with 0.5 cm increments. Mourtada et al. calculated $g_L(r)$ at 21 distances. At 12 distances in common with the study by Chen et al., the results of Mourtada et al. were on average within 2% of the results of Chen et al. and were 3.1%, 3.9%, and 7.0% higher at 5, 6, and 7 cm, respectively. This was considered good agreement given the experimental uncertainties. Because of this good agreement between the MC and measured $g_L(r)$ datasets, the large radial range of 0.1 cm to 10 cm and the high resolution, the MC-based $g_L(r)$ results of Mourtada et al. were selected for ${}_{\text{CON}}g_L(r)$.

A6.3. Model AgX100 anisotropy functions

Chen et al. measured $F(r, \theta)$ from 1 cm to 6 cm with 1 cm increments and at polar angles of 0° to 90° with 10° increments. Mourtada et al. reported MC results of $F(r, \theta)$ at 0.25, 0.5, 1, 2, 3, 5, and 7 cm and with high angular resolution. To maximize the data comparison with Chen et al., Mourtada et al. kindly shared their high-resolution data as used for generating their Fig. 5. Comparing the $F(r, \theta)$ results from Chen et al. at 54 common positions with the study by Mourtada et al. yielded an average difference of 1.6%, with maximum differences of 19% or more occurring at $\theta = 0°$. Excluding comparisons at this polar angle, the agreement improved with an average difference of only 0.2% and a maximum difference of 8% over the ranges of 1 cm to 6 cm and $10° \leq \theta \leq 90°$. Given the relatively good agreement between the candidate datasets and the higher spatial and angular resolution of the study by Mourtada et al., their MC results were selected as the ${}_{\text{CON}}F(r, \theta)$ dataset.

A7. CIVATECH ONCOLOGY MODEL CS10 ^{103}PD SOURCE

The CivaString™ model CS10 ^{103}Pd source was introduced by CivaTech Oncology, Inc. (Research Triangle Park, NC, USA) in 2014. The nominal overall shape is a right cylinder (10.9 mm length and 0.85 mm outer diameter), see Fig. 1(g). An unusual feature is that the source is flexible, due to the organic polymer encapsulation. The model CS10 source is currently posted on the Registry, and is part of the CivaString family of sources having L_{eff} ranging from 1 cm to 6 cm in 1 cm increments. Within each 1 cm length are four wells containing ^{103}Pd and a centrally positioned gold marker (0.80 mm long and 0.25 mm diameter). As the NIST WAFAC is limited to measurements of sources having $L \leq 1$ cm, calibrations for longer sources must be performed through comparisons with the model CS10. Both publications that evaluated dosimetry for the model CS10 source used $L = 1.00$ cm.

Rivard et al.[79] reported results of MC calculations on the dosimetry parameters for the CivaString family of sources, having L_{eff} ranging from 1 cm to 6 cm in 1 cm increments. Version 1.60 of the MCNP5 radiation transport code[55] and the *F4 and F6 tally estimators were used for determinations of air kerma and absorbed dose to water, respectively. The ^{103}Pd photon energy spectrum was taken from the NNDC database[22] and is based on the spectrum evaluated by De Frenne,[80] which did not differ substantially from that recommended in the 2004 AAPM TG-43U1 report.[2] Due to the plastic encapsulation, the influence on dosimetry results when including the 2.7 keV emissions from ^{103}Pd was examined, but these photons contributed $\leq 0.1\%$ of the dose to water beyond 0.13 mm from the encapsulation. The mass-energy absorption coefficients used to convert photon energy fluence in vacuum to air kerma were taken from NIST.[56] The photoatomic cross-section libraries were based on ENDF/B-VI.[72] Air kerma was scored using a 5 keV energy cutoff in vacuum 30 cm from the source in a voxel covering $90.0° \pm 7.5°$ whose center was positioned on the source transverse plane to approximate the NIST WAFAC measurement geometry. Absorbed dose to water was scored in a 40 cm diameter spherical water phantom at distances of 0.05 cm to 1 cm in 0.05 cm increments and at distances of 1 cm to 15 cm in 0.1 cm increments. Polar angle sampling was from $0° \leq \theta \leq 180°$ in 1° increments. MC studies in vacuum and water both used 10^9 photon histories.

Reed et al. published results for both TLD measurements and MC calculations of the model CS10 source.[81] Measurements performed using TLD-100 1 mm^3 cubes calibrated with ^{60}Co photons based on the methods of Nunn et al.[42] Irradiations were performed in two high-purity $30.0 \times 30.0 \times 0.1$ cm^3 PMMA phantoms having independent composition analyses. This material was chosen over solid water mixtures due to the reduced uncertainties when correcting measured results to yield absorbed dose to water. One phantom was drilled to accommodate TLDs for measurements of $g_L(r)$ while the other phantom had holes drilled for $F(r, \theta)$ measurements. In all cases, at least 5 cm of backscattering material at each detector position was added so that measurements were performed under appropriately large scatter conditions. Following the CLA recommendations for measurements of $_{\text{EXP}}\Lambda$,[7] three model CS10 ^{103}Pd sources were calibrated at NIST. To yield dose to water, Reed et al. corrected TLD measurements in phantom through simulating the experimental conditions using the MCNP5 version 1.60 radiation transport code[55] with the same cross-section libraries and similar methods as Rivard,[79] but with the MCPLIB84 photoatomic cross-section library.[82] Measurements by Reed et al.[81] also included use of a NaI scintillation detector to evaluate azimuthal asymmetry of radiation emissions due to the noncylindrically symmetric design of the ^{103}Pd wells. For three different model CS10 sources, they observed that $\geq 95\%$ of the measurement points distributed uniformly around the sources were within 1.2% of the mean value. Their MC calculations also indicated that dosimetric concerns for azimuthal asymmetry were unfounded. MC methods used to evaluate the TG-43 dosimetry parameters were performed with the model CS10 source centrally positioned within a 30 cm diameter water sphere. MC estimation of air kerma using a 5 keV energy cutoff were scored in vacuum 30 cm from the source in a voxel covering $90.0° \pm 7.5°$ whose center was positioned on the source transverse plane to approximate the NIST WAFAC aperture. All MC calculations by Reed et al. utilized 10^{10} photon histories.

A7.1. Model CS10 dose-rate constant

Rivard reported a MC result of $\Lambda = (0.623 \pm 0.008)$ cGy h^{-1} U^{-1}.[79] Reed et al.[81] reported a MC result of $\Lambda = (0.622 \pm 0.009)$ cGy h^{-1} U^{-1} and a TLD-measured value in PMMA for Λ in water of (0.660 ± 0.027) cGy h^{-1} U^{-1}. The TLD value from Reed et al. was selected as $_{\text{EXP}}\Lambda$. The Λ MC results from Rivard et al. and Reed et al. agreed within 0.2%, and their average was taken as $_{\text{MC}}\Lambda = (0.623 \pm 0.006)$ cGy h^{-1} U^{-1}. An equally weighted average of $_{\text{EXP}}\Lambda$ and $_{\text{MC}}\Lambda$ yielded $_{\text{CON}}\Lambda = (0.641 \pm 0.017)$ cGy h^{-1} U^{-1}. The $_{\text{MC}}\Lambda$ value was 5.7% lower than the $_{\text{EXP}}\Lambda$ value and within two standard deviations of the measurement uncertainties.

A7.2. Model CS10 radial dose function

Reed et al.[81] reported TLD and MC $g_L(r)$ results at ten distances. Their MC results were lower than their measured results by 14%, 20%, and 26% at 3, 4, and 5 cm, respectively. At nine distances in common with Rivard et al.,[79] the MC results of Reed et al. were within 0.4% of those from Rivard et al. for 0.5 cm to 5 cm. Because of the good agreement with other $g_L(r)$ datasets, the large radial range of 0.05 cm to 15 cm, and the high resolution, the MC-based $g_L(r)$ results of Rivard et al.[79] were selected for $_{\text{CON}}g_L(r)$. Reed et al. advised against use of the 1D dose calculation formalism when the source orientation is known because of substantial dose calculation errors in comparison to the 2D dose calculation

formalism. Consequently, no $g_P(r)$ are recommended for this source model.

A7.3. Model CS10 anisotropy functions

Reed et al.[74] measured and calculated $F(r, \theta)$ at 1, 2, 3, and 4 cm and polar angles of 0° to 90° with 10° increments. Their results were in agreement within 0.2% on average, with the largest differences occurring along the source long axis with discrepancies of 4.9% at $F(r = 1$ cm, $\theta = 0°)$ and 2.6% at $F(r = 4$ cm, $\theta = 0°)$. A comparison of $F(r, \theta)$ results from TLD measurements by Reed et al., to MC results from Rivard et al. at 30 common positions were in agreement within 0.01% on average with the largest differences occurring along the source long axis with discrepancies of 6.2% at $F(r = 1$ cm, $\theta = 0°)$ and 5.8% at $F(r = 4$ cm, $\theta = 0°)$. A comparison of $F(r, \theta)$ results from MC measurements by Reed et al., to MC results from Rivard et al. at 30 common positions were in agreement within 0.2% on average with the largest differences occurring along the source long axis with discrepancies of 1.4% at $F(r = 1$ cm, $\theta = 0°)$ and 3.1% at $F(r = 4$ cm, $\theta = 0°)$. Given the good agreement with the other datasets and the larger range of radii and high resolution of polar angles covered by the MC-based $F(r, \theta)$ dataset from Rivard et al.,[79] it was selected for ${}_{\text{CON}}F(r, \theta)$.

Reed et al.[81] included $\phi_{an}(r)$ results from their TLD and MC results, as well as from the MC results of Rivard et al.[79] However, they advised against use of the 1D dose calculation formalism when the source orientation is known because of substantial dose calculation errors in comparison to the 2D dose calculation formalism due to volume averaging over dose as a function of polar angle. They reported that dose errors would exceed +84% and −90% near the source ends or at the source transverse bisector, respectively, when using the 1D dose calculation formalism. This effect has been shown to cause < 2% differences in D_{90} for LDR prostate implants with conventional seeds.[83,84] However, the magnitude and spatial extent of these dose calculation errors are larger for this source model (i.e., $L = 1.00$ cm) than for sources having $L \leq 0.4$ cm. Consequently, no ${}_{\text{CON}}\phi_{an}(r)$ are recommended for this source model.

A8. IBT MODEL 1031L ^{103}PD SOURCE

The InterSource™ model 1031L ^{103}Pd source was introduced in 2002 by International Brachytherapy SA (Seneffe, Belgium) and distributed by IBt, Inc. (Norcross, GA, USA). It is no longer in production, but previously met the AAPM brachytherapy dosimetric prerequisites and the AAPM CLA subcommittee requirements. The source was comprised of two hollow titanium tubes with circumferential laser welding at the ends, see Fig. 1(h). The capsule length was 4.5 mm with a 0.81 mm outer diameter and a 0.5 mm diameter hollow inner section. Between these two titanium tubes were sandwiched a 45 μm thick, 1.27 mm long Pt(90% mass) + Ir (10% mass) radiopaque marker and three organic matrices containing ^{103}Pd. The middle section containing ^{103}Pd was reported by the manufacturer to be 0.5 mm long and 9 μm thick, while the two outer sections were 0.8 mm long and 15 μm thick. The ^{103}Pd spanned 3.7 mm in greatest linear extent. Meigooni et al.[85] and Reniers et al.[86] used L_{eff}=0.37 cm, while Taylor and Rogers used $L_{\text{eff}} = 0.435$ cm based on the approach recommended in the 2004 TG-43U1 report.[2] This latter value was chosen as ${}_{\text{CON}}L_{\text{eff}} = 0.435$ cm.

Meigooni et al.[85] reported dosimetry results of TLD measurements and MC calculations of the model 1031L ^{103}Pd source. Measurements were performed using TLD-100 chips and 1 mm^3 cubes calibrated using 6 MV photons from a linac. Irradiations were performed in slabs of model 457 SolidWater™ (Radiation Measurements, Inc., Middleton, WI, USA) where one phantom had holes to accommodate TLDs for measurements of $g_L(r)$ while the other phantom had holes for TLD measurements of $F(r, \theta)$. The TLD chips were used for measurements at $r > 2$ cm while the smaller TLD cubes were used for $r \leq 2$ cm to increase signal at larger distances while minimizing detector volume averaging at smaller distances. Measurements of Λ used three sources calibrated at NIST, following the CLA source calibration recommendations. To convert TLD response to dose to water results, Meigooni et al. corrected measurements in phantom through MC studies of the experimental conditions using the PTRAN radiation transport code.[87] This software was also used by Meigooni et al. to obtain values of Λ and the other dosimetry parameters in both SolidWater™ and water. The ^{103}Pd photon spectrum was taken from the NCRP handbook,[88] with photoatomic cross-sections libraries from DLC-99[89] and photon fluence multiplied by mass-energy absorption coefficients from Hubbell and Seltzer.[56] A total of 2.1×10^6 photon histories were used for MC calculations in water.

Reniers et al.[86] also reported dosimetry results of TLD measurements and MC calculations of the model 1031L ^{103}Pd source. Measurements were performed using TLD-100 1 mm^3 cubes calibrated using 6 MV photons from a linac. Irradiations were performed in a slab of model 457 SolidWater™ with at least 5 cm of backscattering material at each detector position added so that measurements were performed under appropriately large scatter conditions. Measurements of Λ used three sources with calibrations performed by the manufacturer that were traceable to NIST. To convert TLD response to dose to water results, Reniers et al. corrected measurements in phantom through MC simulations of the experimental conditions using the MCNP4B radiation transport code.[90] This software was also used by Reniers et al. to obtain values of Λ and the other dosimetry parameters in both SolidWater™ and water. Unspecified were the s_K calculation geometry, the number of photon histories for s_K calculations in air and for dose calculations in water, and the source of the ^{103}Pd photon spectrum. Reniers et al. used the MCNP4B default cross-section libraries, based on the data of Storm and Israel,[91] later shown by DeMarco et al. to be erroneous for the photon energies pertinent to this study.[92] Consequently, results from Reniers et al. were excluded from derivation of depth-dependent consensus data such as $g_L(r)$.

Taylor and Rogers[15] reported the results of MC calculations for the model 1031L ^{103}Pd source in their database.[14] MC calculations were performed with an EGSnrc-based user-code called BrachyDose, which used a track-length estimator to score collision kerma per history in each voxel. XCOM photon cross-section data was employed, as well as photon spectra from the TG-43U1 report. By simulating up to $4x10^{10}$ histories, Type A uncertainties were maintained at less than 2% for dosimetry parameters calculated at 10 cm from the source. s_K was calculated in vacuum with a 5 keV photon cutoff to maintain consistency with the NIST WAFAC standard. Results were reported for both a point-like detector and for a voxel subtending a solid angle similar to that of the NIST WAFAC.

A8.1. Model 1031L dose-rate constant

Meigooni et al.[85] reported TLD results in SolidWater™ of (0.664 ± 0.033) cGy h^{-1} U^{-1}, MC results in SolidWater™ of (0.660 ± 0.020) cGy h^{-1} U^{-1}, and MC results in water of (0.696 ± 0.021) cGy h^{-1} U^{-1}. Correcting the TLD measurements in SolidWater™ by the ratio of MC results in water to SolidWater™ (a factor of 1.053) yielded a TLD measurement of Λ in water of (0.700 ± 0.044) cGy h^{-1} U^{-1}. Source strengths used for the TLD measurements of Λ in SolidWater™ by Meigooni et al. were based on the calibration of three sources subject to the 1999 NIST WAFAC anomaly,[2] such that the corrected S_K results for this batch were 4.0% lower.[93] Consequently, the TLD measurement of Λ in water was corrected to (0.728 ± 0.046) cGy h^{-1} U^{-1}.

Reniers et al.[86] reported TLD results in SolidWater™ of (0.672 ± 0.047) cGy h^{-1} U^{-1}, MC results in SolidWater™ of (0.657 ± 0.007) cGy h^{-1} U^{-1}, and MC results in water of (0.692 ± 0.007) cGy h^{-1} U^{-1}, with only statistical uncertainties contributing to the MC results. These three values were correctly stated in their abstract, but their MC and TLD results in WT1 were reversed in Table 5 of their publication. Correcting the TLD measurements in SolidWater™ by the ratio of MC results in water to SolidWater™ (a factor of 1.055) yielded a TLD measurement of Λ in water of (0.708 ± 0.046) cGy h^{-1} U^{-1}.

Taylor and Rogers[15] reported MC results for the point detector of (0.664 ± 0.002) cGy h^{-1} U^{-1} and (0.663 ± 0.002) cGy h^{-1} U^{-1} for the NIST WAFAC measurement geometry, with only statistical uncertainties contributing to the MC results. These values were indistinguishable within the reported statistical uncertainties. This was to be expected given that the source design did not introduce any shielding of the radiation emissions near the source transverse plane.

The corrected TLD results of Meigooni et al. and Reniers et al. were within 3.7% and agreed within their uncertainties. The average value was selected for $_{EXP}\Lambda$ = (0.718 ± 0.033) cGy h^{-1} U^{-1}. Results from the three MC studies agreed within a range of 2.6% about the average, and their average was selected for $_{MC}\Lambda$ = (0.684 ± 0.007) cGy h^{-1} U^{-1}. An equally weighted average of $_{EXP}\Lambda$ and $_{MC}\Lambda$ yielded $_{CON}\Lambda$ = (0.701 ± 0.020) cGy h^{-1} U^{-1}. The $_{MC}\Lambda$ value was 4.8% lower than the $_{EXP}\Lambda$ value and within two standard deviations of the measurement uncertainties.

A8.2. Model 1031L radial dose function

Meigooni et al.[85] measured $g_L(r)$ at 12 distances. These TLD measurements were corrected with the ratio of MC results in water to SolidWater™ to obtain measured values in water. Their MC results were within 9% of their measured results over the range of 0.5 cm to 10 cm. Taylor and Rogers[15] reported $g_L(r)$ results from 0.05 cm to 10 cm with high resolution close to the source. Their $g_L(r_0)$ value (0.9942) was set equal to unity.

The TLD and MC results of Meigooni et al. were corrected for $_{CON}L_{eff}$ = 0.435 cm to make direct comparisons with the $g_L(r)$ results from Taylor and Rogers, which used L_{eff} = 0.435 cm. At positions common to each dataset used for comparisons to Taylor and Rogers, the TLD results of Meigooni et al. were within 10% for 0.5–6 cm with worse agreement at larger distances (e.g., maximum discrepancy of 23% at 8 cm). For a similar comparison of MC results from Meigooni et al., agreement with Taylor and Rogers was within 10% for 0.2–5 cm with discrepancies up to 15% at larger distances and 41% at 0.1 cm. These differences at very close distances may be related to the different lengths of the active component modeled by Taylor and Rogers. The results from Taylor and Rogers were selected as $_{CON}g_L(r)$ due to the large radial range and high resolution, and use of modern photoatomic cross-sections libraries.

A8.3. Model 1031L anisotropy functions

Meigooni et al.[85] measured $F(r, \theta)$ in SolidWater™ at 2, 3, 5, and 7 cm at polar angles of 0°, 15°, 45°, 60°, and 90° and performed MC estimations also in SolidWater™ at 0.5, 1, 2, 3, 5, and 7 cm and at polar angles from 0° to 90° with 5° binning. When correcting their TLD results to yield $F(r, \theta)$ in water, the results at 16 common positions were in agreement within 2% on average with the largest differences occurring along the source long axis with discrepancies of 17% at $F(r = 3$ cm, $\theta = 15°)$ and 19% at $F(r = 2$ cm, $\theta = 0°)$.

Reniers et al.[86] measured $F(r, \theta)$ in SolidWater™ at 2, 3, and 5 cm at polar angles from 0° to 90° with 10° binning and performed MC estimations also in SolidWater™ at these same distances at polar angles from 0° to 90° with 5° binning. When correcting their TLD results to yield $F(r, \theta)$ in water, the results at 27 common positions were in agreement within 2% on average with the largest differences occurring along the source long axis with a maximum of 16% at $F(r = 2$ cm, $\theta = 0°)$.

Comparisons of TLD results from Meigooni et al. and Reniers et al. were not performed as there were only six common positions (radii of 2, 3, and 5 cm and polar angles of 0° and 60°). Results of MC calculations in SolidWater™

from Meigooni et al. and Reniers et al. at 27 common positions were in agreement within 1% on average with the largest difference of 10% occurring at $F(r = 5\ \text{cm}, \theta = 20°)$. Upon close examination, it was evident that the MC results from Reniers et al. in SolidWater™ at $r = 2$ cm were identical to those in water, which may have been reported in error.

Taylor and Rogers[15] reported $F(r, \theta)$ in water for 0.1 cm to 10 cm at polar angles from 0° to 90° with assorted bin widths. The $F(r, \theta)$ results from Taylor and Rogers compared with those from Meigooni et al. (corrected for $L_{\text{eff}} = 0.435$ cm) at 90 common positions were in agreement within 5% for $30° \le \theta \le 90°$. However, agreement worsened as polar angles diminished with results from Meigooni et al. being a factor of two and three larger than those of Taylor and Rogers at $F(r = 1\ \text{cm}, \theta = 0°)$ and $F(r = 5\ \text{cm}, \theta = 0°)$, respectively. The $F(r, \theta)$ results from Taylor and Rogers compared with those from Reniers et al. (corrected for $L_{\text{eff}} = 0.435$ cm) at 54 common positions were in agreement within 4% for $30° \le \theta \le 90°$. However, agreement worsened as polar angles diminished with results from Reniers et al. being a 15% lower than those of Taylor and Rogers at $F(r = 5\ \text{cm}, \theta = 0°)$. Given the aforementioned comparisons to the other datasets and the larger range of radii with high resolution of polar angles covered by the MC-based $F(r, \theta)$ dataset from Taylor and Rogers, it was selected for ${}_{\text{CON}}F(r, \theta)$.

A9. IBT MODEL 1032P ^{103}PD SOURCE

The OptiSeed™ model 1032P ^{103}Pd source was introduced in 2005 by International Brachytherapy SA (Seneffe, Belgium) and distributed by IBt, Inc. (Norcross, GA, USA). It is no longer in production, but previously met the AAPM brachytherapy dosimetric prerequisites and the AAPM CLA subcommittee requirements. The source was shaped like a right cylinder (5.00 mm long and 0.80 mm outer diameter) with concave spherical sockets at both ends to accommodate spacers for custom stranding preceding implantation, see Fig. 1(i). This plastic encapsulation contained a centrally positioned gold marker (2.00 mm long and 0.45 mm diameter) with two cylindrical polymer-based ^{103}Pd carriers (0.7 mm long and 0.4 mm diameter) spaced 3.10 mm apart and offset 1.55 mm from the source center. There was a 0.20 mm air gap between the gold marker and each of the ^{103}Pd carriers. The ^{103}Pd spanned 3.80 mm in greatest linear extent. Bernard and Vynckier[94] used $L_{\text{eff}} = 0.37$ cm, while and Wang and Hertel[95] and Taylor and Rogers[14] used $L_{\text{eff}} = 0.38$ cm based on the approach recommended in the 2004 TG-43U1 report.[2] The dosimetric study by Khan et al.[96] did not report a value for L_{eff} and only examined Λ. A value of ${}_{\text{CON}}L_{\text{eff}} = 0.38$ cm was selected.

Bernard and Vynckier[94] reported dosimetry results of TLD measurements and MC estimations of the model 1032P ^{103}Pd source. Measurements were performed using TLD-100 1 mm^3 cubes calibrated using 6 MV photons from a linac. Irradiations were performed in slabs of model 457 SolidWater™ (Radiation Measurement Inc., Middletown, WI, USA) where one slab was machined with holes to accommodate TLDs for measurements of $g_{\text{L}}(r)$ while the other slab was machined with holes for TLD measurements of $F(r, \theta)$. Measurements of Λ used four sources calibrated at NIST following the CLA source calibration recommendations.[7] To convert TLD response to dose to water results, Bernard and Vynckier corrected measurements in phantom through MC simulations of the experimental conditions using the MCNP4C radiation transport code,[97] using erroneous photoelectric cross-section data from Storm and Israel.[91,98] Consequently, these data were not considered for deriving consensus data.

Wang and Hertel[95] also reported dosimetry results of TLD measurements and MC estimations of the model 1032P ^{103}Pd source. Measurements were also performed using TLD-100 1 mm^3 cubes calibrated using ^{60}Co NIST-traceable calibrations. Irradiations were performed in a $30 \times 30 \times 20$ cm^3 VirtualWater™ phantom from Med-Cal, Inc. (Verona, WI, USA). Measurements of Λ used two sources with calibrations performed by NIST. To convert TLD response to dose to water results, Wang and Hertel corrected measurements in phantom through MC simulations of the experimental conditions using the MCNP5 radiation transport code. This software was also used by Wang and Hertel to obtain values of Λ and the other dosimetry parameters in both VirtualWater and water. The ^{103}Pd photon spectrum was taken from the ICRP Publication 38.[99] MCNP default photoatomic cross-sections libraries were based on ENDF/B-VI release 8. The MCNP F6 tally was used to estimate kerma within voxels. At 10 cm in air on the source transverse plane, s_{K} was estimated with a 5 keV energy cutoff, but without simulating the NIST WAFAC measurement geometry. The number of photon histories for derivation of Λ and the other dosimetry parameters was unspecified.

Taylor and Rogers[15] reported the results of MC calculations for the model 1032P ^{103}Pd source in their database. MC calculations were performed with an EGSnrc-based user-code called BrachyDose, which used a track-length estimator to score collision kerma per history in each voxel. XCOM photon cross-section data were employed, as well as photon spectra from the TG-43U1 report. By simulating up to 4×10^{10} histories, Type A uncertainties were reduced to less than 2% for dosimetry parameters calculated at 10 cm from the source. s_{K} was calculated in vacuum with a 5 keV photon cutoff to maintain consistency with the NIST WAFAC standard. Results were reported for both a point-like detector and for a voxel subtending a solid angle similar to that of the NIST WAFAC.

Other related literature includes Abboud et al.,[100] who reported dosimetry results using MC and TLD for a similar source (OptiSeed$^{\text{exp}}$) having the central gold marker replaced with polyetheretherketon, and by Mowlavi and Yazdani[101] who reported MC results in soft tissue. Dosimetry results from both of these papers were not included in formulating a consensus dataset for the model 1032P ^{103}Pd source.

A9.1. Model 1032P dose-rate constant

For VirtualWater, Wang and Hertel[95] reported a TLD result of (0.727 ± 0.050) cGy h^{-1} U^{-1} and a MC result of (0.716 ± 0.015) cGy h^{-1} U^{-1}. In water, Wang and Hertel reported a TLD result of (0.675 ± 0.054) cGy h^{-1} U^{-1} and a MC result of (0.665 ± 0.014) cGy h^{-1} U^{-1}. Taylor and Rogers[15] reported MC results for the point detector of (0.670 ± 0.002) cGy h^{-1} U^{-1} and (0.669 ± 0.002) cGy h^{-1} U^{-1} for the NIST WAFAC geometry, with only statistical uncertainties contributing to the MC results. These values were indistinguishable within the reported statistics. This was to be expected given that the source design did not introduce any shielding of the radiation emissions near the source transverse plane. Khan et al.[96] reported TLD results in water of (0.675 ± 0.051) cGy h^{-1} U^{-1}. Derivation of ${}_{EXP}\Lambda$ = (0.675 ± 0.037) cGy h^{-1} U^{-1} included TLD results from Wang and Hertel and by Khan et al. Derivation of ${}_{MC}\Lambda$ = (0.667 ± 0.007) cGy h^{-1} U^{-1} included results from Wang and Hertel and by Taylor and Rogers. An equally weighted average of ${}_{EXP}\Lambda$ and ${}_{MC}\Lambda$ yielded ${}_{CON}\Lambda$ = (0.671±0.019) cGy h^{-1} U^{-1}. The ${}_{MC}\Lambda$ value was 1.2% lower than the ${}_{EXP}\Lambda$ value and within the standard uncertainty of the measurements.

A9.2. Model 1032P radial dose function

Comparison of the MC results in water from Wang and Hertel to MC results in water from Taylor and Rogers[15] at 24 common distances over 0.1 cm to 7 cm demonstrated good agreement with an average discrepancy of 1.4% and a maximum discrepancy of 3.3% at 7 cm. The MC results of Taylor and Rogers were selected as ${}_{CON}g_L(r)$ given their larger range, smoother behavior, and higher resolution in comparison to MC results from Wang and Hertel. Taylor and Rogers[15] reported $g_L(r)$ results from 0.05 cm to 10 cm with high resolution close to the source. Their $g_L(r_0)$ value (0.9994) was set equal to unity.

A9.3. Model 1032P anisotropy functions

Wang and Hertel[95] reported TLD and MC $F(r, \theta)$ results in VirtualWater™ at 2, 3, 5, and 7 cm from 0° to 90° with 10° binning, and MC results in water from 0.5 to 7 cm covering from 0° to 90° with 5° binning. When correcting their TLD results to yield $F(r, \theta)$ in water, the results at 32 common positions were in agreement within 1% on average, but with discrepancies of 9% at $F(r = 5\text{ cm}, \theta = 20°)$ and $F(r = 7\text{ cm}, \theta = 60°)$.

Taylor and Rogers[15] reported $F(r, \theta)$ in water for 0.1 cm to 10 cm at polar angles from 0° to 90° with assorted bin widths. The MC results in water from Wang and Hertel were compared to Taylor and Rogers, where the $F(r = 7.0\text{ cm}, \theta)$ results of Wang and Hertel were compared to the $F(r = 7.5\text{ cm}, \theta)$ results of Taylor and Rogers. There was excellent agreement at all 72 common positions with no discrepancy exceeding 1.4%. Given the relatively good agreement between the candidate MC datasets and the higher spatial and angular resolution of the study by Taylor and Rogers, their MC results were selected as the ${}_{CON}F(r, \theta)$ dataset.

A10. ISOAID MODEL IAPD-103A ^{103}PD SOURCE

The ADVANTAGE™ model IAPd-103A ^{103}Pd source was introduced in 2006 by IsoAid, LLC (Port Richey, FL, USA). The source is currently posted on the Registry and consists of four polystyrene resin spheres (0.5 mm diameter) absorbed throughout with ^{103}Pd. Two resin spheres are placed on either side of a right cylindrical silver marker (1.25 mm length and 0.50 mm diameter). These items are sealed within a titanium capsule having a 4.50 mm outer length, 0.80 mm outer diameter, 0.35 mm endweld thicknesses, and 0.050 mm wall thickness, see Fig. 1(j). Given the assumption that the resin spheres and silver marker are positioned uniformly within the void within the titanium capsule, Meigooni et al.[102] used a value of L_{eff} = 0.361 cm. Sowards[103] used a value of L_{eff}=0.34 cm and Taylor and Rogers[15] used a value of L_{eff} = 0.362 cm. An independent evaluation using the dimensional information provided in Meigooni et al. and Taylor and Rogers led to selection of the ${}_{CON}L_{eff}$ = 0.362 cm value as used in Taylor and Rogers, which negligibly differs from the L_{eff} value used by Meigooni et al.

Meigooni et al.[102] reported dosimetry results of TLD measurements and MC estimations of the model IAPd-103A ^{103}Pd source. Measurements performed using TLD-100 chips calibrated using 6 MV photons from a linac. Irradiations were performed in slabs of model 457 SolidWater™ (Radiation Measurement Inc., Middletown, WI, USA) where one slab was machined with holes to accommodate TLDs for measurements of $g_L(r)$ while the other slab was machined with holes for TLD measurements of $F(r, \theta)$. The data reported at each measurement position was the average from at least 16 separate measurements. Measurements of Λ used sources calibrated at NIST following the CLA source calibration recommendations.[7] To convert TLD response to dose to water results, Meigooni et al. corrected measurements in phantom through MC simulations of the experimental conditions using version 7.3 of the PTRAN[87] radiation transport code and the next flight point kerma estimator, photon cross-section libraries based on ENDF/B-VI release 8,[72] and mass-energy absorption coefficients from Hubbell and Seltzer to convert photon energy fluence to absorbed dose.[56] Using an inverse-square correction, s_K was estimated in a 30.0-cm diameter dry air sphere on the source transverse plane with a 5 keV energy cutoff, but without simulating the NIST WAFAC active volume geometry. Up to 5×10^6 histories per simulation were used such that statistical uncertainties (k = 1) were < 2% for $r \leq 5$ cm. While the ^{103}Pd photon spectrum was not specified, the spatial distribution of ^{103}Pd emissions was assumed to be uniformly distributed within the resin spheres.

Sowards[103] reported MC results using version 7.44 of the PTRAN code with the same next flight point kerma estimator

as well as the same approach to deriving s_K as Meigooni et al. A total of 10^7 photon histories were used for calculations in water. Sowards reported that PTRAN employs the ^{103}Pd photon spectrum from the Medical Internal Radiation Dosimetry (MIRD) pamphlet.[104]

Taylor and Rogers[15] reported the results of MC calculations for the model IAPd-103A ^{103}Pd source in their database. MC calculations were performed with an EGSnrc-based user-code called BrachyDose, which used a track-length estimator to score collision kerma per history in each voxel. XCOM photon cross-section data were employed, as well as photon spectra from the TG-43U1 report. By simulating up to 4×10^{10} histories, Type A uncertainties were less than 2% for dosimetry parameters calculated at 10 cm from the source. s_K was calculated in vacuum with a 5 keV photon cutoff to maintain consistency with the NIST WAFAC standard. Results were reported for both a point-like detector and for a voxel subtending a solid angle similar to that of the NIST WAFAC.

A10.1. Model IAPd-103A dose-rate constant

Meigooni et al.[102] measured (0.68 ± 0.05) cGy h^{-1} U^{-1} in SolidWater™, which was corrected to (0.70 ± 0.06) cGy h^{-1} U^{-1} for water using MC-based calculations in both SolidWater™ and water. Meigooni et al. MC estimations in SolidWater™ (0.67 ± 0.02) cGy h^{-1} U^{-1} and water (0.69 ± 0.02) cGy h^{-1} U^{-1} were in agreement with TLD-measured results to within 1%. Sowards[103] calculated (0.709 ± 0.014) cGy h^{-1} U^{-1} in water, which was within 1% of the measured result and 3% of the simulated result from Meigooni et al. Taylor and Rogers[15] reported (0.687 ± 0.001) cGy h^{-1} U^{-1} for MC estimation of a point detector and the NIST WAFAC geometry. However, Rodriguez and Rogers later reported MC results of Λ = (0.661 ± 0.002) cGy h^{-1} U^{-1} using the NIST WAFAC geometry,[44] where the difference with Taylor and Rogers[15] was attributed to a minor MC coding error. An average of the three MC estimations produced $_{MC}\Lambda$ = (0.687 ± 0.008) cGy h^{-1} U^{-1}. The sole measured result in water from Meigooni et al. was selected as the $_{EXP}\Lambda$ value, and averaged with $_{MC}\Lambda$ to yield $_{CON}\Lambda$ = (0.693 ± 0.031) cGy h^{-1} U^{-1}. The $_{MC}\Lambda$ value was 1.9% lower than the $_{EXP}\Lambda$ value and within the standard uncertainty of the measurements.

A10.2. Model IAPd-103A radial dose function

Meigooni et al.[102] reported TLD and MC $g_L(r)$ results in SolidWater™ at 0.5, 1, 1.5, 2, 3, 4, 5, 6, and 7 cm and MC results in water for $0.2 \le r \le 8$ cm. The MC results were used to correct the TLD measurements in SolidWater™ to yield measured results in water. Their TLD and MC results in water were in agreement on average within 1% with a maximum discrepancy of 9% at 6 cm and 7 cm. Comparing the results from Sowards[103] to Meigooni et al. MC results in water at 15 common distances covering 0.2–6 cm and corrected to $_{CON}L_{eff}$ = 0.362 cm, the average agreement was within 0.4% with no discrepancies beyond 2%. However, the MC results from Sowards were 4% lower at 7 cm and 17% lower at 8 cm than MC results in water from Meigooni et al. Comparing the results from Sowards to Meigooni et al. TLD results in water at seven common distances covering 0.5–5 cm and corrected to $_{CON}L_{eff}$ = 0.362 cm, the average agreement was within 0.1% with no discrepancies greater than 5%. However, the TLD results in water from Meigooni et al. were 9% higher at 6 cm and 12% higher at 7 cm than MC results from Sowards.

Comparing MC results in water from both Taylor and Rogers and Meigooni et al., the average agreement was 2% for 0.2–6 cm with a maximum discrepancy of 5%, and discrepancies of 9% at 7 cm and 22% at 8 cm. The TLD results in water from Meigooni et al. for 0.5–5 cm at common distances were on average 2% higher than the Taylor and Rogers results. Results from Meigooni et al. were 12% higher at 6 cm and 19% higher at 7 cm than Taylor and Rogers. Results from Taylor and Rogers[15] and from Sowards were in 2% agreement on average for 0.2–9 cm with a maximum discrepancy of 6%, and had discrepancies of 8% at 9.5 cm and 20% at 0.1 cm.

The MC results of Sowards in comparison to results from Taylor and Rogers were in substantially better agreement than the comparison of MC results from Meigooni et al. to results from Taylor and Rogers. TLD results in water from Meigooni et al. in comparison to the MC results in water from Meigooni et al., Sowards, and Taylor and Rogers at 7 cm were 9%, 13%, and 19% higher, respectively, and demonstrated a trend of worsened agreement with increasing distance. Because the MC results of Taylor and Rogers included a larger range and higher resolution in comparison to MC results from Sowards, the MC results from Taylor and Rogers were selected for $_{CON}g_L(r)$. Taylor and Rogers[15] reported $g_L(r)$ results from 0.05 cm to 10 cm with high resolution close to the source. Their $g_L(r_0)$ value (1.0067) was set equal to unity.

A10.3. Model IAPd-103A anisotropy functions

Meigooni et al.[102] reported MC $F(r, \theta)$ results in water at 0.5, 1, 2, 3, 4, and 5 cm from 0° to 90° with 5° binning. For the purposes of the current report, the authors provided the TLD and MC results in SolidWater™ as presented in their Fig. 4. When correcting their TLD results to yield $F(r, \theta)$ in water, the results at 30 common positions were in agreement within 10% on average except at $F(r = 1$ cm, $\theta = 0°)$ where a 31% discrepancy was observed. This was confirmed upon examination of their Fig. 3(a).

Sowards reported MC $F(r, \theta)$ results in water at 0.5, 1, 2, 3, 4, 5, 6, and 7 cm from 0° to 90° with 5° binning. For direct comparisons with results from Meigooni et al.[102] and Taylor and Rogers,[15] the Sowards results were corrected with line-source geometry functions for a common value of L_{eff} = 0.362 cm. MC results in water from Sowards compared to Meigooni et al. at 108 common positions were in

agreement within 3% on average, but differences up to 30% were observed, most commonly occurring between 0° and 30° at the smallest common distance (i.e., 0.5 cm). Excluding results near the source ends, the maximum discrepancy reduced to 13%.

The MC results in water from Meigooni et al. compared to Taylor and Rogers at 108 common positions were in agreement within 2% on average, but differences up to 21% were observed, most commonly occurring between 0° and 20° at 0.5 cm and 1 cm. Excluding results near the source ends, the maximum discrepancy reduced to 7%. MC results in water from Sowards compared to Taylor and Rogers at 126 common positions were in agreement within 4% on average, but differences up to 40% were observed, most commonly occurring between 0° and 30° at 0.5 cm and 1 cm. Excluding results near the source ends, the maximum discrepancy reduced to 13%. Given the agreement between the candidate MC datasets and the higher spatial and angular resolution of the study by Taylor and Rogers, their MC results were selected as the ${}_{\mathrm{CON}}F(r, \theta)$ dataset.

The TLD results in water from Meigooni et al. compared to Taylor and Rogers at the aforementioned 30 common positions were in agreement within 1% on average with differences within 10% except at $F(r = 1\ \mathrm{cm}, \theta = 0°)$ where a 16% discrepancy was observed.

A11. ISORAY MEDICAL MODEL CS-1 REV2 ^{131}CS SOURCE

The Proxcelan™ model CS-1 Rev2 ^{131}Cs source was introduced in 2004 by IsoRay Medical, Inc. (Richland, WA, USA). The source is currently posted on the Registry, and consists of a titanium tubing capsule having inner and outer diameters of 0.713 mm and 0.824 mm, respectively, 0.056 mm wall thickness, flat disk-shaped ends that are 0.10 mm thick, and a total outer length of 4.50 mm, see Fig. 1(k). Sealed inside is a glass tube (0.30 mm inner diameter and 0.40 mm outer diameter) coated with ceramic (containing ^{131}Cs) with a final outer diameter ranging from 0.56 to 0.65 mm. Inside the glass tube is a 0.25 mm diameter gold marker. The glass tube, ceramic coating, and gold marker are all 4.0 ± 0.1 mm long as reported by the manufacturer.

Murphy et al.[105] reported dosimetry results of TLD measurements and MC estimations of the model CS-1 Rev0 ^{131}Cs source with $L = 0.41$ cm. Measurements were performed using TLD-100 1 mm^3 cubes and TLD-700 chips calibrated using a highly filtered 40 keV x-ray beam to achieve a detector energy response correction value. Irradiations were performed in slabs of VirtualWater™ from Med-Cal, Inc. (Verona, WI, USA) where several slabs were machined to accommodate TLD cubes close to the source and TLD chips at farther distances from the source. Measurements of Λ used four sources calibrated at NIST following the CLA source calibration recommendations.[7] Using the MCNP4C radiation transport code,[97] brachytherapy dosimetry parameters were also determined in water and VirtualWater with annular ring detectors using the F6 tally to estimate absorbed dose. The MCNP4C default cross-section libraries were used. Unspecified were the s_K calculation geometry and the source of the ^{131}Cs photon spectrum. The number of photon histories per simulation ranged from 10^8 to 10^9.

Chen et al.[106] reported dosimetry results of TLD measurements of the model CS-1 Rev1 ^{131}Cs source with $L = 0.41$ cm. Measurements were performed in a SolidWater™ phantom (Radiation Measurements, Inc., Middleton, WI, USA) using TLD-100 chips and 1 mm^3 cubes calibrated with 6 MV photons from a linac. Measurements of Λ were linked to source strength calibrations reported by the

TABLE AI. For the 11 low-energy photon-emitting brachytherapy sources included in this report, the initial dates used by NIST and ADCLs for air-kerma strength calibrations are listed. Also listed are the consensus dose-rate constant values ${}_{\mathrm{CON}}\Lambda$, their standard uncertainties ($k = 1$), and the active length ${}_{\mathrm{CON}}L$ or effective length ${}_{\mathrm{CON}}L_{\mathrm{eff}}$ for each source model.

Manufacturer, source model, and radionuclide	Calibration date used by NIST and ADCLs	${}_{\mathrm{CON}}\Lambda$ (cGy ·h^{-1} U^{-1})	${}_{\mathrm{CON}}L$ or ${}_{\mathrm{CON}}L_{\mathrm{eff}}$ (cm)
Eckert & Ziegler BEBIG GmbH, I25.S17, ^{125}I	April 22, 2005[a]	0.933±0.025	0.346
Eckert & Ziegler BEBIG GmbH, I25.S17plus, ^{125}I	December 3, 2013	0.940±0.025	0.34
Eckert & Ziegler BEBIG GmbH, I25.S18, ^{125}I	August 1, 2008[b]	0.893±0.032	0.275
Elekta AB, 130.002, ^{125}I	April 14, 2006	0.954±0.043	0.34
Oncura, Inc., 9011, ^{125}I	July 18, 2008	0.933±0.028	0.28
Theragenics, Corp., AgX100, ^{125}I	August 16, 2010	0.952±0.043	0.35
CivaTech Oncology, Inc., CS10, ^{103}Pd	December 19, 2013	0.641±0.017	1.00
IBt, Inc., 1031L, ^{103}Pd	October 6, 2001[c]	0.701±0.020	0.435
IBt, Inc., 1032P, ^{103}Pd	March 28, 2005	0.671±0.019	0.38
IsoAid, LLC, IAPd-103A, ^{103}Pd	December 4, 2006	0.693±0.031	0.362
IsoRay Medical, Inc., CS-1 Rev2, ^{131}Cs	May 22, 2006	1.056±0.013	0.40

[a]NIST provided a calibration standard for the model I25.S17 ^{125}I source, but the standard was not transferred to the ADCLs.
[b]Five ^{125}I sources labeled as model 1252K were initially sent by IBt-Bebig to NIST. This calibration standard was then transferred to the ADCLs. Two additional sources labeled as model I25.S18 were sent to NIST by IBt-BEBIG in 2010, but they were not sent to the ADCLs to transfer the calibration standard.
[c]For the two batches of model 1031L sources calibrated at NIST in 1999 preceding discovery of the 1999 NIST WAFAC anomaly, the percentage difference change in the Λ value from the 1999 value was +4.8% on average.

manufacturer using equipment calibrated with sources calibrated with the NIST WAFAC measurement geometry.

As Murphy et al.[105] and Chen et al.[106] studied a different source model than the current model, that is, CS-1 Rev2, these studies were excluded as candidates from subsequent derivations of consensus data.

Wittman and Fisher[107] reported results of MC calculations on the dosimetry parameters for the model CS-1 Rev2 ^{131}Cs source using the MCNP5 (version 1.30)[108] photon transport simulation code and the default photoatomic cross-section libraries based on ENDF/B-VI[72] and ^{131}Cs photon spectrum taken from the NNDC. The MCNP *F4 tally (using mass-energy absorption coefficients from the NIST XCOM database to convert photon energy fluence to absorbed dose)[56] and the F6 tally for absorbed dose were both used and compared. Approximately 10^8 photon histories were used per simulation. The NIST WAFAC geometry was modeled with the 86.36 μm thick aluminized-mylar filter and no subsequent 5 keV cutoff. A value of $L = 0.40$ cm was used.

Rivard[109] reported results of MC calculations on the dosimetry parameters for the model CS-1 Rev2 ^{131}Cs source with $L = 0.40$ cm. Version 1.40 of the MCNP5 radiation transport code was used with default photoatomic cross-section libraries based on ENDF/B-VI[72] and ^{131}Cs photon spectrum taken from the NNDC. Absorbed dose was determined from the MCNP *F4 and F6 tally estimators of photon energy

TABLE AII. Radial dose function consensus values for 11 low-energy photon-emitting brachytherapy sources using the line-source approximation (values from Table IA) for derivation of $_{CON}g_L(r)$ values (upper half of table) and the point-source approximation for $_{CON}g_P(r)$ values (lower half of table). Values of $_{CON}g_P(r)$ are not provided for the CivaTech model CS10 ^{103}Pd source as the 2D dose calculation formalism is recommended for this elongated source. Data in boldface indicate that values were interpolated toward presenting datasets for all 11 sources on a common mesh. Data were italicized if they were acquired from a candidate dataset differing from the principal dataset.

r (cm)	BEBIG S17	BEBIG S17plus	BEBIG S18	Elekta 130.002	Oncura 9011	Theragenics AgX100	CivaTech CS10	IBt 1031L	IBt 1032P	IsoAid 1APd-103A	IsoRay CS-1 Rev2
Line-source approximation, $_{CON}g_L(r)$											
0.10	1.072	1.059	1.169	1.042	*1.036*	1.066	1.010	1.016	0.628	0.788	0.960
0.15	1.090	1.080	**1.152**	**1.062**	*1.057*	1.086	1.164	1.170	0.957	1.080	0.971
0.25	1.100	1.092	**1.121**	**1.085**	**1.081**	1.098	1.263	1.301	1.200	1.254	0.989
0.50	1.077	1.073	1.070	1.078	1.072	1.076	1.232	1.264	1.229	1.238	1.006
0.75	1.042	1.040	**1.033**	**1.044**	**1.039**	1.042	1.124	1.135	1.124	1.122	1.009
1.00	1.000	1.000	1.000	1.000	1.000	1.000	1.000	1.000	1.000	1.000	1.000
1.50	0.908	0.909	0.932	0.907	0.908	0.908	0.770	0.766	0.767	0.758	0.962
2.00	0.811	0.814	0.855	0.808	0.811	0.813	0.580	0.576	0.576	0.569	0.908
3.00	0.635	0.635	0.689	0.627	0.629	0.633	0.320	0.316	0.316	0.313	0.777
4.00	0.484	0.482	0.538	0.477	0.477	0.482	0.1726	0.1718	0.1708	0.1686	0.642
5.00	0.362	0.363	0.420	0.357	0.357	0.361	0.0924	0.0931	0.0904	0.0911	0.518
6.00	0.267	0.270	0.315	0.265	0.265	0.269	0.0496	0.0489	0.0483	0.0487	0.411
7.00	0.1977	0.1995	0.235	0.1963	0.1960	0.1990	0.0268	0.0268	0.0261	0.0265	0.323
8.00	0.1454	0.1467	0.1720	0.1442	0.1440	0.1470	0.01471	0.01507	0.01419	0.01472	0.251
9.00	0.1064	0.1087	0.1250	0.1058	0.1060	0.1080	0.00816	0.00892	0.00794	0.00841	0.1931
10.00	0.0782	0.0792	0.0990	0.0776	0.0780	0.0790	0.00473	0.00543	0.00464	0.00504	0.1481
Point source approximation, $_{CON}g_P(r)$											
0.10	0.655	0.647	0.806	0.643	*0.708*	0.647		0.541	0.363	0.469	0.538
0.15	0.817	0.810	**0.938**	**0.802**	*0.856*	0.811		0.792	0.690	0.795	0.685
0.25	0.972	0.965	**1.031**	**0.962**	**0.992**	0.968		1.087	1.038	1.097	0.845
0.50	1.047	1.044	1.051	1.049	1.052	1.046		1.211	1.189	1.201	0.970
0.75	1.035	1.033	**1.029**	**1.036**	**1.034**	1.034		1.122	1.114	1.113	0.999
1.00	1.000	1.000	1.000	1.000	1.000	1.000		1.000	1.000	1.000	1.000
1.50	0.913	0.914	0.935	0.912	0.911	0.913		0.772	0.772	0.763	0.969
2.00	0.817	0.820	0.859	0.813	0.815	0.819		0.582	0.581	0.574	0.917
3.00	0.640	0.640	0.693	0.632	0.633	0.639		0.320	0.320	0.316	0.786
4.00	0.488	0.487	0.541	0.481	0.480	0.487		0.1743	0.1728	0.1703	0.650
5.00	0.365	0.367	0.423	0.360	0.359	0.365		0.0945	0.0914	0.0921	0.525
6.00	0.270	0.272	0.317	0.268	0.267	0.272		0.0497	0.0489	0.0492	0.417
7.00	0.1996	0.201	0.236	0.1982	0.1972	0.201		0.0273	0.0264	0.0268	0.327
8.00	0.1468	0.1481	0.1731	0.1456	0.1449	0.1485		0.01530	0.01436	0.01487	0.254
9.00	0.1075	0.1098	0.1258	0.1068	0.1067	0.1091		0.00905	0.00803	0.00850	0.1956
10.00	0.0790	0.0800	0.0996	0.0783	0.0785	0.0798		0.00551	0.00469	0.00510	0.1501

TABLE AIII. $_{CON}F(r, \theta)$ data for the BEBIG model I25.S17 ^{125}I source, taken directly from Taylor and Rogers.[15]

	r (cm)									
Polar angle θ (°)	0.10	0.25	0.50	0.75	1	2	3	5	7.5	10
0		0.197	0.212	0.255	0.294	0.401	0.465	0.540	0.613	0.646
2		0.199	0.213	0.267	0.331	0.483	0.559	0.629	0.671	0.696
5		0.217	0.335	0.397	0.430	0.522	0.567	0.628	0.676	0.702
7		0.273	0.368	0.413	0.451	0.544	0.591	0.650	0.689	0.712
10		0.431	0.425	0.472	0.509	0.595	0.636	0.686	0.723	0.747
15		0.624	0.553	0.586	0.614	0.679	0.709	0.746	0.779	0.788
20		0.795	0.664	0.681	0.700	0.748	0.767	0.799	0.821	0.838
25		0.906	0.751	0.757	0.769	0.802	0.817	0.839	0.854	0.858
30	1.110	0.976	0.821	0.817	0.824	0.849	0.858	0.869	0.884	0.891
40	1.034	1.011	0.922	0.907	0.909	0.916	0.915	0.922	0.927	0.941
50	1.010	0.952	0.990	0.970	0.967	0.964	0.959	0.961	0.964	0.963
60	1.003	0.975	1.026	1.016	1.009	1.000	0.988	0.983	0.987	0.992
70	1.000	0.989	0.991	1.032	1.032	1.024	1.012	1.005	1.005	0.999
80	1.000	0.997	0.997	0.996	1.001	1.030	1.021	1.019	1.023	1.019

TABLE AIV. $_{CON}F(r, \theta)$ data for the BEBIG model I25.S17plus ^{125}I source, taken directly from Pantelis et al.[54]

	r (cm)									
Polar angle θ (°)	0.25	0.50	0.75	1	1.5	2	3	5	7	10
0	0.211	0.208	0.255	0.287	0.347	0.400	0.469	0.556	0.606	0.694
2	0.213	0.212	0.275	0.344	0.449	0.508	0.573	0.645	0.673	0.711
5	0.240	0.367	0.426	0.455	0.500	0.534	0.579	0.636	0.675	0.705
7	0.339	0.397	0.431	0.464	0.514	0.549	0.596	0.648	0.688	0.719
10	0.502	0.444	0.484	0.516	0.563	0.594	0.637	0.682	0.716	0.740
15	0.697	0.570	0.595	0.619	0.652	0.676	0.709	0.745	0.766	0.786
20	0.869	0.681	0.690	0.705	0.729	0.746	0.769	0.796	0.812	0.824
25	0.971	0.771	0.767	0.776	0.791	0.802	0.817	0.837	0.849	0.859
30	1.023	0.840	0.829	0.832	0.842	0.849	0.858	0.866	0.879	0.886
40	1.036	0.942	0.920	0.916	0.916	0.918	0.920	0.922	0.930	0.930
50	0.970	1.007	0.984	0.976	0.970	0.969	0.966	0.961	0.964	0.964
60	0.989	1.033	1.025	1.017	1.009	1.004	0.997	0.989	0.992	0.989
70	0.999	0.995	1.036	1.034	1.030	1.028	1.021	1.010	1.011	1.003
80	1.003	1.000	0.999	1.005	1.032	1.030	1.025	1.017	1.017	1.014

TABLE AV. $_{CON}F(r, \theta)$ data for the BEBIG model I25.S18 ^{125}I source, taken directly from Abboud et al.[57]

	r (cm)								
Polar angle θ (°)	0.5	1	2	3	4	5	6	7	10
0	0.457	0.640	0.769	0.811	0.846	0.852	0.857	0.878	0.869
10	0.782	0.846	0.893	0.907	0.916	0.920	0.922	0.923	0.924
20	0.874	0.925	0.939	0.943	0.953	0.948	0.956	0.949	0.956
30	0.921	0.955	0.958	0.966	0.969	0.967	0.969	0.965	0.966
40	0.947	0.967	0.972	0.978	0.980	0.978	0.979	0.971	0.979
50	0.967	0.987	0.984	0.987	0.989	0.990	0.988	0.989	0.989
60	0.966	0.992	0.988	0.995	0.998	0.992	0.996	0.992	0.994
70	0.986	0.999	0.997	0.997	1.001	1.001	1.002	0.996	0.997
80	0.985	1.001	0.997	1.000	1.000	0.998	1.002	0.999	1.003

TABLE AVI. $_{CON}F(r, \theta)$ data for the Elekta model 130.002 ^{125}I source, taken from personal communication with Karaiskos.[68]

	r (cm)									
Polar angle θ (°)	0.1	0.2	0.5	0.7	1	2	3	5	7	10
0			0.203	0.247	0.290	0.387	0.463	0.551	0.598	0.640
2			0.214	0.260	0.325	0.462	0.535	0.601	0.638	0.667
5			0.330	0.378	0.423	0.509	0.561	0.624	0.659	0.682
7			0.367	0.396	0.436	0.527	0.575	0.639	0.679	0.690
10			0.414	0.448	0.490	0.572	0.621	0.675	0.700	0.723
15			0.531	0.555	0.588	0.652	0.688	0.725	0.751	0.771
20		1.030	0.637	0.649	0.671	0.721	0.749	0.779	0.790	0.807
25	1.294	1.007	0.720	0.723	0.741	0.778	0.797	0.821	0.830	0.850
30	1.127	0.962	0.790	0.784	0.794	0.824	0.839	0.858	0.862	0.875
40	1.038	0.944	0.899	0.882	0.882	0.895	0.904	0.912	0.921	0.923
50	1.010	0.967	0.970	0.953	0.949	0.952	0.954	0.956	0.960	0.959
60	1.002	0.982	1.003	1.000	0.997	0.990	0.990	0.989	0.989	0.986
70	1.000	0.992	0.984	1.014	1.017	1.018	1.014	1.013	1.005	1.005
80	1.000	0.997	0.995	0.994	0.999	1.021	1.019	1.016	1.017	1.007

TABLE AVII. $_{CON}F(r, \theta)$ data for the Oncura model 9011 ^{125}I source, taken directly from Rivard.[71] Data formatted as boldface were interpolated from the consensus $_{CON}F(r, \theta)$ dataset.

	r (cm)										
Polar angle θ (°)	0.1	0.25	0.5	0.7	1.0	1.5	2	3	5	7	10
0		0.157	0.199	0.234	0.281	0.344	0.386	0.450	0.551	0.580	0.589
2		**0.170**	0.226	0.299	0.364	0.422	0.457	0.511	0.572	0.607	0.628
5		0.247	0.277	0.311	0.354	0.407	0.448	0.505	0.569	0.610	0.646
7		**0.289**	0.304	0.342	0.388	0.440	0.481	0.534	0.596	0.632	0.665
10		0.433	0.398	0.428	0.465	0.512	0.544	0.588	0.644	0.674	0.709
15	1.104	0.618	0.549	0.561	0.585	0.618	0.642	0.675	0.716	0.737	0.756
20	1.091	0.732	0.666	0.669	0.682	0.704	0.721	0.743	0.771	0.788	0.804
25	1.033	0.807	0.748	0.748	0.757	0.771	0.782	0.798	0.818	0.830	0.843
30	1.006	0.860	0.809	0.807	0.811	0.821	0.830	0.843	0.856	0.864	0.874
40	0.989	0.927	0.890	0.887	0.889	0.893	0.898	0.904	0.910	0.916	0.920
50	0.988	0.963	0.943	0.940	0.939	0.941	0.943	0.946	0.949	0.950	0.954
60	0.992	0.970	0.976	0.975	0.974	0.974	0.975	0.975	0.976	0.976	0.978
70	0.996	0.987	0.995	0.996	0.995	0.996	0.995	0.994	0.993	0.991	0.988
80	0.999	0.997	0.996	0.997	1.004	1.004	1.005	1.003	1.002	1.000	0.998

fluence and track length, respectively, with the former multiplied by mass-energy absorption coefficients from the NIST XCOM database to convert photon energy fluence to absorbed dose.[56] Each simulation was performed with 2 x 10^9 photon histories. Absorbed dose to water was scored in a 40 cm diameter spherical water phantom. In addition to water, absorbed dose was determined in SolidWater™ and VirtualWater™ for comparisons with other publications. Some of the reported $F(r, \theta)$ data were mistakenly transposed.[110] Air kerma was scored using a 5 keV energy cutoff in vacuum 30 cm from the source in a voxel covering 90.0° ± 7.5° whose center was positioned on the source transverse plane to approximate the NIST WAFAC aperture.

Wang and Zhang[111] reported results of MC calculations on the dosimetry parameters for the model CS-1 Rev2 ^{131}Cs source using the MCNP5 (version 1.40) photon transport simulation code and the default photoatomic cross-section libraries based on ENDF/B-VI[72] and ^{131}Cs photon spectrum taken from the NNDC. The MCNP *F5 tally using mass-energy absorption coefficients from the NIST XCOM database was used to convert photon energy fluence to absorbed dose.[56] For each simulation, 2 × 10^8 photon histories were used. In addition to water, absorbed dose was determined in SolidWater™ and VirtualWater™ for comparisons with other publications. Air kerma was scored using a 5 keV energy cutoff in air over distances of 0.5 cm to 25 cm. A value of L = 0.41 cm was used.

Melhus and Rivard[112] reported results of MC calculations on the dosimetry parameters for the model CS-1 Rev2 ^{131}Cs source using the MCNP5 (version 1.40) photon transport simulation code, principally for evaluating eye plaque dose

TABLE AVIII. $_{CON}F(r, \theta)$ data for the Theragenics model AgX100 ^{125}I source, taken from personal communication with Mourtada et al.[77]

	r (cm)									
Polar angle θ (°)	0.25	0.5	0.7	1.0	1.5	2	3	5	7	10
0	0.207	0.216	0.250	0.289	0.354	0.400	0.465	0.537	0.586	0.639
2	0.212	0.215	0.250	0.314	0.411	0.470	0.532	0.595	0.637	0.659
5	0.221	0.314	0.357	0.400	0.454	0.493	0.549	0.610	0.646	0.681
7	0.251	0.342	0.380	0.429	0.484	0.522	0.572	0.634	0.667	0.703
10	0.416	0.405	0.446	0.490	0.543	0.578	0.624	0.673	0.702	0.726
15	0.627	0.539	0.566	0.600	0.638	0.664	0.699	0.735	0.756	0.775
20	0.803	0.653	0.666	0.689	0.717	0.736	0.759	0.786	0.804	0.819
25	0.916	0.744	0.747	0.761	0.779	0.793	0.812	0.829	0.843	0.851
30	0.989	0.815	0.811	0.818	0.830	0.840	0.852	0.865	0.873	0.880
40	1.027	0.918	0.906	0.905	0.907	0.910	0.914	0.920	0.923	0.926
50	0.959	0.987	0.971	0.964	0.961	0.961	0.960	0.959	0.962	0.958
60	0.981	1.030	1.018	1.008	1.000	0.997	0.993	0.987	0.988	0.986
70	0.994	0.988	1.035	1.037	1.028	1.024	1.017	1.009	1.008	0.999
80	0.999	0.996	0.997	1.002	1.030	1.030	1.027	1.021	1.017	1.014

TABLE AIX. $_{CON}F(r, \theta)$ data for the CivaTech model CS10 ^{103}Pd source, taken directly from Rivard et al.,[79] except for underlined data which were extrapolated from the consensus $_{CON}F(r, \theta)$ dataset.

	r (cm)									
Polar angle θ (°)	0.1	0.25	0.5	0.75	1	2	3	5	7	10
0				1.059	0.976	0.864	0.847	0.847	0.896	0.742
2				1.086	1.013	0.936	0.925	0.920	0.936	0.943
5			1.266	1.157	1.093	1.011	0.990	0.979	0.978	1.019
7			1.281	1.174	1.116	1.034	1.013	0.993	0.986	0.999
10		1.287	1.292	1.183	1.130	1.052	1.029	1.011	1.001	0.996
15		1.271	1.274	1.183	1.135	1.065	1.042	1.024	1.011	1.008
20		1.252	1.244	1.173	1.132	1.068	1.047	1.027	1.016	1.011
25	1.358	1.229	1.213	1.159	1.124	1.066	1.047	1.028	1.018	1.008
30	1.296	1.203	1.183	1.141	1.112	1.063	1.046	1.029	1.021	1.010
40	1.187	1.149	1.128	1.104	1.085	1.050	1.037	1.025	1.017	1.009
50	1.113	1.099	1.083	1.069	1.058	1.035	1.026	1.018	1.010	1.006
60	1.061	1.057	1.046	1.039	1.034	1.021	1.016	1.010	1.007	1.006
70	1.025	1.025	1.021	1.017	1.015	1.010	1.007	1.004	1.001	1.003
80	1.005	1.007	1.005	1.003	1.003	1.002	1.002	1.000	0.998	1.000

distributions and benchmarking a 3-radionuclide dosimetry comparison. The default photoatomic cross-section libraries based on ENDF/B-VI[72] were used, along with the ^{131}Cs photon spectrum taken from the NNDC and mass-energy absorption coefficients from the NIST XCOM database to convert *F4 photon energy fluence to absorbed dose.[56] Using 2×10^8 photon histories, statistical uncertainties for estimation of s_K were < 0.1% with statistical uncertainties in water < 0.4% on the transverse plane for $r \leq 7$ cm or ~0.03% at $r = 1$ cm. Air kerma was scored using a 5 keV energy cutoff in vacuum 30 cm from the source in a voxel covering 90.0° ± 7.5° whose center was positioned on the source transverse plane to approximate the NIST WAFAC measurement geometry, and similarly modeled in detail with a 86.36 μm thick aluminized-mylar filter and no subsequent 5 keV cutoff as done by Wittman and Fisher.[107] A value of $L = 0.40$ cm was used.

Tailor et al.[113] reported dosimetry results of TLD measurements of the model CS-1 Rev2 ^{131}Cs source with $L = 0.40$ cm. Measurements were performed in water with TLD-100 powder calibrated with 6 MV photons from a linac using ^{60}Co NIST-traceable calibrations and a detector energy response correction value of 0.699 between ^{131}Cs and ^{60}Co photons. The TLD powder was contained within a 0.14 cm diameter glass capillary tubing positioned within a (30 cm)^3 cubic water phantom.[114] TLD powder response was calibrated with 6 MV photons from a linac using ^{60}Co NIST-traceable calibrations and a detector energy response correction value of 0.699 between ^{131}Cs and ^{60}Co photons. Measurements of Λ were linked to source strength calibrations

TABLE AX. $_{CON}F(r, \theta)$ for the IBt model 1031L ^{103}Pd source, taken directly from Taylor and Rogers.[15]

	r (cm)									
Polar angle θ (°)	0.1	0.25	0.5	0.75	1	2	3	5	7.5	10
0	0.000	0.623	0.194	0.224	0.276	0.406	0.460	0.520	0.574	0.661
2	0.000	0.612	0.233	0.284	0.344	0.414	0.441	0.473	0.531	0.608
5	0.000	0.558	0.399	0.393	0.409	0.444	0.470	0.501	0.546	0.635
7	0.000	0.555	0.503	0.473	0.466	0.480	0.500	0.527	0.572	0.639
10	0.000	0.681	0.579	0.522	0.511	0.517	0.533	0.555	0.596	0.681
15	0.000	0.748	0.654	0.611	0.596	0.595	0.604	0.621	0.652	0.714
20	0.000	0.917	0.696	0.674	0.670	0.662	0.669	0.675	0.708	0.734
25	0.896	1.027	0.739	0.716	0.713	0.712	0.719	0.728	0.748	0.794
30	0.952	1.083	0.782	0.758	0.756	0.753	0.757	0.765	0.777	0.817
40	0.897	1.100	0.869	0.835	0.831	0.828	0.832	0.838	0.851	0.873
50	0.902	1.074	0.933	0.906	0.902	0.893	0.897	0.895	0.906	0.909
60	0.926	1.043	0.972	0.958	0.955	0.945	0.948	0.940	0.945	0.949
70	0.964	1.022	0.991	0.983	0.985	0.976	0.978	0.972	0.980	0.963
80	0.992	1.007	0.998	0.995	0.998	0.995	0.994	0.991	0.989	0.988

TABLE AXI. $_{CON}F(r, \theta)$ data for the IBt model 1032P ^{103}Pd source, taken directly from Taylor and Rogers.[15]

	r (cm)									
Polar angle θ (°)	0.1	0.25	0.5	0.75	1	2	3	5	7.5	10
0		0.1417	1.074	0.891	0.823	0.753	0.736	0.741	0.752	0.787
2		1.241	1.075	0.893	0.823	0.752	0.740	0.743	0.757	0.764
5		1.766	1.076	0.893	0.828	0.761	0.750	0.750	0.763	0.770
7		1.749	1.075	0.900	0.836	0.773	0.761	0.763	0.773	0.788
10		2.198	1.083	0.914	0.853	0.793	0.781	0.784	0.794	0.795
15		1.907	1.090	0.936	0.880	0.827	0.816	0.816	0.829	0.841
20		1.776	1.091	0.957	0.907	0.862	0.853	0.850	0.860	0.867
25		1.644	1.089	0.975	0.934	0.895	0.888	0.893	0.898	0.890
30	1.401	1.524	1.086	0.993	0.961	0.927	0.921	0.919	0.925	0.916
40	1.301	1.326	1.078	1.016	0.994	0.969	0.963	0.960	0.970	0.954
50	1.196	1.187	1.060	1.022	1.006	0.992	0.987	0.990	0.990	0.972
60	1.105	1.093	1.039	1.019	1.010	1.003	1.001	1.004	1.008	0.994
70	1.047	1.035	1.021	1.012	1.008	1.005	1.002	1.008	1.017	0.992
80	1.013	1.007	1.006	1.005	1.004	1.002	1.000	1.010	1.012	1.008

reported by the manufacturer using equipment having a NIST-traceable calibration.

Zhang et al.[115] reported results of MC calculations on the dosimetry parameters for the model CS-1 Rev2 ^{131}Cs source using the MCNPX (version 2.5.0)[75] photon transport simulation code, principally for evaluating eye plaque dose distributions and benchmarking for a dosimetry comparison between ^{131}Cs and ^{125}I. The default photoatomic cross-section libraries based on ENDF/B-VI[72] were used, along with the ^{131}Cs photon spectrum taken from the NNDC and mass-energy absorption coefficients from the NIST XCOM database to convert *F4 photon energy fluence to absorbed dose.[56] Using 2×10^8 photon histories, statistical uncertainties for estimation of s_K were < 0.1%. The geometry for s_K calculations was not specified. A value of $L = 0.40$ cm was used.

Chiu-Tsao et al.[116] reported results of MC calculations on the dosimetry parameters for the model CS-1 Rev2 ^{131}Cs source using the MCNP5 (version 1.60)[55] photon transport simulation code, principally for evaluating dose distributions in radiochromic film and benchmarking for a dosimetry comparison between ^{131}Cs and ^{125}I. The default photoatomic cross-section libraries based on ENDF/B-VI[72] were used, along with the ^{131}Cs photon spectrum taken from the NNDC and mass-energy absorption coefficients from the NIST XCOM database to convert *F4 photon energy fluence to absorbed dose.[56] In water and vacuum, 10^{11} and 10^{10} photon histories were simulated to achieve negligible statistical uncertainties. Air kerma was scored using a 5 keV energy cutoff in vacuum 30 cm from the source in a voxel covering 90.0° ± 7.5° whose center was positioned on the source transverse plane to approximate

TABLE AXII. $_{CON}F(r, \theta)$ data for the IsoAid model IAPd-103A ^{103}Pd source, taken directly from Taylor and Rogers.[15]

	r (cm)									
Polar angle θ (°)	0.1	0.25	0.5	0.75	1	2	3	5	7.5	10
0		0.232	0.223	0.233	0.244	0.284	0.305	0.340	0.397	0.491
2		0.237	0.225	0.235	0.246	0.286	0.309	0.338	0.396	0.494
5		0.265	0.235	0.243	0.253	0.291	0.315	0.346	0.399	0.495
7		0.299	0.245	0.252	0.261	0.299	0.323	0.355	0.407	0.507
10		0.395	0.274	0.274	0.281	0.319	0.343	0.371	0.425	0.531
15		0.649	0.351	0.338	0.341	0.375	0.397	0.426	0.481	0.566
20		0.898	0.467	0.433	0.429	0.454	0.473	0.498	0.543	0.622
25		1.051	0.585	0.538	0.527	0.543	0.554	0.573	0.613	0.687
30	2.008	1.116	0.684	0.632	0.616	0.623	0.630	0.645	0.675	0.733
40	1.545	1.112	0.839	0.778	0.756	0.753	0.756	0.762	0.784	0.819
50	1.299	1.070	0.933	0.888	0.866	0.857	0.855	0.855	0.873	0.896
60	1.152	1.037	0.980	0.954	0.941	0.936	0.932	0.927	0.943	0.945
70	1.067	1.017	0.997	0.988	0.978	0.978	0.976	0.977	0.977	0.956
80	1.018	1.005	1.001	0.996	0.989	0.996	0.994	0.980	0.999	0.992

TABLE AXIII. $_{CON}F(r, \theta)$ data for the IsoRay model CS-1 Rev2 ^{131}Cs source, obtained from Rivard[111,112] without angular averaging. Data formatted as boldface were interpolated from the consensus $_{CON}F(r, \theta)$ dataset.

	r (cm)									
Polar angle θ (°)	0.1	0.25	0.5	0.7	1	2	3	5	7	10
0		0.622	0.829	0.851	0.845	0.837	0.838	0.843	0.853	0.833
2		**0.670**	0.796	0.806	0.818	0.839	0.842	0.846	0.845	0.847
5		0.731	0.781	0.761	0.750	0.764	0.780	0.800	0.810	0.819
7		**0.730**	0.718	0.706	0.713	0.746	0.769	0.794	0.808	0.816
10		0.707	0.678	0.690	0.709	0.752	0.776	0.801	0.815	0.826
15		0.759	0.720	0.734	0.753	0.791	0.811	0.831	0.840	0.847
20		0.843	0.778	0.788	0.803	0.832	0.847	0.862	0.868	0.871
25	1.161	0.887	0.828	0.834	0.845	0.866	0.876	0.886	0.891	0.896
30	1.113	0.915	0.868	0.870	0.878	0.894	0.902	0.910	0.912	0.916
40	1.031	0.949	0.923	0.923	0.926	0.935	0.939	0.943	0.944	0.944
50	1.009	0.971	0.958	0.957	0.959	0.963	0.964	0.966	0.967	0.966
60	1.002	0.985	0.978	0.978	0.980	0.981	0.982	0.982	0.982	0.983
70	1.000	0.993	0.990	0.991	0.992	0.993	0.993	0.993	0.993	0.992
80	1.000	0.998	0.998	0.997	0.998	0.999	0.999	0.999	0.998	0.998

the NIST WAFAC measurement geometry. A value of $_{CON}L$ = 0.40 cm was selected.

A11.1. Model CS-1 Rev2 dose-rate constant

Wittman and Fisher[107] reported a Λ value in water of (1.040 ± 0.023) cGy h^{-1} U^{-1} using MC methods that accounted for the NIST WAFAC geometry. Rivard[109] reported a Λ value in water of (1.046 ± 0.019) cGy h^{-1} U^{-1} using MC methods that accounted for the NIST WAFAC geometry. Wang and Zhang[111] reported a Λ value in water of (1.048 ± 0.026) cGy h^{-1} U^{-1} using MC methods. Melhus and Rivard[112] reported a Λ value in water of (1.052 ± 0.027) cGy h^{-1} U^{-1} using MC methods that accounted for the NIST WAFAC geometry. Tailor et al.[113] reported a Λ value in water of (1.063 ± 0.023) cGy h^{-1} U^{-1} using TLD powder. Zhang et al.[115] reported a Λ value in water of (1.059 ± 0.026) cGy h^{-1} U^{-1} using MC methods. Chiu-Tsao et al.[116] reported a Λ value in water of (1.053 ± 0.014) cGy h^{-1} U^{-1} using MC methods that accounted for the NIST WAFAC geometry. TLD results from Tailor et al. were selected for $_{EXP}\Lambda$. MC results in water from Wittman and Fisher, Rivard, Wang and Zhang, Melhus and Rivard, Zhang et al., and Chiu-Tsao et al. were averaged to obtain $_{MC}\Lambda$ = (1.050 ± 0.009) cGy h^{-1} U^{-1}. The average of $_{EXP}\Lambda$ and $_{MC}\Lambda$ yielded $_{CON}\Lambda$ = (1.056 ± 0.013) cGy h^{-1} U^{-1}. The $_{MC}\Lambda$ value was 1.3% lower than the $_{EXP}\Lambda$ value and within the standard uncertainty of the measurements.

TABLE AXIV. The consensus 1D anisotropy function $_{CON}\phi_{an}(r)$ data as a function of distance for the brachytherapy sources included in the current report were typically derived from $_{CON}F(r, \theta)$ by numerical integration of the dose rate with respect to solid angle. Interpolated data are highlighted in boldface while extrapolated data are underlined. Results for the model CS10 ^{103}Pd source are not included since the 2D dose calculation formalism is recommended for this source model.

r (cm)	BEBIG S17	BEBIG S17plus	BEBIG S18	Elekta 130.002	Oncura 9011	Theragenics AgX100	IBt 1031L	IBt 1032P	IsoAid IAPd-103A	IsoRay CS-1 Rev2
0.10	1.125	1.169	0.989	1.252	*1.519*	1.175	1.132	1.273	1.411	1.241
0.15	1.287	1.169	0.989	**1.221**	*1.366*	1.353	1.704	1.776	1.610	1.431
0.25	1.138	1.169	0.989	**1.121**	**1.048**	1.151	1.363	1.615	1.237	1.223
0.50	0.982	0.994	0.989	0.964	0.946	0.981	0.986	1.112	0.928	1.008
0.75	0.960	0.968	**0.989**	**0.943**	**0.932**	**0.959**	0.931	1.032	0.878	0.976
1.00	0.955	0.961	0.988	0.939	0.929	0.953	0.917	1.005	0.858	**0.966**
1.50	**0.955**	0.958	**0.986**	0.938	0.930	0.951	**0.908**	**0.992**	**0.856**	0.961
2.00	0.955	0.958	0.983	0.942	0.932	0.952	0.899	0.979	0.853	0.960
3.00	0.951	0.957	0.986	0.946	0.936	0.953	0.900	0.973	0.853	0.961
4.00	0.950	0.960	0.988	0.948	0.938	0.954	0.898	0.967	0.858	0.963
5.00	0.954	0.956	0.987	0.952	0.941	0.954	0.898	0.975	0.856	0.963
6.00	**0.956**	0.960	0.989	0.953	0.942	0.955	**0.902**	**0.977**	**0.862**	0.964
7.00	**0.959**	0.960	0.985	0.953	0.944	0.956	**0.905**	**0.979**	**0.869**	0.964
8.00	**0.960**	0.963	**0.986**	0.955	0.944	0.956	**0.909**	**0.978**	**0.875**	0.964
9.00	**0.961**	0.955	**0.986**	0.955	0.946	0.958	**0.913**	**0.973**	**0.882**	0.965
10.00	0.962	0.961	0.987	0.955	0.946	0.957	0.916	0.968	0.889	0.965

A11.2. Model CS-1 Rev2 radial dose function

Rivard[109] reported MC results in water from 0.05 cm to 15 cm, Wang and Zhang[111] reported MC results in water from 0.2 cm to 15 cm, Melhus and Rivard[112] reported MC results in water from 0.1 cm to 7 cm, and Zhang et al.[115] reported MC results in water from 0.05 cm to 10 cm. Comparing these data to those from Rivard at common distances, agreement of results from Wang and Zhang with Rivard was within 0.3% on average with a maximum discrepancy of 1.6%. Agreement of results from Melhus and Rivard with Rivard was within 0.03% on average with a maximum discrepancy of 0.3%. Comparing results from Zhang et al. to those from Rivard at common distances, agreement was not as good. Average agreement was 4% with a maximum discrepancy of 21% at 10 cm with differences increasing monotonically for distance greater than 1 cm. Comparing TLD results from Tailor et al. to MC results from Rivard at common distances, agreement for $r < 6$ cm was within 0.1% on average. However, differences increased with distance with discrepancies of 7% at 7 cm and 15% at 10 cm. The MC results of Rivard were selected as $_{CON}g_L(r)$ given their larger range, smoother behavior, higher resolution, and the aforementioned comparisons to MC results from Wang and Zhang, Melhus and Rivard, and Zhang et al.

A11.3. Model CS-1 Rev2 anisotropy functions

Rivard[109] reported MC results in water for 0.05 cm to 15 cm and from 0° to 90° with 5° binning, with mistyped results at 0.5 cm and 0.75 cm corrected in an erratum.[110] Wang and Zhang[111] reported MC results in water for 0.5–10 cm and also from 0° to 90° with 5° binning. Tailor et al.[113] reported results using TLD powder in water at 1, 2, 3, 5, and 7 cm at an assortment of polar angles. When correcting their MC results from Wang and Zhang to use $_{CON}L$ = 0.40 cm for a direct comparison with MC results from Rivard, the results at 162 common positions were in agreement within 0.3% on average, with the largest differences occurring near the source long axis with discrepancies of 4% at F (r = 1 cm, θ = 5°) and 5% at F(r = 10 cm, θ = 0°). For the TLD results from Tailor et al., comparison of $F(r, \theta)$ at 302 common positions with the MC results of Rivard were in agreement within 1.28% on average, with the largest differences occurring close to the source long axis with discrepancies of 6% at F(r = 1 cm, θ = 10°) and 3% at F(r = 2 cm, θ = 5°). Given the good agreement with the other datasets and the larger range of radii and polar angles covered by the MC-based $F(r, \theta)$ dataset from Rivard,[109,110] it was selected for $_{CON}F(r, \theta)$.

[a]Author to whom correspondence should be addressed. Electronic mail: markjrivard@gmail.com.

REFERENCES

1. Nath R, Anderson LL, Luxton G, Weaver KA, Williamson JF, Meigooni AS. Dosimetry of interstitial brachytherapy sources: recommendations of the AAPM Radiation Therapy Committee Task Group No. 43. *Med Phys*. 1995;22:209–234.
2. Rivard MJ, Coursey BM, DeWerd LA, et al. Update of AAPM Task Group No. 43 Report: a revised AAPM protocol for brachytherapy dose calculations. *Med Phys*. 2004;31:633–674.
3. Rivard MJ, Butler WM, DeWerd LA, et al. Erratum: update of AAPM Task Group No. 43 Report: a revised AAPM protocol for

brachytherapy dose calculations [Med. Phys. 31, 633-674 (2004)]. *Med Phys*. 2004;31:3532–3533.
4. Rivard MJ, Butler WM, DeWerd LA, et al. Supplement to the 2004 update of the AAPM Task Group No. 43 Report. *Med Phys*. 2007;34:2187–2205.
5. Rivard MJ, Butler WM, DeWerd LA, et al. Erratum: supplement to the 2004 update of the AAPM Task Group No. 43 Report [Med. Phys. 34, 2187-2205 (2007)]. *Med Phys*. 2010;37:2396.
6. Williamson JF, Coursey BM, DeWerd LA, Hanson WF, Nath R. Dosimetric prerequisites for routine clinical use of new low energy photon interstitial brachytherapy sources. *Med Phys*. 1998;25:2269–2270.
7. DeWerd LA, Huq MS, Das IJ, et al. Procedures for establishing and maintaining consistent air-kerma strength standards for low-energy, photon-emitting brachytherapy sources: recommendations of the Calibration Laboratory Accreditation Subcommittee of the American Association of Physicists in Medicine. *Med Phys*. 2004;31:675–681.
8. Beaulieu L, Carlsson Tedgren Å, Carrier J-F, et al. Report of the Task Group 186 on model-based dose calculation methods in brachytherapy beyond the TG-43 formalism: current status and recommendations for clinical implementation. *Med Phys*. 2012;39:6208–6236.
9. Brachytherapy Source Registry. Joint AAPM/IROC Houston Registry of Brachytherapy Sources Meeting the AAPM Dosimetric Prerequisites; 2017. http://rpc.mdanderson.org/RPC/BrachySeeds/Source_Registry.htm, last accessed June 7, 2017.
10. Rivard MJ, Melhus CS, Williamson JF. Brachytherapy dose calculation formalism, dataset evaluation, and treatment planning system implementation, Chap. 13. In: Rogers DWO, Cygler JE, eds. *Clinical Dosimetry for Radiotherapy: AAPM Summer School*. Madison, WI: Medical Physics Publishing, Inc.; 2009:403–436. ISBN 97818 88340846.
11. Li Z, Das RK, DeWerd LA, et al. Dosimetric prerequisites for routine clinical use of photon emitting brachytherapy sources with average energy higher than 50 keV. *Med Phys*. 2007;34:37–40.
12. Pérez-Calatayud J, Ballester F, Das RK, et al. Dose calculation for photon-emitting brachytherapy sources with average energy higher than 50 keV: report of the AAPM and ESTRO. *Med Phys*. 2012;39:2904–2929.
13. BRAPHYQS Working Group of GEC-ESTRO; 2017. http://www.estro.org/about/governance-organisation/committees-activities/gec-estro-braphyqs, last accessed June 7, 2017.
14. Carleton Laboratory for Radiotherapy Physics; 2017. http://www.physics.carleton.ca/clrp/seed_database, last accessed June 7, 2017.
15. Taylor REP, Rogers DWO. An EGSnrc Monte Carlo-calculated database of TG-43 parameters. *Med Phys*. 2008;35:4228–4241.
16. Taylor REP, Rogers DWO. EGSnrc Monte Carlo calculated dosimetry parameters for ^{192}Ir and ^{169}Yb brachytherapy sources. *Med Phys*. 2008;35:4933–4944.
17. Taylor REP, Yegin G, Rogers DWO. Benchmarking BrachyDose: voxel based EGSnrc Monte Carlo calculations of TG-43 dosimetry parameters. *Med Phys*. 2007;34:445–457.
18. Russell KR, Tedgren ÅC, Ahnesjö A. Brachytherapy source characterization for improved dose calculations using primary and scatter dose separation. *Med Phys*. 2005;32:2739–2752.
19. Williamson JF, Baker RS, Li Z. A convolution algorithm for brachytherapy dose computations in heterogeneous geometries. *Med Phys*. 1991;18:1256–1265.
20. DeWerd LA, Ibbott GS, Meigooni AS, et al. A dosimetric uncertainty analysis for photon-emitting brachytherapy sources: report of AAPM Task Group No. 138 and GEC-ESTRO. *Med Phys*. 2011;38:782–801.
21. Venselaar J, Perez-Calatayud J. *A Practical Guide to Quality Control of Brachytherapy Equipment*, 1st ed. Brussels, Belgium: ESTRO; 2004. European Guidelines for Quality Assurance in Radiotherapy: Booklet No. 8.
22. National Nuclear Data Center, Brookhaven National Laboratory. NUDAT 2.6; 2017. National Nuclear Data Center, Brookhaven National Laboratory. http://www.nndc.bnl.gov/nudat2/index.jsp, last accessed June 7, 2017.
23. Rivard MJ, Granero D, Perez-Calatayud J, Ballester F. Influence of photon energy spectra from brachytherapy sources on Monte Carlo simulations of kerma and dose rates in water and air. *Med Phys*. 2010;37:869–876.
24. Rodriguez M, Rogers DWO. On determining dose rate constants spectroscopically. *Med Phys*. 2013;40:011713, 10 pp.
25. NCRP Report No. 58. *A Handbook of Radioactivity Measurements Procedures: with Nuclear Data for Some Biomedically Important Radionuclides, Reevaluated Between August, 1983 and April, 1984*, 2nd ed. Bethesda, MD: National Council on Radiation Protection and Measurements; 1994.
26. National Institute of Standards and Technology; 2017. https://www.nist.gov/pml/x-ray-transition-energies-database, last accessed June 7, 2017.
27. The Lund/LBNL Nuclear Data Search; 2017. http://nucleardata.nuclear.lu.se/toi/, last accessed June 7, 2017.
28. Laboratoire National Henri Becquerel; 2017. http://www.nucleide.org/DDEP_WG/DDEPdata.htm, last accessed June 7, 2017.
29. Chen Z, Nath R. Photon spectrometry for the determination of the dose-rate constant of low-energy photon-emitting brachytherapy sources. *Med Phys*. 2007;34:1412–1430.
30. U.S. Standard Atmosphere. Washington, D.C.: National Oceanic and Atmospheric Administration; 1976. NOAA-S/T 76-1562, October 1976.
31. Griffin SL, DeWerd LA, Micka JA, Bohm TD. The effect of ambient pressure on well chamber response: experimental results with empirical correction factors. *Med Phys*. 2005;32:700–709.
32. Bohm TD, Griffin SL, DeLuca PM, DeWerd LA. The effect of ambient pressure on well chamber response: Monte Carlo calculated results for the HDR 1000 Plus. *Med Phys*. 2005;32:1103–1114.
33. La Russa DJ, Rogers DWO. An EGSnrc investigation of the P_{TP} correction factor for ion chambers in kilovoltage x-rays. *Med Phys*. 2006;33:4590–4599.
34. La Russa DJ, McEwen M, Rogers DWO. An experimental and computational investigation of the standard temperature-pressure correction factor for ion chambers in kilovoltage x rays. *Med Phys*. 2007;34:4690–4699.
35. Tornero-López AM, Guirado D, Perez-Calatayud J, et al. Dependence with air density of the response of the PTW sourcecheck ionization chamber for low energy brachytherapy sources. *Med Phys*. 2013;40:122103. 6 pp.
36. Williamson JF, Rivard MJ. Thermoluminescent detector and Monte Carlo techniques for reference-quality brachytherapy dosimetry, Chap. 14. In: Rogers DWO, Cygler JE, eds. *Clinical Dosimetry Measurements in Radiotherapy.* Madison, Wisconsin: Medical Physics Publishing; 2009:437–499.
37. Mitch MG, DeWerd LA, Minniti R, Williamson JF. Treatment of uncertainties radiation dosimetry, Chap. 22. In: Rogers DWO, Cygler JE, eds. *Clinical Dosimetry Measurements in Radiotherapy.* Madison, Wisconsin: Medical Physics Publishing; 2009:723–757.
38. Williamson JF, Meigooni AS. Quantitative dosimetry methods for brachytherapy, Chap. 5. In: Williamson JF, Thomadsen BR, Nath R, eds. *Brachytherapy Physics*. Madison, Wisconsin: Medical Physics Publishing; 1995:87–134.
39. Rogers DWO. General characteristics of radiation dosimeters and a terminology to describe them, Chap. 4. In: Rogers DWO, Cygler JE, eds. *Clinical Dosimetry Measurements in Radiotherapy.* Madison, Wisconsin: Medical Physics Publishing; 2009:137–145.
40. DeWerd LA, Bartol LJ, Davis SD. Thermoluminescence dosimetry, Chap. 24. In: Rogers DWO, Cygler JE, eds. *Clinical Dosimetry Measurements in Radiotherapy.* Madison, Wisconsin: Medical Physics Publishing; 2009:815–840.
41. Davis SD, Ross CK, Mobit PN, Van der Zwan L, Chase WJ, Shortt KR. The response of LiF thermoluminescent dosemeters to photon beams in the energy range from 30 kV x rays to ^{60}Co gamma rays. *Radiat Prot Dosim*. 2003;106:33–43.
42. Nunn AA, Davis SD, Micka JA, DeWerd LA. LiF:Mg, Ti TLD response as a function of photon energy for moderately filtered x-ray spectra in the range of 20–250 kVp relative to ^{60}Co. *Med Phys*. 2008;35:1859–1869.
43. Carlsson Tedgren Å, Hedman A, Grindborg J-E, Carlsson GA. Response of LiF:Mg, Ti thermoluminescent dosimeters at photon energies relevant to dosimetry of brachytherapy (<1 MeV). *Med Phys*. 2011;38:5539–5550.

44. Rodriguez M, Rogers DWO. Effect of improved TLD dosimetry on the determination of dose rate constants for ^{125}I and ^{103}Pd brachytherapy seeds. *Med Phys*. 2014;41:114301, 15 pp.
45. Reed JL, Rasmussen BE, Davis SD, Micka JA, Culberson WS, DeWerd LA. Determination of the intrinsic energy dependence of LiF: Mg,Ti thermoluminescent dosimeters for ^{125}I and ^{103}Pd brachytherapy sources relative to ^{60}Co. *Med Phys*. 2014;41:122103, 11 pp.
46. Olko P. Microdosimetric interpretation of thermoluminescence efficiency of LiF:Mg, Cu, P (MCP-N) detectors for weakly and densely ionising radiations. *Rad Prot Dosim*. 1996;65:151–158.
47. Horowitz YS. Letter to the editor-update on AAPM Task Group No. 43 report-brachytherapy and TLD. *Radiat Prot Dosim*. 2009;133:124–125.
48. Horowitz YS, Moscovitch M. Highlights and pitfalls of 20 years of application of computerised glow curve analysis to thermoluminescence research and dosimetry. *Rad Prot Dosim*. 2013;153:1–22.
49. Carlsson Tedgren Å, Elia R, Hedtjärn H, Olsson S, Carlsson GA. Determination of absorbed dose to water around a clinical HDR 192Ir source using LiF:Mg, Ti TLDs demonstrates an LET dependence of detector response. *Med Phys*. 2012;39:1133–1140.
50. Massillon-JL G, Cabrera-Santiago A, Minniti R, O'Brien M, Soares CG. Influence of phantom materials on the energy dependence of LiF: Mg, Ti thermoluminescent dosimeters exposed to 20–300 kV narrow x-ray spectra, ^{137}Cs and ^{60}Co photons. *Phys Med Biol*. 2014;59:4149–4166.
51. Lymperopoulou G, Papagiannis P, Sakelliou L, et al. Monte Carlo and thermoluminescence dosimetry of the new IsoSeed® model I25.S17 ^{125}I interstitial brachytherapy seed. *Med Phys*. 2005;32:3313–3317.
52. Moutsatsos A, Pantelis E, Papagiannis P, Baltas D. Experimental determination of the Task Group-43 dosimetric parameters of the new I25.S17plus ^{125}I brachytherapy source. *Brachytherapy*. 2014;13:618–626.
53. Kennedy RM, Davis SD, Micka JA, DeWerd LA. Experimental and Monte Carlo determination of the TG-43 dosimetric parameters for the model 9011 THINSeed™ brachytherapy source. *Med Phys*. 2010;37:1681–1688.
54. Pantelis E, Papagiannis P, Anagnostopoulos G, Baltas D. New ^{125}I brachytherapy source IsoSeed I25.S17plus: Monte Carlo dosimetry simulation and comparison to sources of similar design. *J Contemp Brachytherapy*. 2013;5:240–249.
55. Brown F, Kiedrowski B, Bull J. MCNP5-1.60 Release Notes, LA-UR-10-06235; 2010.
56. Hubbell JH, Seltzer SM. Tables of x-ray mass attenuation coefficients and mass energy-absorption coefficients 1 keV to 20 MeV for elements Z = 1 to 92 and 48 additional substances of dosimetric interest. NISTIR 5632; 1995.
57. Abboud F, Hollows M, Scalliet P, Vynckier S. Experimental and theoretical dosimetry of a new polymer encapsulated iodine-125 source—smartseed: dosimetric impact of fluorescence x rays. *Med Phys*. 2010;37:2054–2062.
58. Van Gellekom MPR, Moerland MA, Van Vulpen M, Wijrdeman HK, Battermann JJ. Quality of permanent prostate implants using automated delivery with seedSelectron™ versus manual insertion of RAPID Strands™. *Radiother Oncol*. 2004;73:49–56.
59. Rivard MJ, Radford Evans D-A, Kay I. A technical evaluation of the Nucletron FIRST system: conformance of a remote afterloading brachytherapy seed implantation system to manufacturer specifications and AAPM Task Group report recommendations. *J Appl Clin Med Phys*. 2005;6:22–50.
60. Podder TK, Beaulieu L, Caldwell B, et al. AAPM and GEC-ESTRO guidelines for image-guided robotic brachytherapy: report of Task Group 192. *Med Phys*. 2014;41:101501, 27 pp.
61. Anagnostopoulos G, Baltas D, Karaiskos P, Sandilos P, Papagiannis P, Sakelliou L. Thermoluminescent dosimetry of the selectSeed ^{125}I interstitial brachytherapy seed. *Med Phys*. 2002;29:709–716.
62. Papagiannis P, Sakelliou L, Anagnostopoulos G, Baltas D. On the dose rate constant of the selectSeed ^{125}I interstitial brachytherapy seed. *Med Phys*. 2006;33:1522–1523.
63. Karaiskos P, Papagiannis P, Sakelliou L, Anagnostopoulos G, Baltas D. Monte Carlo dosimetry of the selectSeed ^{125}I interstitial brachytherapy seed. *Med Phys*. 2001;28:1753–1760.
64. Scofield JH. Theoretical photoionization cross sections from 1 to 1,500 keV. Lawrence Livenmore Laboratory Report No. UCRL-51326; 1973.
65. Hubbell JH, Veigele WJ, Briggs EA, Brown RT, Cromer DT, Howerton RJ. Atomic form factors, incoherent scattering functions, and photon scattering cross sections. *J Phys Chem Ref Data*. 1975;4:471–538.
66. Hubbell JH, Øverbø I. Relativistic atomic form factors and photon coherent scattering cross sections. *J Phys Chem Ref Data*. 1979;8:69–105.
67. Plechaty EF, Cullen DE, Howerton RJ. Tables and graphs of photo-interaction cross sections from 0.1 keV to 100 MeV derived from the LLL Evaluated Nuclear Data Library. UCRL-50400, Vol. 6, Rev. 3, Lawrence Livermore Laboratory; 1981.
68. Karaiskos P. Personal communication, December 22, 2003; 2003.
69. Roberts G, Al-Qaisieh B, Bownes P, Henry A, Thwaites D. Evaluation of the visibility of a new thinner ^{125}I radioactive source for permanent prostate brachytherapy. *Brachytherapy*. 2012;11:460–467.
70. Robertson AKH, Basran PS, Thomas SD, Wells D. CT, MR, and ultrasound image artifacts from prostate brachytherapy seed implants: the impact of seed size. *Med Phys*. 2012;39:2061–2068.
71. Rivard MJ. Monte Carlo radiation dose simulations and dosimetric comparison of the model 6711 and 9011 ^{125}I brachytherapy sources. *Med Phys*. 2009;36:486–491.
72. White MC. *Photoatomic Data Library MCPLIB04: A New Photoatomic Library Based on Data from ENDF/B-VI release 8, Memorandum LA-UR-03-1019*. Los Alamos, NM: Los Alamos National Laboratory; 2003.
73. Dolan J, Li Z, Williamson JF. Monte Carlo and experimental dosimetry of an ^{125}I brachytherapy seed. *Med Phys*. 2006;33:4675–4684.
74. Mason J, Al-Qaisieh B, Bownes P, Henry A, Thwaites D. Monte Carlo investigation of I-125 interseed attenuation for standard and thinner seeds in prostate brachytherapy with phantom validation using a MOSFET. *Med Phys*. 2013;40:031717, 10 pp.
75. Pelowitz DB. MCNPX User's Manual Version 2.5.0. Los Alamos National Laboratory Report No. LA-CP-05-0369; 2005.
76. Rivard MJ. Erratum: Monte Carlo radiation dose simulations and dosimetric comparison of the model 6711 and 9011 ^{125}I brachytherapy sources [Med. Phys. 36, 486-491 (2009)]. *Med Phys*. 2010;37:1459.
77. Mourtada F, Mikell J, Ibbott G. Monte Carlo calculations of AAPM Task Group Report No. 43 dosimetry parameters for the ^{125}I I-Seed AgX100 source model. *Brachytherapy*. 2012;11:237–244.
78. Chen Z, Bongiorni P, Nath R. Experimental characterization of the dosimetric properties of a newly designed I-Seed model AgX100 ^{125}I interstitial brachytherapy source. *Brachytherapy*. 2012;11:476–482.
79. Rivard MJ, Reed JL, DeWerd LA. ^{103}Pd strings: Monte Carlo assessment of a new approach to brachytherapy source design. *Med Phys*. 2014;41:011716, 11 pp.
80. De Frenne D. Nuclear data sheets for A = 103. *Nucl Data Sheets*. 2009;110:2081–2256.
81. Reed JL, Rivard MJ, Micka JA, Culberson WS, DeWerd LA. Experimental and Monte Carlo dosimetric characterization of a 1 cm ^{103}Pd brachytherapy source. *Brachytherapy*. 2014;13:657–667.
82. Brown FB. Status of cross-section data libraries for MCNP. Los Alamos National Laboratory Report No.LA-UR-13-23040, Los Alamos, NM, April 29, 2013; 2013.
83. Chng N, Spadinger I, Rasoda R, Morris WJ, Salcudean S. Prostate brachytherapy postimplant dosimetry: seed orientation and the impact of dosimetric anisotropy in stranded implants. *Med Phys*. 2012;39:721–731.
84. Collins Fekete CA, Plamondon M, Martin A-G, Vigneault E, Verhaegen F, Beaulieu L. Quantifying the effect of seed orientation in post-planning dosimetry of low-dose-rate prostate brachytherapy. *Med Phys*. 2014;41:101704, 9 pp.
85. Meigooni AS, Sowards K, Soldano M. Dosimetric characteristics of the intersource^{103} palladium brachytherapy source. *Med Phys*. 2000;27:1093–1100.
86. Reniers B, Vynckier S, Scalliet P. Dosimetric study of a new palladium seed. *Appl Radiat Isot*. 2002;57:805–811.

87. Williamson JF. Monte Carlo evaluation of kerma at a point for photon transport problems. *Med Phys*. 1987;14:567–576.
88. NCRP. A handbook of radioactivity measurements procedures. NCRP Report No. 58, National Council on Radiation Protection and Measurements, Bethesda, MD; 1985.
89. Roussin RW, Knight JR, Hubbell JH, Howerton RJ. Description of the DLC-99/HUGO package of photon interaction. Oak Ridge National Laboratory, RSIC Data Library Collection, Radiation Shielding Center, December, Report ORNL/RSIC-46, Oak-Ridge, TN; 1983.
90. Briesmeister JF. MCNP-A General Monte Carlo N-Particle Transport Code System, Version 4B, LA-12625-M; 1997.
91. Storm E, Israel H. Photon cross-sections from 1 keV to 100 MeV for elements *Z*=1 to *Z*=100. *Nucl Data Sect A*. 1970;7:566–575.
92. DeMarco JJ, Wallace RE, Boedeker K. An analysis of MCNP cross-sections and tally methods for low-energy photon emitters'. *Phys Med Biol*. 2002;47:1321–1332.
93. Mitch M. Personal communication, October 9; 2014.
94. Bernard S, Vynckier S. Dosimetric study of a new polymer encapsulated palladium-103 seed. *Phys Med Biol*. 2005;50:1493–1504.
95. Wang Z, Hertel N. Determination of dosimetric characteristics of OptiSeed™ a plastic brachytherapy ^{103}Pd source. *Appl Radiat Isot*. 2005;63:311–321.
96. Khan S, Chen ZJ, Nath R. Photon energy spectrum emitted by a novel polymer-encapsulated ^{103}Pd source and its effect on the dose rate constant. *Med Phys*. 2008;35:1403–1406.
97. Briesmeister JF. MCNP—A general Monte Carlo N-particle transport code—Version 4C. Los Alamos National Laboratory Report LA-13709-M, March 2000; 2000.
98. Storm E, Israel HI. Photon cross sections from 0.001 to 100 MeV for elements 1 through 100. Los Alamos Laboratory Report LA-3753; 1969.
99. International Commission on Radiological Protection. *ICRP Publication 38: Radionuclide Transformations: Energy and Intensity of Emissions*. Oxford, U.K.: Pergamon Press Inc.; 2008.
100. Abboud F, Scalliet P, Vynckier S. An experimental palladium-103 seed (OptiSeed^{exp}) in a biocompatible polymer without a gold marker: characterization of dosimetric parameters including the interseed effect. *Med Phys*. 2008;35:5841–5850.
101. Mowlavi AA, Yazdani M. Determination of the TG-43 dosimetry parameters and isodose curves of ^{103}Pd source model OptiSeed™ in soft tissue phantom. *Elixir Pharmacy*. 2011;38:4178–4181.
102. Meigooni AS, Dini SA, Awan SB, Dou K, Koona RA. Theoretical and experimental determination of dosimetric characteristics for ADVANTAGE™ Pd-103 brachytherapy source. *Appl Radiat Isot*. 2006;64:881–887.
103. Sowards KT. Monte Carlo dosimetric characterization of the IsoAid ADVANTAGE ^{103}Pd brachytherapy source. *J Appl Clin Med Phys*. 2007;8:18–25.
104. Dillman LT, Van der Lage FC. Radionuclide Decay Schemes and Nuclear Parameters for Use in Radiation-Dose Estimates. NM/MIRD pamphlet No. 10. Revised edition. New York (NY): Society of Nuclear Medicine, Medical Internal Radiation Dose Committee; 1975.
105. Murphy MK, Piper RK, Greenwood LR, et al. Evaluation of the new cesium-131 seed for use in low-energy x-ray brachytherapy. *Med Phys*. 2004;31:1529–1538.
106. Chen Z, Bongiorni P, Nath R. Dose rate constant of a cesium-131 interstitial brachytherapy seed measured by thermoluminescent dosimetry and gamma-ray spectrometry. *Med Phys*. 2005;32:3279–3285.
107. Wittman RS, Fisher DR. Multiple-estimate Monte Carlo calculation of the dose rate constant for a cesium-131 interstitial brachytherapy seed. *Med Phys*. 2007;34:49–54.
108. X-5 Monte Carlo Team. MCNP—A general Monte Carlo N-particle transport code, version 5—volume I: Overview and Theory. LA-UR-03-1987, April, 2003 revised September, 2005; 2005.
109. Rivard MJ. Brachytherapy dosimetry parameters calculated for a ^{131}Cs source. *Med Phys*. 2007;34:754–762.
110. Rivard MJ. Erratum: brachytherapy dosimetry parameters calculated for a ^{131}Cs source [Med. Phys. 34, 754–762 (2007)]. *Med Phys*. 2009;36:279.
111. Wang J, Zhang H. Dosimetric characterization of model CS-1 cesium-131 brachytherapy source in water phantoms and human tissues with MCNP5 Monte Carlo simulation. *Med Phys*. 2008;35:1571–1579.
112. Melhus CS, Rivard MJ. COMS eye plaque brachytherapy dosimetry simulations for ^{103}Pd, ^{125}I, and ^{131}Cs. *Med Phys*. 2008;35:3364–3371.
113. Tailor R, Ibbott G, Lampe S, Warren WB, Tolani N. Dosimetric characterization of a ^{131}Cs brachytherapy source by thermoluminescence dosimetry in liquid water. *Med Phys*. 2008;35:5861–5868.
114. Tailor R, Tolani N, Ibbott GS. Thermoluminescence dosimetry measurements of brachytherapy sources in liquid water. *Med Phys*. 2008;35:4063–4069.
115. Zhang H, Martin D, Chiu-Tsao ST, Meigooni AS, Thomadsen BR. A comprehensive dosimetric comparison between ^{131}Cs and ^{125}I brachytherapy sources for COMS eye plaque implant. *Brachytherapy*. 2010;9:362–372.
116. Chiu-Tsao S-T, Napoli JJ, Davis SD, Hanley J, Rivard MJ. Dosimetry for ^{131}Cs and ^{125}I seeds in solid water phantom using radiochromic EBT film. *Appl Radiat Isot*. 2014;92:102–114.